

# Numerical methods for nonlocal and fractional models

Marta D’Elia

*Center for Computing Research*

*Sandia National Laboratories, Albuquerque, New Mexico 87185, USA*

`mdelia@sandia.gov`

<https://sites.google.com/site/martadeliawebsite>

Qiang Du

*Department of Applied Physics and Applied Mathematics,  
and Data Science Institute*

*Columbia University, New York, NY 10027 USA*

`qd2125@columbia.edu`

<http://www.columbia.edu/~qd2125>

Christian Glusa

*Center for Computing Research*

*Sandia National Laboratories, Albuquerque, New Mexico 87185, USA*

`caglusa@sandia.gov`

Max Gunzburger

*Department of Scientific Computing*

*Florida State University, Tallahassee, Florida 32306, USA*

`mgunzburger@fsu.edu`

<https://www.sc.fsu.edu/gunzburg>

Xiaochuan Tian

*Department of Mathematics*

*University of Texas, Austin 78751, USA*

`xtian@math.utexas.edu`

<https://web.ma.utexas.edu/users/xtian>

Zhi Zhou

*Department of Applied Mathematics*

*The Hong Kong Polytechnic University, Kowloon, Hong Kong, China*

`zhizhou@polyu.edu.hk`

<https://sites.google.com/site/zhizhou0125>

Partial differential equations (PDEs) are used, with huge success, to model phenomena arising across all scientific and engineering disciplines. However, across an equally wide swath, there exist situations in which PDE models fail to adequately model observed phenomena or are not the best available model for that purpose. On the other hand, in many situations, *nonlocal models* that account for interaction occurring at a distance have been shown to more faithfully and effectively model observed phenomena that involve possible singularities and other anomalies. In this article, we consider a generic nonlocal model, beginning with a short review of its definition, the properties of its solution, its mathematical analysis, and specific concrete examples. We then provide extensive discussions about numerical methods, including finite element, finite difference, and spectral methods, for determining approximate solutions of the nonlocal models considered. In that discussion, we pay particular attention to a special class of nonlocal models that are the most widely studied in the literature, namely those involving fractional derivatives. The article ends with brief considerations of several modeling and algorithmic extensions which serve to show the wide applicability of nonlocal modeling.

## CONTENTS

### PART 1: Nonlocal diffusion models, including fractional models

1	General models for nonlocal diffusion	5
2	Weak formulations of nonlocal models	12
3	Fractional diffusion models	19

### PART 2: Numerical methods for nonlocal and fractional models

4	Introductory remarks	29
5	Finite element methods for nonlocal models	31
6	Finite element methods for the integral fractional Laplacian	40
7	Finite element methods for the spectral fractional Laplacian	43
8	Spectral-Galerkin methods for nonlocal diffusion	46
9	Spectral-Galerkin methods for fractional diffusion	51
10	Finite difference methods for the strong form of nonlocal diffusion	60
11	Numerical methods for the strong form of fractional diffusion	64
12	Conditioning and fast solvers	71

### PART 3: Selected extensions

13	Weakly coercive indefinite, and non-self-adjoint problems	74
14	Nonlocal convection-diffusion problems	77
15	Inverse problems	81
16	Variational inequalities and obstacle problems	89
17	Reduced-order modeling	91
18	Time-dependent nonlocal problems	95
19	Connections to stochastic processes	98
20	A turbulent flow application	101
21	Peridynamics models for solid mechanics	103
22	Image denoising	106
	References	111

## PART ONE

### Nonlocal diffusion models, including fractional models

In an attempt to make the article as self-contained as is possible or as is practical, in this part we introduce the model equations and provide results about solutions of those equations that, in Part 2, are used in the development and analysis of numerical methods. We focus on a general class of *nonlocal models* that are characterized by interactions at a distance through the use of integral equation formulations as opposed to partial differential equations. For the same applications setting, the nonlocal models considered feature different representations of physics<sup>1</sup> than do partial differential equation models. *Fractional derivative models* are an example of the general class of models we consider. Because there exists a large body of mathematical and computational literature devoted to fractional derivative models, that class of models is given special attention throughout the article. However, also highlighted are the opportunities afforded by the more general nonlocal models we consider that are not available through the use of fractional models.

Throughout, we use the following notational conventions; exceptions made to these conventions should not cause confusion. Please note that the adherence to these conventions become less strict as one moves from Part 1 to Part 2 to Part 3.

---

Roman letters:	functions depending on a single point, e.g., $u(\mathbf{x})$ , $\mathbf{v}(\mathbf{x})$ , $\mathbf{D}(\mathbf{x})$
Greek letters:	function depending on two points, e.g., $\eta(\mathbf{x}, \mathbf{y})$ , $\boldsymbol{\nu}(\mathbf{x}, \mathbf{y})$ , $\boldsymbol{\Theta}(\mathbf{x}, \mathbf{y})$
plain font:	scalar-valued functions, e.g., $u(\mathbf{x})$ , $\eta(\mathbf{x}, \mathbf{y})$
boldface font:	vector-valued functions, e.g., $\mathbf{u}(\mathbf{x})$ , $\boldsymbol{\nu}(\mathbf{x}, \mathbf{y})$
upper-case boldface font:	tensor-valued functions, e.g., $\mathbf{D}(\mathbf{x})$ , $\boldsymbol{\Theta}(\mathbf{x}, \mathbf{y})$
calligraphy font:	operators, functionals, bilinear forms, e.g., $\mathcal{A}$ , $\mathcal{D}$ , $\mathcal{L}$

---

In choosing these notational conventions, our goal is to be as consistent as is possible or practical throughout the article. Unfortunately, because of the different notations adopted in the literature, the notations used in the article may differ from those used in some of the cited books and papers.

<sup>1</sup> Throughout, for the sake of economy of exposition, we refer to physics as the setting for the generic models we consider. Of course, those models also arise in all other physical science settings as well as in engineering and the biological and social sciences.

## 1. General models for nonlocal diffusion

We consider an integral equation model that is a nonlocal analog of the classical Poisson problem

$$\begin{cases} -\mathcal{L}_0 u := -\nabla \cdot (\mathbf{D} \nabla u) = f(\mathbf{x}) & \forall \mathbf{x} \in \Omega \\ \mathcal{B}u = g(\mathbf{x}) & \forall \mathbf{x} \in \partial\Omega, \end{cases} \quad (1.1)$$

where  $\Omega \in \mathbb{R}^d$  denotes a bounded, open domain having boundary  $\partial\Omega$ ,  $f(\mathbf{x})$  and  $g(\mathbf{x})$  denote given functions defined on  $\Omega$  and  $\partial\Omega$ , respectively, and  $\mathbf{D}(\mathbf{x})$  denotes a given symmetric, positive definite  $d \times d$  matrix. For the boundary conditions operator  $\mathcal{B}$ , we have the choices

$$\mathcal{B}u = \begin{cases} u & \Leftarrow \text{Dirichlet boundary condition} \\ (\mathbf{D} \nabla u) \cdot \mathbf{n} & \Leftarrow \text{Neumann boundary condition} \\ (\mathbf{D} \nabla u) \cdot \mathbf{n} + r(\mathbf{x})u & \Leftarrow \text{Robin boundary condition} \end{cases} \quad (1.2)$$

as well as mixed boundary conditions, e.g., Dirichlet and Neumann boundary condition applied on disjoint, covering parts of the boundary. The problem (1.1) is a model for, e.g., steady-state diffusion.

As will be immediately clear, the nonlocal model we consider is not an integral or boundary integral reformulation of the problem (1.1) based on, e.g., the use of Green's functions, but rather models different physics than does (1.1).

Given the bounded, open domain  $\Omega \in \mathbb{R}^d$  and given a constant  $\delta > 0$ , we define the *interaction domain* corresponding to  $\Omega$  as

$$\Omega_{\mathcal{I}_\delta} := \{\mathbf{y} \in \mathbb{R}^d \setminus \Omega \text{ such that } \mathbf{y} \in B_\delta(\mathbf{x}) \text{ for some } \mathbf{x} \in \Omega\}, \quad (1.3)$$

where  $B_\delta(\mathbf{x})$  denotes the ball of radius  $\delta$  centered at  $\mathbf{x}$ . We refer to  $\delta$  as the *interaction radius* or *horizon*. The nomenclature “interaction” used here is appropriate because  $\Omega_{\mathcal{I}_\delta}$  contains all points in the complement domain  $\mathbb{R}^d \setminus \Omega$  that are within a distance  $\delta$  of some point in  $\Omega$ . Note that the four cases

$$0 < \delta \ll \text{diam } \Omega, \quad \text{diam } \Omega \ll \delta < \infty, \quad \delta \approx \text{diam } \Omega, \quad \text{and} \quad \delta = \infty \quad (1.4)$$

are all of interest. An illustration of the first two cases is given in Figure 1.1. For the fourth case we have that the interaction domain  $\Omega_{\mathcal{I}_\infty} = \mathbb{R}^d \setminus \Omega$ . Also, the case of  $\Omega = \mathbb{R}^d$  is of considerable interest.

For  $\delta > 0$ , we consider the nonlocal problem for a scalar-valued function  $u(\mathbf{x})$  defined on  $\Omega \cup \Omega_{\mathcal{I}_\delta}$  given by

$$\begin{cases} -\mathcal{L}_\delta u = f(\mathbf{x}) & \forall \mathbf{x} \in \Omega \\ \mathcal{V}u = g(\mathbf{x}) & \forall \mathbf{x} \in \Omega_{\mathcal{I}_\delta}. \end{cases} \quad (1.5)$$

Note that *the constraint  $\mathcal{V}u = g$  is applied on the domain  $\Omega_{\mathcal{I}_\delta}$  having nonzero*

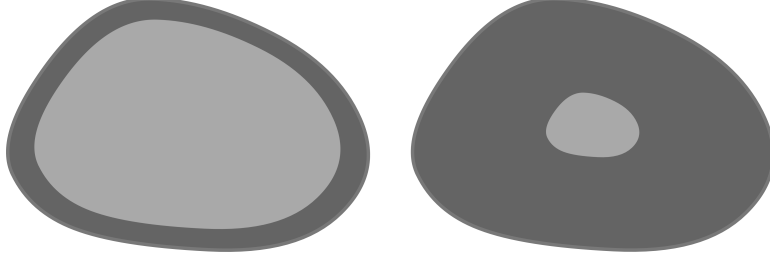


Figure 1.1.  $\Omega$  is in light gray whereas  $\Omega_{T_\delta}$  is in dark gray and has thickness  $\delta$ . Left:  $\delta$  smaller than the diameter of  $\Omega$ . Right:  $\delta$  larger than the diameter of  $\Omega$ .

*volume* in  $\mathbb{R}^d$  in contrast to the constraint  $\mathcal{B}u = g$  in (1.2) that is applied on the boundary surface  $\partial\Omega$ . For this reason we refer to  $\mathcal{V}u = g$  as being a *volume constraint* and to (1.5) as being a *volume-constrained problem* (Du, Gunzburger, Lehoucq and Zhou 2012a).

In (1.5), we have that  $f(\mathbf{x})$  and  $g(\mathbf{x})$  denote given scalar-valued functions defined on  $\Omega$  and  $\Omega_{T_\delta}$ , respectively, and

$$\mathcal{L}_\delta u(\mathbf{x}) := 2 \int_{\Omega \cup \Omega_{T_\delta}} (u(\mathbf{y}) - u(\mathbf{x})) \gamma_\delta(\mathbf{x}, \mathbf{y}) d\mathbf{y} \quad \forall \mathbf{x} \in \Omega, \quad (1.6)$$

where  $\gamma_\delta(\mathbf{x}, \mathbf{y})$  is a symmetric function, i.e.,

$$\gamma_\delta(\mathbf{x}, \mathbf{y}) = \gamma_\delta(\mathbf{y}, \mathbf{x}), \quad (1.7)$$

and, for any  $\mathbf{x}$ ,

$$\text{supp}(\gamma_\delta(\mathbf{x}, \mathbf{y})) = B_\delta(\mathbf{x}), \quad (1.8)$$

i.e.,  $\gamma_\delta(\mathbf{x}, \mathbf{y}) = 0$  whenever  $|\mathbf{y} - \mathbf{x}| > \delta$ . We note that in some of the specific cases we consider below, the integral in (1.6) has to be viewed in the principal-value sense. For notation simplicity, we omit “p.v.” in front of the integral sign even in such cases. The operator  $\mathcal{L}_\delta$  is a nonlocal analog of the PDE operator  $\nabla \cdot (\mathbf{D} \nabla u)$ . That connection is made explicit in Section 1.1. The nonlocal model (1.5) is a nonlocal analog of the local PDE diffusion model (1.1).

Analogous to (1.2), we have the choice of volume constraints

$$\mathcal{V}u = \begin{cases} u & \Leftarrow \text{Dirichlet volume constraint} \\ \mathcal{N}_\delta u & \Leftarrow \text{Neumann volume constraint} \\ \mathcal{N}_\delta u + r(\mathbf{x})u & \Leftarrow \text{Robin volume constraint} \end{cases} \quad (1.9)$$

as well as mixed types of volume constraints, where we have the *nonlocal*

*Neumann or nonlocal flux operator*

$$\mathcal{N}_\delta u := -2 \int_{\Omega \cup \Omega_{\mathcal{I}_\delta}} (u(\mathbf{y}) - u(\mathbf{x})) \gamma_\delta(\mathbf{x}, \mathbf{y}) d\mathbf{y} \quad \forall \mathbf{x} \in \Omega_{\mathcal{I}_\delta}. \quad (1.10)$$

The operator  $\mathcal{N}_\delta$  plays the role that the normal derivative does for the classical PDE case. In fact, both  $(\mathbf{D}\nabla u) \cdot \mathbf{n}$  and  $\mathcal{N}_\delta u$  denote fluxes into a point  $\mathbf{x}$ , with  $\mathbf{x} \in \partial\Omega$  for the PDE case and  $\mathbf{x} \in \Omega_{\mathcal{I}_\delta}$  in the nonlocal case. It is obvious that the definitions of the operators  $\mathcal{L}_\delta$  and  $\mathcal{N}_\delta$  involve exactly the same integrand but have different domains of definition, i.e.,  $\Omega$  for the former and  $\Omega_{\mathcal{I}_\delta}$  for the latter. So, clearly, they can be combined into a single operator defined over  $\Omega \cup \Omega_{\mathcal{I}_\delta}$ . However, as is made clear below, it is convenient to keep using the two operators. For a detailed discussion about nonlocal fluxes, see (Du et al. 2012a, Du, Gunzburger, Lehoucq and Zhou 2013a).

Because points  $\mathbf{x}$  only interact with points  $\mathbf{y} \in B_\delta(\mathbf{x})$ , (1.6) and (1.10) can be equivalently written as

$$\mathcal{L}_\delta u := 2 \int_{B_\delta(\mathbf{x})} (u(\mathbf{y}) - u(\mathbf{x})) \gamma_\delta(\mathbf{x}, \mathbf{y}) d\mathbf{y} \quad \forall \mathbf{x} \in \Omega \quad (1.11)$$

and

$$\mathcal{N}_\delta u := -2 \int_{(\Omega \cup \Omega_{\mathcal{I}_\delta}) \cap B_\delta(\mathbf{x})} (u(\mathbf{y}) - u(\mathbf{x})) \gamma_\delta(\mathbf{x}, \mathbf{y}) d\mathbf{y} \quad \forall \mathbf{x} \in \Omega_{\mathcal{I}_\delta}, \quad (1.12)$$

respectively, where we have used the facts that due to the definition of the interaction domain  $\Omega_{\mathcal{I}_\delta}$ ,  $(\Omega \cup \Omega_{\mathcal{I}_\delta}) \cap B_\delta(\mathbf{x}) = B_\delta(\mathbf{x})$  for  $\mathbf{x} \in \Omega$  but  $(\Omega \cup \Omega_{\mathcal{I}_\delta}) \cap B_\delta(\mathbf{x}) \subset B_\delta(\mathbf{x})$  for  $\mathbf{x} \in \Omega_{\mathcal{I}_\delta}$ .

### 1.1. A brief review of a nonlocal vector calculus

To make some sense of how the model (1.5) arises and why we refer to it as a nonlocal analog of the model (1.1), we need to first introduce some elements of a nonlocal vector calculus. Note that in this article, we also use elements of the *fractional calculus*. However, because there are many excellent references about the fractional calculus and its applications (see, e.g., (Baleanu, Diethelm, Scalas and Trujillo 2016, Mainardi 1997, Meerschaert and Sikorskii 2012)) we do not discuss them here.

The classical vector calculus provides a set of tools that are in ubiquitous use for the modeling, analysis, discretization, and numerical analysis of partial differential equation (PDE) models, an obvious example being the use of Green's first identity to transform the strong formulation of a PDE into a weak formulation. The foundation of that calculus are the familiar divergence, gradient, and curl differential operators upon which an edifice is built that includes vector identities (e.g.,  $\operatorname{div} \operatorname{curl} \mathbf{v} = 0$ ), integral theorems (e.g., Gauss' theorem), and much, much more.

A nonlocal vector calculus has been developed (Gunzburger and Lehoucq 2010, Du et al. 2012a, Du et al. 2013a, Alali, Gunzburger and Liu 2015, Mengesha and Du 2016, Du 2019, D'Elia, Flores, Li, Radu and Yu 2019a) to deal with nonlocal models such as (1.5) in much the same way as the classical vector calculus is used to deal with PDE models such as (1.1). Here, mostly following (Du et al. 2013a), we provide a brief introduction into the nonlocal vector calculus, including notions that are used in the rest of the article. We remark that certain elements of the nonlocal vector calculus have previously appeared in, e.g., (Coulhon and Grigoryan 1998, Zhou and Schölkopf 2005, Gilboa and Osher 2008, L  zoray, Ta and Elmoataz 2010, Lou, Zhang, Osher and Bertozzi 2010, Jiang, Lim, Yao and Ye 2011). However, the discussions in those papers, compared to that in (Du et al. 2013a), are limited in scope and in application and provide only a partial development of a nonlocal vector calculus that mimics the classical vector calculus.

The foundation of the nonlocal vector calculus are *integral* operators that mimic the three differential operators upon which the classical vector calculus is built.

Given the vector-valued functions  $\boldsymbol{\nu}_\delta(\mathbf{x}, \mathbf{y}) : (\Omega \cup \Omega_{\mathcal{I}_\delta}) \times (\Omega \cup \Omega_{\mathcal{I}_\delta}) \rightarrow \mathbb{R}^d$  and  $\boldsymbol{\alpha}_\delta(\mathbf{x}, \mathbf{y}) : (\Omega \cup \Omega_{\mathcal{I}_\delta}) \times (\Omega \cup \Omega_{\mathcal{I}_\delta}) \rightarrow \mathbb{R}^d$ , the action of the *nonlocal divergence operator*  $\mathcal{D}_\delta : \Omega \cup \Omega_{\mathcal{I}_\delta} \rightarrow \mathbb{R}$  on  $\boldsymbol{\nu}(\mathbf{x}, \mathbf{y})$  is defined as

$$(\mathcal{D}_\delta \boldsymbol{\nu})(\mathbf{x}) := \int_{\Omega \cup \Omega_{\mathcal{I}_\delta}} (\boldsymbol{\nu}(\mathbf{y}, \mathbf{x}) + \boldsymbol{\nu}(\mathbf{x}, \mathbf{y})) \cdot \boldsymbol{\alpha}_\delta(\mathbf{x}, \mathbf{y}) \mathcal{X}_{B_\delta(\mathbf{x})}(\mathbf{y}) d\mathbf{y} \quad (1.13)$$

$$\forall \mathbf{x} \in \Omega \cup \Omega_{\mathcal{I}_\delta},$$

where  $\boldsymbol{\alpha}_\delta(\mathbf{x}, \mathbf{y})$  denotes an antisymmetric function, i.e.,  $\boldsymbol{\alpha}_\delta(\mathbf{y}, \mathbf{x}) = -\boldsymbol{\alpha}_\delta(\mathbf{x}, \mathbf{y})$  for all  $\mathbf{x}, \mathbf{y} \in \Omega \cup \Omega_{\mathcal{I}_\delta}$ , and  $\mathcal{X}_{(\cdot)}(\cdot)$  denotes the indicator function. Note that unlike its differential counterpart  $\nabla \cdot$ , the nonlocal operator  $\mathcal{D}_\delta$  is not uniquely defined, i.e., not only do we have an unspecified parameter  $\delta > 0$ , but we also have said nothing about  $\boldsymbol{\alpha}_\delta(\mathbf{x}, \mathbf{y})$  other than it is an antisymmetric function. The choices one makes for  $\delta$  and especially  $\boldsymbol{\alpha}_\delta(\mathbf{x}, \mathbf{y})$  can result in operators having very different properties. Thus,  $\delta$  and  $\boldsymbol{\alpha}_\delta(\mathbf{x}, \mathbf{y})$  are modeling choices dictated by the specific application one considers. We have already mentioned, in (1.4), the wide choices of  $\delta$  that are of interest; several choices for  $\boldsymbol{\alpha}_\delta(\mathbf{x}, \mathbf{y})$  are considered in Section 2.2.1.

Simple manipulations show that, under suitable regularity assumptions that we do not dwell on here,

$$\int_{\Omega \cup \Omega_{\mathcal{I}_\delta}} v \mathcal{D}_\delta \boldsymbol{\nu} d\mathbf{x} = \int_{\Omega \cup \Omega_{\mathcal{I}_\delta}} \int_{\Omega \cup \Omega_{\mathcal{I}_\delta}} \boldsymbol{\nu} \cdot \mathcal{D}_\delta^* v d\mathbf{y} d\mathbf{x} \quad (1.14)$$

where

$$(\mathcal{D}_\delta^* u)(\mathbf{x}, \mathbf{y}) := -(u(\mathbf{y}) - u(\mathbf{x})) \boldsymbol{\alpha}_\delta(\mathbf{x}, \mathbf{y}) \mathcal{X}_{B_\delta(\mathbf{x})}(\mathbf{y}) \quad (1.15)$$

$$\forall \mathbf{x}, \mathbf{y} \in \Omega \cup \Omega_{\mathcal{I}_\delta}.$$



From (1.14), it is natural to refer to operator  $\mathcal{D}_\delta^*$  as being the *adjoint operator* corresponding to  $\mathcal{D}_\delta$ . With  $\mathcal{D}_\delta^*$  being the adjoint of  $\mathcal{D}_\delta$ , one may formally refer to  $-\mathcal{D}_\delta^*$  as being a *nonlocal gradient operator*.

Let  $\Theta_\delta(\mathbf{x}, \mathbf{y}) : (\Omega \cup \Omega_{\mathcal{I}_\delta}) \times (\Omega \cup \Omega_{\mathcal{I}_\delta}) \rightarrow \mathbb{R}^{d \times d}$  denote a tensor-valued function that is symmetric in the function sense, i.e.,  $\Theta_\delta(\mathbf{x}, \mathbf{y}) = \Theta_\delta(\mathbf{y}, \mathbf{x})$ , and is symmetric and positive definite in the matrix sense. Then, from the definitions of the nonlocal divergence and gradient operators, we have that

$$\begin{aligned} -\mathcal{D}_\delta(\Theta_\delta \mathcal{D}_\delta^* u) \\ = 2 \int_{\Omega \cup \Omega_{\mathcal{I}_\delta}} (u(\mathbf{y}) - u(\mathbf{x})) \alpha_\delta(\mathbf{x}, \mathbf{y}) \cdot (\Theta_\delta(\mathbf{x}, \mathbf{y}) \alpha_\delta(\mathbf{x}, \mathbf{y})) \mathcal{X}_{B_\delta(\mathbf{x})}(\mathbf{y}) d\mathbf{y}. \end{aligned} \quad (1.16)$$

For all  $\mathbf{x}, \mathbf{y} \in \Omega \cup \Omega_{\mathcal{I}_\delta}$ , we define the *kernel*  $\gamma_\delta(\mathbf{x}, \mathbf{y})$  as

$$\gamma_\delta(\mathbf{x}, \mathbf{y}) := \alpha_\delta(\mathbf{x}, \mathbf{y}) \cdot (\Theta_\delta(\mathbf{x}, \mathbf{y}) \alpha_\delta(\mathbf{x}, \mathbf{y})) \mathcal{X}_{B_\delta(\mathbf{x})}(\mathbf{y}). \quad (1.17)$$

Note that  $\gamma_\delta(\mathbf{x}, \mathbf{y})$  defined in this way satisfies the symmetry condition (1.7) and the support condition (1.8), where the former follows from the fact that  $\mathcal{X}_{B_\delta(\mathbf{x})}(\mathbf{y})$  is itself a symmetric function, i.e., if  $\mathbf{y} \in B_\delta(\mathbf{x})$  then necessarily  $\mathbf{x} \in B_\delta(\mathbf{y})$ .

We then have that (1.16) can be expressed as

$$\begin{aligned} \mathcal{D}_\delta(\Theta_\delta \mathcal{D}_\delta^* u) &= -2 \int_{\Omega \cup \Omega_{\mathcal{I}_\delta}} (u(\mathbf{y}) - u(\mathbf{x})) \gamma_\delta(\mathbf{x}, \mathbf{y}) d\mathbf{y} \\ &= -2 \int_{B_\delta(\mathbf{x})} (u(\mathbf{y}) - u(\mathbf{x})) \gamma_\delta(\mathbf{x}, \mathbf{y}) d\mathbf{y}, \end{aligned} \quad (1.18)$$

where  $\gamma_\delta(\mathbf{x}, \mathbf{y})$  is given by (1.17) and  $\mathcal{D}_\delta$  and  $\mathcal{D}_\delta^*$  are given by (1.13) and (1.15), respectively.

Of course, we recognize that

$$\mathcal{D}_\delta(\Theta_\delta \mathcal{D}_\delta^* u) = -\mathcal{L}_\delta u, \quad (1.19)$$

where  $\mathcal{L}_\delta u$  is defined in (1.6) or (1.11). The fact that the operator  $\mathcal{L}_\delta$  can be written as a composition of nonlocal divergence and gradient operators justifies referring to (1.5) as a nonlocal Poisson problem, i.e.,  $\mathcal{L}_\delta u$  may be viewed as a nonlocal analog of  $\nabla \cdot (\mathbf{D} \nabla u)$  for suitable choices of  $\alpha_\delta(\mathbf{x}, \mathbf{y})$ , and, if  $\Theta_\delta$  is the identity tensor,  $\mathcal{L}_\delta u$  is indeed a nonlocal analog of the  $\Delta u$ .

**Remark 1.1.** *Variable coefficients in nonlocal models.* An advantage accruing from the nonlocal calculus is that, through compositions such as (1.16) or (1.18), it provides a natural means for generalizing nonlocal constant coefficient operators such as the fractional Laplace operator to variable coefficient settings in a manner completely analogous to how one defines variable coefficient operators in the PDE case. As an example, in Section 3.4, we describe one way this can be done for fractional diffusion models.  $\square$

The final bit of the nonlocal vector calculus that we need is a (generalized) nonlocal Green's first identity. In the context of this section, that identity is given by (Du et al. 2013a)

$$\int_{\Omega \cup \Omega_{\mathcal{I}_\delta}} v \mathcal{D}_\delta(\Theta_\delta \mathcal{D}_\delta^* u) d\mathbf{y} = \int_{\Omega \cup \Omega_{\mathcal{I}_\delta}} \mathcal{D}_\delta^* v \cdot (\Theta_\delta \mathcal{D}_\delta^* u) d\mathbf{y} d\mathbf{x}. \quad (1.20)$$

We have that

$$\mathcal{D}_\delta^* v \cdot (\Theta_\delta \mathcal{D}_\delta^* u) = (v(\mathbf{y}) - v(\mathbf{x}))(u(\mathbf{y}) - u(\mathbf{x}))\gamma_\delta(\mathbf{x}, \mathbf{y}) \quad (1.21)$$

so that substituting (1.18), (1.10), and (1.21) into (1.20) results in the equivalent form of the nonlocal Green's first identity given by

$$\begin{aligned} \int_{\Omega \cup \Omega_{\mathcal{I}_\delta}} \int_{\Omega \cup \Omega_{\mathcal{I}_\delta}} (v(\mathbf{y}) - v(\mathbf{x}))(u(\mathbf{y}) - u(\mathbf{x}))\gamma_\delta(\mathbf{x}, \mathbf{y}) d\mathbf{y} d\mathbf{x} \\ = - \int_{\Omega} v(\mathbf{x}) \mathcal{L}_\delta u(\mathbf{x}) d\mathbf{x} + \int_{\Omega_{\mathcal{I}_\delta}} v(\mathbf{x}) \mathcal{N}_\delta u(\mathbf{x}) d\mathbf{x}. \end{aligned} \quad (1.22)$$

Given our comments about nonlocal fluxes, etc., we recognize (1.22) as a nonlocal analog of the (generalized) local Green's first identity

$$\int_{\Omega} \nabla v \cdot (\mathbf{D} \nabla u) d\mathbf{x} = - \int_{\Omega} v \nabla \cdot (\mathbf{D} \nabla u) d\mathbf{x} + \int_{\partial\Omega} v \mathbf{n} \cdot (\mathbf{D} \nabla u) d\mathbf{x}.$$

Derivations in a more rigorous functional analytic setting of nonlocal integral identities such as (1.22) and the connection to their local analogs can be found in (Mengesha and Du 2016, Du 2019).

**Remark 1.2.** *The roles played in the kernel by operator definitions and constitutive functions.* It is important to differentiate between the roles that the functions  $\alpha_\delta(\mathbf{x}, \mathbf{y})$  and  $\Theta_\delta(\mathbf{x}, \mathbf{y})$  have in the nonlocal models we are considering. It is clear that  $\alpha_\delta(\mathbf{x}, \mathbf{y})$  serves to define operators (i.e.,  $\mathcal{D}_\delta$ ,  $\mathcal{D}_\delta^*$ , and  $\mathcal{N}_\delta$  given by (1.13), (1.15), and (1.10), respectively), *irrespective of how those operators are used*. On the other hand,  $\Theta_\delta(\mathbf{x}, \mathbf{y})$  serves as a constitutive function. Thus, both  $\alpha_\delta(\mathbf{x}, \mathbf{y})$  and  $\Theta_\delta(\mathbf{x}, \mathbf{y})$  are modeling choices. Both influence the properties of solutions of nonlocal models such as their regularity. Of course, the situation is much the same in the local PDE case, i.e., the operators  $\nabla \cdot$  and  $\nabla$  are defined irrespective of how they are used and  $\mathbf{D}(\mathbf{x})$  denotes a constitutive tensor.  $\square$

**Remark 1.3.** *Choices that define a nonlocal diffusion model.* Recapitulating, to define a specific nonlocal diffusion model, one must make three modeling choices:

- the horizon  $\delta$  that defines the extent of nonlocal interactions
- the antisymmetric function  $\alpha_\delta(\mathbf{x}, \mathbf{y})$  that defines the nonlocal divergence operator  $\mathcal{D}_\delta$  and nonlocal gradient operator  $-\mathcal{D}_\delta^*$

- the constitutive tensor  $\Theta_\delta(\mathbf{x}, \mathbf{y})$  that defines the properties of the media.

These three choices are all that enter into the definition (1.17) of the kernel  $\gamma_\delta(\mathbf{x}, \mathbf{y})$  so that specifying them uniquely defines the operator  $\mathcal{L}_\delta$ .  $\square$

**Remark 1.4.** *Additional operators of the nonlocal vector calculus.* The composition of the nonlocal divergence operator  $\mathcal{D}_\delta$  and its adjoint operator  $\mathcal{D}_\delta^*$  are the only nonlocal operators needed to define the nonlocal operator  $\mathcal{L}_\delta$  that operates on scalar-valued functions. However, other aspects of the nonlocal vector calculus such as nonlocal vector identities and nonlocal operators acting on vector-valued functions make use of additional nonlocal operators.

Thus, in addition to  $\mathcal{D}_\delta$  and  $\mathcal{D}_\delta^*$ , we have the nonlocal gradient operator  $\mathcal{G}_\delta$  defined by, for a scalar-valued function  $\nu(\mathbf{x}, \mathbf{y})$ ,

$$(\mathcal{G}_\delta \nu)(\mathbf{x}) := \int_{\Omega \cup \Omega_{\mathcal{I}_\delta}} (\nu(\mathbf{y}, \mathbf{x}) + \nu(\mathbf{x}, \mathbf{y})) \alpha_\delta(\mathbf{x}, \mathbf{y}) \mathcal{X}_{B_\delta(\mathbf{x})}(\mathbf{y}) d\mathbf{y} \quad (1.23)$$

for all  $\mathbf{x} \in \Omega \cup \Omega_{\mathcal{I}_\delta}$  and its adjoint operator  $\mathcal{G}_\delta^*$  given by, for a vector-valued function  $\mathbf{u}(\mathbf{x})$ ,

$$(\mathcal{G}_\delta^* \mathbf{u})(\mathbf{x}, \mathbf{y}) = -(\mathbf{u}(\mathbf{y}) - \mathbf{u}(\mathbf{x})) \cdot \alpha_\delta(\mathbf{x}, \mathbf{y}) \mathcal{X}_{B_\delta(\mathbf{x})}(\mathbf{y}) \quad (1.24)$$

for all  $\mathbf{x}, \mathbf{y} \in \Omega \cup \Omega_{\mathcal{I}_\delta}$ . Similarly, we have the nonlocal curl operator  $\mathcal{C}_\delta$  defined by, for a vector-valued function  $\boldsymbol{\nu}(\mathbf{x}, \mathbf{y})$ ,

$$(\mathcal{C}_\delta \boldsymbol{\nu})(\mathbf{x}) := \int_{\mathbb{R}^d} (\boldsymbol{\nu}(\mathbf{y}, \mathbf{x}) + \boldsymbol{\nu}(\mathbf{x}, \mathbf{y})) \times \alpha_\delta(\mathbf{x}, \mathbf{y}) \mathcal{X}_{B_\delta(\mathbf{x})}(\mathbf{y}) d\mathbf{y} \quad (1.25)$$

for all  $\mathbf{x} \in \Omega \cup \Omega_{\mathcal{I}_\delta}$  and its adjoint operator  $\mathcal{C}_\delta^*$  defined by, for a vector-valued function  $\mathbf{u}(\mathbf{x})$ ,

$$(\mathcal{C}_\delta^* \mathbf{u})(\mathbf{x}, \mathbf{y}) = -\alpha_\delta(\mathbf{x}, \mathbf{y}) \times (\mathbf{u}(\mathbf{y}) - \mathbf{u}(\mathbf{x})) \mathcal{X}_{B_\delta(\mathbf{x})}(\mathbf{y}) \quad (1.26)$$

for all  $\mathbf{x}, \mathbf{y} \in \Omega \cup \Omega_{\mathcal{I}_\delta}$ . Thus, in the nonlocal vector calculus we have pairs of divergence operators  $\mathcal{D}_\delta$  and  $-\mathcal{G}_\delta^*$ , gradient operators  $\mathcal{G}_\delta$  and  $-\mathcal{D}_\delta^*$ , and curl operators  $\mathcal{C}_\delta$  and  $\mathcal{C}_\delta^*$ , with  $\mathcal{D}_\delta, \mathcal{G}_\delta, \mathcal{C}_\delta$  acting on functions of two points, i.e.,  $\boldsymbol{\nu}(\mathbf{x}, \mathbf{y})$  and  $\nu(\mathbf{x}, \mathbf{y})$ , and  $\mathcal{D}_\delta^*, \mathcal{G}_\delta^*, \mathcal{C}_\delta^*$  acting on functions of one point, i.e.,  $\mathbf{u}(\mathbf{x})$  and  $u(\mathbf{x})$ .

With these operators in hand, we have the nonlocal vector identities

$$\begin{cases} \mathcal{D}_\delta(\mathcal{C}_\delta^* \mathbf{u}) = 0 & \mathcal{C}_\delta(\mathcal{G}_\delta^* u) = 0 \\ \mathcal{D}_\delta(\mathcal{D}_\delta^* \mathbf{u}) = \mathcal{G}_\delta(\mathcal{G}_\delta^* \mathbf{u}) + \mathcal{C}_\delta(\mathcal{C}_\delta^* \mathbf{u}) \end{cases} \quad (1.27)$$

that are nonlocal analogs of  $\nabla \cdot (\nabla \times \mathbf{u}) = 0$ ,  $\nabla \times (\nabla u) = 0$ , and  $\Delta \mathbf{u} = \nabla \cdot (\nabla \mathbf{u}) = \nabla(\nabla \cdot \mathbf{u}) - \nabla \times (\nabla \times \mathbf{u})$ , respectively. In particular, we can view  $-\mathcal{D}_\delta(\mathcal{D}_\delta^* \mathbf{u}) = -\mathcal{G}_\delta(\mathcal{G}_\delta^* \mathbf{u}) - \mathcal{C}_\delta(\mathcal{C}_\delta^* \mathbf{u})$  as a nonlocal vector Laplacian.

In addition, the operators introduced in this remark are used in (D'Elia et

al. 2019a) to define the nonlocal Hodge-Helmholtz decomposition of vector-valued function that depend on two points  $\mathbf{x}$  and  $\mathbf{y}$ . Note that the operators  $\mathcal{D}_\delta$ ,  $\mathcal{D}_\delta^*$ ,  $\mathcal{G}_\delta$ , and  $\mathcal{G}_\delta^*$ , as operators between functions of two points  $\mathbf{x}$  and  $\mathbf{y}$  and functions of one point  $\mathbf{x}$  or  $\mathbf{y}$ , do not recover their classical counterparts in the local limit  $\delta \rightarrow 0$ . Thus, in parallel to them, additional examples of nonlocal operators acting on vector-valued functions of one point only are introduced in (Du et al. 2013a) and further analyzed in (Mengesha and Du 2016, Du 2019, Du, Tao, Tian and Yang 2019d, Lee and Du 2019b). In fact, a nonlocal Helmholtz decomposition of a vector-valued function  $\mathbf{u}(\mathbf{x})$  can be established which recovers the classical one in the local limit; see (Lee and Du 2019b). These operators can also be used to construct a nonlocal analog of the Stokes equation, which was used to provide a foundation for the analysis of smoothed particle hydrodynamics (Du and Tian 2019, Lee and Du 2019b). Some of these developments can be found in Section 21.  $\square$

## 2. Weak formulations of nonlocal models

The model (1.5) is a strong formulation of a nonlocal problem that is required to hold pointwise on  $\Omega \cup \Omega_{\mathcal{I}_\delta}$ . In this section, we consider a weak formulation corresponding to (1.5) and then relate that formulation to a minimization principle. We conclude the section by providing specific examples of the kernels  $\gamma_\delta(\mathbf{x}, \mathbf{y})$  and their associated energy spaces.

### 2.1. Function spaces, weak formulations, and well posedness

#### 2.1.1. Function spaces and norms

We define the “energy” space

$$V(\Omega \cup \Omega_{\mathcal{I}_\delta}) = \{v(\mathbf{x}) \in L^2(\Omega \cup \Omega_{\mathcal{I}_\delta}) : \|v\|_{V(\Omega \cup \Omega_{\mathcal{I}_\delta})} < \infty\}, \quad (2.1)$$

where  $\|\cdot\|_{V(\Omega \cup \Omega_{\mathcal{I}_\delta})}$  denotes the “energy” norm defined as

$$\begin{aligned} \|v\|_{V(\Omega \cup \Omega_{\mathcal{I}_\delta})} = & \left( \int_{\Omega \cup \Omega_{\mathcal{I}_\delta}} \int_{\Omega \cup \Omega_{\mathcal{I}_\delta}} (v(\mathbf{y}) - v(\mathbf{x}))^2 \gamma_\delta(\mathbf{x}, \mathbf{y}) d\mathbf{y} d\mathbf{x} \right. \\ & \left. + \|v\|_{L^2(\Omega \cup \Omega_{\mathcal{I}_\delta})}^2 \right)^{1/2}. \end{aligned} \quad (2.2)$$

The space  $V(\Omega \cup \Omega_{\mathcal{I}_\delta})$  is by definition a subspace of  $L^2(\Omega \cup \Omega_{\mathcal{I}_\delta})$  and can be shown, for suitably chosen kernels (Mengesha and Du 2013), to be a Hilbert

space that comes equipped with the inner product

$$\begin{aligned} (u, v)_{V(\Omega \cup \Omega_{\mathcal{I}_\delta})} &= \int_{\Omega \cup \Omega_{\mathcal{I}_\delta}} \int_{\Omega \cup \Omega_{\mathcal{I}_\delta}} (v(\mathbf{y}) - v(\mathbf{x}))(u(\mathbf{y}) - u(\mathbf{x}))\gamma_\delta(\mathbf{x}, \mathbf{y}) d\mathbf{y}d\mathbf{x} \\ &\quad + (u, v)_{L^2(\Omega \cup \Omega_{\mathcal{I}_\delta})} \quad \forall u, v \in V(\Omega \cup \Omega_{\mathcal{I}_\delta}). \end{aligned} \quad (2.3)$$

We also have the *constrained energy space*

$$V_c(\Omega \cup \Omega_{\mathcal{I}_\delta}) = \{v(\mathbf{x}) \in V(\Omega \cup \Omega_{\mathcal{I}_\delta}) : v(\mathbf{x}) = 0 \text{ for } \mathbf{x} \in \Omega_{\mathcal{I}_\delta}\}. \quad (2.4)$$

Under suitable conditions on the kernels, we can prove a nonlocal Poincaré inequality (Du et al. 2012a, Du 2019). Thus, we have that the seminorm

$$|v|_{V_c(\Omega \cup \Omega_{\mathcal{I}_\delta})} = \left( \int_{\Omega \cup \Omega_{\mathcal{I}_\delta}} \int_{\Omega \cup \Omega_{\mathcal{I}_\delta}} (v(\mathbf{y}) - v(\mathbf{x}))^2 \gamma_\delta(\mathbf{x}, \mathbf{y}) d\mathbf{y}d\mathbf{x} \right)^{1/2} \quad (2.5)$$

is a norm on  $V_c(\Omega \cup \Omega_{\mathcal{I}_\delta})$  equivalent to the the norm (2.2) with equivalence constants that are independent of  $\delta$ . Correspondingly,  $V_c(\Omega \cup \Omega_{\mathcal{I}_\delta})$  is a Hilbert space equipped with the inner product

$$\begin{aligned} (u, v)_{V_c(\Omega \cup \Omega_{\mathcal{I}_\delta})} &= \int_{\Omega \cup \Omega_{\mathcal{I}_\delta}} \int_{\Omega \cup \Omega_{\mathcal{I}_\delta}} (v(\mathbf{y}) - v(\mathbf{x}))(u(\mathbf{y}) - u(\mathbf{x}))\gamma_\delta(\mathbf{x}, \mathbf{y}) d\mathbf{y}d\mathbf{x} \end{aligned} \quad (2.6)$$

for all  $u, v \in V_c(\Omega \cup \Omega_{\mathcal{I}_\delta})$ . For more detailed discussions of the conditions on the kernels and rigorous proofs of the properties on these spaces, we refer to (Mengesha and Du 2016, Mengesha and Du 2015, Du 2019).

We also have the “*trace*” space  $V_t(\Omega_{\mathcal{I}_\delta})$

$$V_t(\Omega_{\mathcal{I}_\delta}) = \{v(\mathbf{x}) = w(\mathbf{x})|_{\Omega_{\mathcal{I}_\delta}} \text{ for } \mathbf{x} \in \Omega_{\mathcal{I}_\delta} \text{ and } w(\mathbf{x}) \in V(\Omega \cup \Omega_{\mathcal{I}_\delta})\}. \quad (2.7)$$

Of course,  $V_t(\Omega_{\mathcal{I}_\delta})$  is not a trace space in the usual sense because it does not involve restrictions to lower-dimensional surfaces, but instead involves restrictions to the domain  $\Omega_{\mathcal{I}_\delta}$  having finite volume in  $\mathbb{R}^d$ . However, one can view  $V_t(\Omega_{\mathcal{I}_\delta})$  as a nonlocal analog of the trace space  $H^{1/2}(\partial\Omega)$  for functions belonging to  $H^1(\Omega)$ . A norm on  $V_t(\Omega_{\mathcal{I}_\delta})$  is given by

$$\begin{aligned} \|v\|_{V_t(\Omega_{\mathcal{I}_\delta})} &= \left( \int_{\Omega_{\mathcal{I}_\delta}} \int_{\Omega_{\mathcal{I}_\delta}} (v(\mathbf{y}) - v(\mathbf{x}))^2 \gamma_\delta(\mathbf{x}, \mathbf{y}) d\mathbf{y}d\mathbf{x} + \|v\|_{L^2(\Omega_{\mathcal{I}_\delta})}^2 \right)^{1/2}. \end{aligned} \quad (2.8)$$

We denote by  $V_d(\Omega)$  the *dual space* corresponding to  $V(\Omega \cup \Omega_{\mathcal{I}_\delta})$  that is defined in the usual way, using the  $L^2$  inner product to define the duality pairing and to also define a norm  $\|\cdot\|_{V_d(\Omega)}$  on that space.

As mentioned in Remark 1.2, specific function spaces are defined by making specific choices for  $\alpha_\delta(\mathbf{x}, \mathbf{y})$ . For some choices, the function spaces so

defined can be shown to be equivalent to standard function spaces such as Sobolev spaces. See Section 2.2.1 for some examples.

### 2.1.2. Weak formulations and well posedness

A weak formulation of the problem (1.5) with  $\mathcal{V}u = u$  is defined as follows.

$$\begin{aligned} & \text{Given } \gamma_\delta(\mathbf{x}, \mathbf{y}) \text{ defined in (1.17) and given } g(\mathbf{x}) \in V_t(\Omega_{\mathcal{I}_\delta}) \\ & \text{and } f(\mathbf{x}) \in V_d(\Omega), \\ & \text{find } u(\mathbf{x}) \in V(\Omega \cup \Omega_{\mathcal{I}_\delta}) \text{ such that} \\ & \begin{cases} \mathcal{A}_\delta(u, v) = \langle f, v \rangle & \forall v \in V_c(\Omega \cup \Omega_{\mathcal{I}_\delta}) \\ u(\mathbf{x}) = g(\mathbf{x}) & \forall \mathbf{x} \in \Omega_{\mathcal{I}_\delta}, \end{cases} \end{aligned} \quad (2.9)$$

where, for all  $u(\mathbf{x}), v(\mathbf{x}) \in V(\Omega \cup \Omega_{\mathcal{I}_\delta})$ , we have the bilinear form

$$\begin{aligned} \mathcal{A}_\delta(u, v) &= \int_{\Omega \cup \Omega_{\mathcal{I}_\delta}} \int_{\Omega \cup \Omega_{\mathcal{I}_\delta}} (v(\mathbf{y}) - v(\mathbf{x}))(u(\mathbf{y}) - u(\mathbf{x})) \gamma_\delta(\mathbf{x}, \mathbf{y}) d\mathbf{y} d\mathbf{x} \end{aligned} \quad (2.10)$$

and, for all  $f(\mathbf{x}) \in V_d(\Omega)$ , we have the linear functional

$$\langle f, v \rangle = \int_{\Omega} f(\mathbf{x}) v(\mathbf{x}) d\mathbf{x}. \quad (2.11)$$

That (2.9)–(2.11) are indeed a weak formulation corresponding to (1.5) is an immediate consequence of setting  $v(\mathbf{x}) = 0$  on  $\Omega_{\mathcal{I}_\delta}$  in the nonlocal Green's first identity (1.22) so that the term involving  $\mathcal{N}_\delta u$  vanishes. Equation (2.9) is a nonlocal analog of the weak formulation of the problem (1.1) with  $\mathcal{B}u = u$  given by  $\int_{\Omega} \nabla v \cdot (\mathbf{D} \nabla u) d\mathbf{x} = \langle f, v \rangle$  for all  $v \in H_0^1(\Omega)$  along with  $u = g$  on  $\partial\Omega$ .

It can be shown that the bilinear form  $\mathcal{A}_\delta(u, v)$  is symmetric and is continuous and coercive with respect to  $V_c(\Omega \cup \Omega_{\mathcal{I}_\delta})$  so that, by the Lax-Milgram theorem, the problem (2.9) is well posed. In particular, we have the a priori estimate with respect to the energy norm for the solution  $u(\mathbf{x})$  of (2.9) given by

$$\|u\|_{V(\Omega \cup \Omega_{\mathcal{I}_\delta})} \leq C_\delta (\|f\|_{V_d(\Omega)} + \|g\|_{V_t(\Omega_{\mathcal{I}_\delta})}), \quad (2.12)$$

where the constant  $C_\delta$  may depend on  $\delta$ , usually in a benign way.

**Remark 2.1.** *A nonlocal Neumann model.* We can, of course, also define a weak formulation of (1.5) for  $\mathcal{V}u = \mathcal{N}_\delta u$ , i.e., for a nonlocal Neumann problem. In this case a weak formulation is given by

$$\begin{cases} \mathcal{A}_\delta(u, v) = \langle f, v \rangle + \int_{\Omega_{\mathcal{I}_\delta}} g(\mathbf{x}) v(\mathbf{x}) d\mathbf{x} & \forall v \in V(\Omega \cup \Omega_{\mathcal{I}_\delta}) \setminus \mathbb{R} \\ \int_{\Omega} f(\mathbf{x}) d\mathbf{x} + \int_{\Omega_{\mathcal{I}_\delta}} g(\mathbf{x}) d\mathbf{x} = 0, \end{cases} \quad (2.13)$$

where the quotient space  $V(\Omega \cup \Omega_{\mathcal{I}_\delta}) \setminus \mathbb{R}$  is used to ensure uniqueness and the compatibility condition on  $f$  and  $g$  must be satisfied to ensure existence. Equation (2.13) is a nonlocal analog of the weak formulation corresponding to (1.1) with  $\mathcal{B}u = (\mathbf{D}\nabla u) \cdot \mathbf{n}$  given by

$$\int_{\Omega} \nabla v \cdot (\mathbf{D}\nabla u) d\mathbf{x} = \int_{\Omega} f v d\mathbf{x} + \int_{\partial\Omega} g v d\mathbf{x}$$

for all  $v \in H^1(\Omega) \setminus \mathbb{R}$  along with the compatibility condition

$$\int_{\Omega} f d\mathbf{x} + \int_{\partial\Omega} g d\mathbf{x} = 0.$$

For the sake of economy of exposition, in the sequel we focus on (2.9) in which  $\mathcal{V}u = u$  and, at times, we even focus on the homogeneous version of (2.9) for which  $g(\mathbf{x}) = 0$ . Most of what is said about (2.9) can be extended to nonlocal Neumann problems. For additional discussions about nonlocal Neumann problems, see, e.g., (Cortazar, Elgueta, Rossi and Wolanski 2008, Du 2019, Mengesha and Du 2016, Mengesha and Du 2015, Tao, Tian and Du 2017, D’Elia, Tian and Yu 2019d).

We note that, although other ways of defining a nonlocal Neumann problem have been proposed, perhaps the one in (2.13) is the most “natural” to the nonlocal vector calculus.  $\square$

### 2.1.3. Relation to an energy minimization principle

The weak formulation (2.9) can also be derived as the Euler-Lagrange equation for an energy minimization principle. Consider the energy functional

$$\begin{aligned} \mathcal{E}_\delta(u; f, \gamma_\delta) = & \frac{1}{2} \int_{\Omega \cup \Omega_{\mathcal{I}_\delta}} \int_{\Omega \cup \Omega_{\mathcal{I}_\delta}} (u(\mathbf{y}) - u(\mathbf{x}))^2 \gamma_\delta(\mathbf{x}, \mathbf{y}) d\mathbf{y} d\mathbf{x} \\ & - \int_{\Omega} f(\mathbf{x}) u(\mathbf{x}) d\mathbf{x} \end{aligned} \quad (2.14)$$

an the minimization principle

$$\begin{aligned} & \text{given } \gamma_\delta(\mathbf{x}, \mathbf{y}) \text{ defined in (1.17) and given } g(\mathbf{x}) \in V_t(\Omega_{\mathcal{I}_\delta}) \\ & \text{and } f(\mathbf{x}) \in V_d(\Omega), \\ & \text{find } u(\mathbf{x}) \in V(\Omega \cup \Omega_{\mathcal{I}_\delta}) \text{ such that} \\ & \mathcal{E}_\delta(u; f, \gamma_\delta) \text{ is minimized} \\ & \text{subject to } u(\mathbf{x}) = g(\mathbf{x}) \text{ for } \mathbf{x} \in \Omega_{\mathcal{I}_\delta}. \end{aligned} \quad (2.15)$$

Using standard techniques from the calculus of variations, one easily sees that (2.9) is indeed the Euler-Lagrange equation corresponding to the energy minimization principle (2.15).

## 2.2. Kernel choices and the corresponding energy spaces

We assume that  $\gamma_\delta(\mathbf{x}, \mathbf{y})$  given by (1.17) can be written in the form

$$\gamma_\delta(\mathbf{x}, \mathbf{y}) = \phi_\delta(\mathbf{x}, \mathbf{y})\theta_\delta(\mathbf{x}, \mathbf{y})\mathcal{X}_{B_\delta(\mathbf{x})}(\mathbf{y}), \quad (2.16)$$

where  $\theta_\delta(\mathbf{x}, \mathbf{y})$  and  $\phi_\delta(\mathbf{x}, \mathbf{y})$  denote positive, symmetric, scalar-valued functions. This form is very general with respect to both operators and constitutive functions. In fact, by setting

$$\boldsymbol{\alpha}_\delta(\mathbf{x}, \mathbf{y}) = \frac{\mathbf{y} - \mathbf{x}}{|\mathbf{y} - \mathbf{x}|} \sqrt{\phi_\delta(\mathbf{x}, \mathbf{y})} \quad (2.17)$$

and

$$\theta_\delta(\mathbf{x}, \mathbf{y}) := \frac{\mathbf{y} - \mathbf{x}}{|\mathbf{y} - \mathbf{x}|} \cdot \left( \boldsymbol{\Theta}_\delta(\mathbf{x}, \mathbf{y}) \frac{\mathbf{y} - \mathbf{x}}{|\mathbf{y} - \mathbf{x}|} \right) \quad (2.18)$$

in (1.17), we arrive at (2.16). Thus, the only assumption made is that  $\boldsymbol{\alpha}_\delta(\mathbf{x}, \mathbf{y})$  is directed along the vector  $\mathbf{y} - \mathbf{x}$ . Note that  $\boldsymbol{\alpha}_\delta(\mathbf{x}, \mathbf{y})$  given by (2.17) is indeed an antisymmetric function whereas  $\theta_\delta(\mathbf{x}, \mathbf{y})$  given by (2.18) is indeed a positive, symmetric function if  $\boldsymbol{\Theta}_\delta(\mathbf{x}, \mathbf{y})$  is symmetric in the function sense and symmetric and positive definite in the matrix sense.

We do not combine  $\theta_\delta(\mathbf{x}, \mathbf{y})$  and  $\phi_\delta(\mathbf{x}, \mathbf{y})$  into a single function because we want to keep separate the operator definition and constitutive roles played by  $\gamma_\delta(\mathbf{x}, \mathbf{y})$ ; note that  $\phi_\delta$  is only related to  $\boldsymbol{\alpha}_\delta$  whereas  $\theta_\delta$  is only related to  $\boldsymbol{\Theta}_\delta$ . Thus, now  $\phi_\delta(\mathbf{x}, \mathbf{y})$  takes over the role of  $\boldsymbol{\alpha}_\delta(\mathbf{x}, \mathbf{y})$  in this regard and  $\theta_\delta(\mathbf{x}, \mathbf{y})$  can be viewed as a constitutive function. Note also that  $\boldsymbol{\alpha}_\delta(\mathbf{x}, \mathbf{y})$  as given by (2.17) can be used to define the “first-order” nonlocal operators  $\mathcal{D}_\delta$  and  $\mathcal{D}_\delta^*$  whereas  $\gamma_\delta(\mathbf{x}, \mathbf{y})$  is used to define the “second-order” nonlocal operator  $\mathcal{L}_\delta$  and the “Neumann” nonlocal operator  $\mathcal{N}_\delta$ . In the sequel, we refer to  $\gamma_\delta(\mathbf{x}, \mathbf{y})$  as the *kernel*,  $\phi_\delta(\mathbf{x}, \mathbf{y})$  as the *kernel function*, and  $\theta_\delta(\mathbf{x}, \mathbf{y})$  as a *constitutive function*.

**Remark 2.2.** *Scalar constitutive tensors.* The case of  $\boldsymbol{\Theta}_\delta(\mathbf{x}, \mathbf{y})$  being a scalar tensor (i.e., if  $\boldsymbol{\Theta}_\delta(\mathbf{x}, \mathbf{y}) = \theta_\delta(\mathbf{x}, \mathbf{y})\mathbf{I}$ , where  $\mathbf{I}$  denotes the identity tensor and  $\theta_\delta(\mathbf{x}, \mathbf{y})$  denotes a scalar-valued function) is by far the most common case considered, just as it is for a scalar diffusivity tensor  $\mathbf{D} = a(\mathbf{x})\mathbf{I}$  in the local PDE case. In this case, (2.18) becomes a tautology. Also, in this case, (1.17) simplifies to

$$\begin{aligned} \gamma_\delta(\mathbf{x}, \mathbf{y}) &= \theta_\delta(\mathbf{x}, \mathbf{y})\boldsymbol{\alpha}_\delta(\mathbf{x}, \mathbf{y}) \cdot \boldsymbol{\alpha}_\delta(\mathbf{x}, \mathbf{y})\mathcal{X}_{B_\delta(\mathbf{x})}(\mathbf{y}) \\ &= \theta_\delta(\mathbf{x}, \mathbf{y})|\boldsymbol{\alpha}_\delta(\mathbf{x}, \mathbf{y})|^2\mathcal{X}_{B_\delta(\mathbf{x})}(\mathbf{y}). \end{aligned} \quad \square$$

**Remark 2.3.** *Homogeneous and inhomogeneous nonlocal operators.* If  $\boldsymbol{\Theta}_\delta(\mathbf{x}, \mathbf{y}) = \boldsymbol{\Theta}_\delta(|\mathbf{y} - \mathbf{x}|)$  and  $\phi_\delta(\mathbf{x}, \mathbf{y}) = \phi_\delta(|\mathbf{y} - \mathbf{x}|)$ , i.e.,  $\boldsymbol{\Theta}_\delta$  and  $\phi_\delta$  are *radial functions*, then (1.5) is a model for a homogeneous medium. This is not surprising because  $\boldsymbol{\Theta}_\delta$  and  $\phi_\delta$  being radial functions means that the nature of the interaction between a point  $\mathbf{x}$  and another point  $\mathbf{y}$  is independent



of the location of the point  $\mathbf{x}$ ; that interaction only depends on the distance  $|\mathbf{y} - \mathbf{x}|$  between  $\mathbf{x}$  and  $\mathbf{y}$ . In this case, (1.5) is a nonlocal analog of the PDE  $-\nabla \cdot (\mathbf{D}\nabla u) = f$  in which  $\mathbf{D}$  is a constant tensor. If in addition  $\Theta_\delta$  is a scalar tensor, (1.5) is a nonlocal analog of the PDE  $-\kappa\Delta u = f$  in which  $\kappa$  is a constant. Thus, to obtain an inhomogeneous model, both  $\Theta_\delta(\mathbf{x}, \mathbf{y})$  and  $\phi_\delta(\mathbf{x}, \mathbf{y})$  cannot be radial functions. Note that  $\phi_\delta(\mathbf{x}, \mathbf{y})$  is indeed often chosen to be a radial function, in which case  $\Theta_\delta(\mathbf{x}, \mathbf{y})$  has to be non-radial for  $\mathcal{L}_\delta$  to be a inhomogeneous operator. It is important to note that a constant coefficient nonlocal problem does not mean that the kernel and constitutive functions are themselves constant functions; they merely need to be radial functions.  $\square$

### 2.2.1. A list of kernel functions in common use

Because  $\theta_\delta(\mathbf{x}, \mathbf{y})$  is a constitutive function which is not specific even within a single application, we focus on choices for the function  $\phi_\delta(\mathbf{x}, \mathbf{y})$  that determines generic properties of a model. However, we again note that because we have assumed that  $\Theta_\delta(\mathbf{x}, \mathbf{y})$  is a symmetric, positive definite tensor, it follows that  $\theta_\delta(\mathbf{x}, \mathbf{y})$  is a positive function for all  $\mathbf{x}, \mathbf{y} \in \Omega \cup \Omega_{\mathcal{I}_\delta}$ .

We also assume, as is usually the case, that for all  $\mathbf{x}, \mathbf{y} \in \Omega \cup \Omega_{\mathcal{I}_\delta}$ , the constitutive function  $\theta_\delta(\mathbf{x}, \mathbf{y})$  is bounded from above and below by constants whose values do not depend on  $\delta$ . In fact, often  $\theta_\delta(\mathbf{x}, \mathbf{y})$  does not depend on  $\delta$ . Thus we focus on a list of kernel functions  $\phi_\delta(\mathbf{x}, \mathbf{y})$ . In Table 2.1, we provide the energy spaces corresponding to the kernel functions we list.

General integrable kernel functions. The kernel function satisfies

$$\int_{\Omega \cup \Omega_{\mathcal{I}_\delta}} |\phi_\delta(\mathbf{x}, \mathbf{y})| d\mathbf{y} < \infty \quad \forall \mathbf{x} \in \Omega \cup \Omega_{\mathcal{I}_\delta}. \quad (2.19)$$

In the design of numerical methods, one may need to differentiate between cases for which

- $\phi_\delta(\mathbf{x}, \mathbf{y})$  is a smooth, bounded function of  $\mathbf{x}$  and  $\mathbf{y}$
- $\phi_\delta(\mathbf{x}, \mathbf{y})$  is a bounded function of  $\mathbf{x}$  and  $\mathbf{y}$  but is not smooth, e.g., a piecewise constant function
- $\phi_\delta(\mathbf{x}, \mathbf{y})$  is a singular but integrable function, e.g.,  $\phi_\delta(\mathbf{x}, \mathbf{y}) \propto 1/|\mathbf{y} - \mathbf{x}|^r$  with  $r < d$ .

“Critical” kernel functions. The kernel function satisfies

$$\phi_\delta(\mathbf{x}, \mathbf{y}) \propto \frac{1}{|\mathbf{y} - \mathbf{x}|^d}. \quad (2.20)$$

We refer to this kernel as *critical* because it “just misses being integrable,” i.e.,  $1/|\mathbf{y} - \mathbf{x}|^{d-\epsilon}$  is integrable for any  $\epsilon > 0$  and for any  $d$ , but is not integrable for any  $d$  if  $\epsilon = 0$ . For the other kernels in this list, the corresponding

energy space is precisely known; see Table 2.1. For critical kernels, that is not the case; what is known is that energy space is a Hilbert space and is a strict subspace of  $L^2(\Omega \cup \Omega_{\mathcal{I}_\delta})$ .

“Peridynamic” kernel functions. The kernel function satisfies

$$\phi_\delta(\mathbf{x}, \mathbf{y}) \propto \frac{1}{|\mathbf{y} - \mathbf{x}|}. \quad (2.21)$$

We refer to this kernel as *peridynamic* because it has the same singular behavior as one of the commonly used kernels in peridynamic models. Note that for  $d = 1$  this kernel function is a member of the critical class whereas for  $d = 2$ , it is integrable and for  $d = 3$  it is square integrable.

Fractional kernel functions. The kernel function satisfies

$$\phi_\delta(\mathbf{x}, \mathbf{y}) \propto \frac{1}{|\mathbf{y} - \mathbf{x}|^{d+2s}}. \quad (2.22)$$

We refer to this kernel as *fractional* because the singularity at  $\mathbf{y} = \mathbf{x}$  is that of the kernel for the fractional Laplace operator. This kernel plays a central role in Section 3.

type	definition	energy space $V(\Omega \cup \Omega_{\mathcal{I}_\delta})$
general integrable	(2.19)	$L^2(\Omega \cup \Omega_{\mathcal{I}_\delta})$
critical	(2.20)	$\subsetneq L^2(\Omega \cup \Omega_{\mathcal{I}_\delta})$
peridynamic	(2.21)	$L^2(\Omega \cup \Omega_{\mathcal{I}_\delta})$ for $d = 2, 3$
fractional	(2.22)	$H^s(\Omega \cup \Omega_{\mathcal{I}_\delta})$

Table 2.1. Kernel functions  $\phi_\delta(\mathbf{x}, \mathbf{y})$  and the corresponding energy spaces  $V(\Omega \cup \Omega_{\mathcal{I}_\delta})$ .

**Remark 2.4.** *Solution smoothness in nonlocal diffusion.* For integrable kernel functions such as the two listed in Table 2.1, the *solution is not smoother than the data*. For example, if  $g(\mathbf{x}) = 0$  and  $f(\mathbf{x}) \in L^2(\Omega)$ , then the solution  $u(\mathbf{x}) = (-\mathcal{L}_\delta)^{-1}f \in L^2(\Omega \cup \Omega_{\mathcal{I}_\delta})$ . Because  $L^2(\Omega)$  includes, e.g., functions with jump discontinuities, this means that if the data  $f(\mathbf{x})$  has a jump discontinuity, so will the solution  $u(\mathbf{x})$ . For the fractional kernel function, we could have  $2s$  derivatives of smoothing, i.e., if the data  $f(\mathbf{x}) \in H^{-s}(\Omega)$ , then  $u(\mathbf{x}) \in H^s(\Omega \cup \Omega_{\mathcal{I}_\delta})$ , where here  $H^s(\Omega \cup \Omega_{\mathcal{I}_\delta})$  denotes

a fractional Sobolev space and  $H^{-s}(\Omega)$  its dual space. Note that for  $s < \frac{1}{2}$ ,  $H^s(\Omega \cup \Omega_{\mathcal{I}_\delta})$  also contains functions having a jump discontinuity.  $\square$

**Remark 2.5.** *Boundedness and decay of kernels.* All the kernel functions listed above (and also many more) satisfy the requirement that there exists a  $0 < \delta_{inner} < \delta$  such that

$$\phi_\delta(\mathbf{x}, \mathbf{y}) \text{ is bounded for } \mathbf{y} \in B_\delta(\mathbf{x}) \setminus B_{\delta_{inner}}(\mathbf{x}),$$

i.e., away from the possible singular point  $\mathbf{y} = \mathbf{x}$ , the kernel functions are bounded so that, e.g., for  $\delta < \infty$ , the kernel functions are integrable over  $B_\delta(\mathbf{x}) \setminus B_{\delta_{inner}}(\mathbf{x})$ . If  $\delta = \infty$ , then, of course, any kernel function choice would be required to be integrable over  $\mathbb{R}^d \setminus B_{\delta_{inner}}(\mathbf{x})$ . For example, if  $\delta = \infty$ , this obviously rules out the use of constant kernel functions.  $\square$

**Remark 2.6.** *Scaling constants and limit behavior.* Often kernel functions take the form

$$\phi_\delta(\mathbf{x}, \mathbf{y}) = C\varphi(\mathbf{x}, \mathbf{y}),$$

where here  $C$  denotes a scaling constant that, depending on the specific instance, may depend on  $\delta$  and also on other parameters appearing in the definition of  $\phi_\delta(\mathbf{x}, \mathbf{y})$ . One approach towards defining the scaling constant  $C$  is to choose it so that in the limit  $\delta \rightarrow 0$ , a nonlocal model and its solution reduces to a local PDE model and its solution, respectively. Another approach is to choose  $C$  so that in the limit  $\delta \rightarrow \infty$ , the nonlocal model and its solution reduce to a well-known model that is posed on  $\mathbb{R}^d$ . In the sequel, we will have occasion to follow both the approaches. In any case, the scaling constant is a modeling choice so that, for example, if neither type of limiting behavior is of interest, then the scaling constant should be chosen based on the physics being modeled.  $\square$

### 3. Fractional diffusion models

In this section, we consider a widely used nonlocal diffusion model that involves the fractional Laplace operator  $-(-\Delta)^s$  with  $s \in (0, 1)$ . In a real sense, fractional diffusion models can be thought of as being a special case of the general nonlocal diffusion models discussed in Sections 1 and 2. After all, fractional diffusion models are defined in terms of a specific choice for the kernel function; see (2.22). On the other hand, the scope of fractional diffusion models and the literature devoted to their analysis, approximation, and application hugely dwarf what is available for other nonlocal diffusion models. Thus, here, a more detailed consideration of fractional models is warranted.

The *integral definition of the fractional Laplacian* is given by, for  $u(\mathbf{x})$  :

$\mathbb{R}^d \rightarrow \mathbb{R}^d$  with  $d \in \mathbb{N}_+$ ,

$$\begin{aligned} (-\Delta)^s u(\mathbf{x}) &= \int_{\mathbb{R}^d} \left( u(\mathbf{x}) - u(\mathbf{y}) \right) \gamma_s(\mathbf{x}, \mathbf{y}) d\mathbf{y} \quad \forall \mathbf{x} \in \mathbb{R}^d \\ \text{with } \gamma_s(\mathbf{x}, \mathbf{y}) &= \frac{C_{d,s}}{|\mathbf{y} - \mathbf{x}|^{d+2s}}. \end{aligned} \quad (3.1)$$

Note that this is one case in which the integral in (3.1) should be interpreted in the principal-value sense. In (3.1),  $C_{d,s}$  is a normalization constant given by

$$C_{d,s} = \frac{2^{2s} s \Gamma\left(s + \frac{d}{2}\right)}{\pi^{d/2} \Gamma(1-s)}, \quad (3.2)$$

where  $\Gamma$  denotes the Gamma function.

The integral representation of the fractional Laplacian given in (3.1) can be viewed as a special case of the nonlocal Laplacian given by (1.6). It is also equivalent to and can be directly derived from the Fourier representation (Valdinoci 2009)

$$\begin{aligned} (-\Delta)^s u(\mathbf{x}) &= \frac{1}{(2\pi)^d} \int_{\mathbb{R}^d} |\boldsymbol{\xi}|^{2s} (u, e^{-i\boldsymbol{\xi} \cdot \mathbf{x}}) e^{i\boldsymbol{\xi} \cdot \mathbf{x}} d\boldsymbol{\xi} \\ &= \mathcal{F}^{-1} \left( |\boldsymbol{\xi}|^{2s} \mathcal{F}\{u\}(\boldsymbol{\xi}) \right) (\mathbf{x}). \end{aligned} \quad (3.3)$$

where  $\mathcal{F}$  denotes the Fourier transform. If  $s = 1$ , the spectral operator (3.3) coincides with the usual PDE Laplacian  $-\Delta$ , whereas it reproduces the identity operator when  $s = 0$ . In fact, it is well-known that  $(-\Delta)^s u(x) \rightarrow u(x)$  as  $s \rightarrow 0^+$  and  $(-\Delta)^s u(x) \rightarrow -\Delta u(x)$  as  $s \rightarrow 1^-$  for a regular function  $u$ ; see, e.g., (Stinga 2019, Theorems 3 and 4) and (Di Nezza, Palatucci and Valdinoci 2012, Proposition 4.4).

The fractional Laplacian (3.1) is often used to model superdiffusion for which the mean-squared particle displacement grows faster than that for PDE models of diffusion. At microscopic scales, in contrast to standard diffusion that is described by Brownian motion, superdiffusion can be described by Lévy flights in which the length of particle jumps follows a heavy tailed distribution, reflecting the long-range interactions between particles. See, e.g., (Metzler and Klafter 2000, Sokolov, Klafter and Blumen 2002) for discussions of the physical background and practical applications of anomalous diffusion.

### 3.1. Integral fractional Laplacian models for diffusion on bounded domains

Letting  $\Omega \subset \mathbb{R}^d$  denote a bounded Lipschitz domain, we define the *integral fractional Laplacian*  $-(-\Delta)^s$  to be the restriction of the full-space operator to functions satisfying a volume constraint on  $\Omega_{\mathcal{I}\infty} := \mathbb{R}^d \setminus \Omega$ , i.e., on the interaction domain corresponding to  $\Omega$ . The *fractional Poisson problem* is

then given by

$$\begin{cases} (-\Delta)^s u = f & \forall \mathbf{x} \in \Omega \\ u = g & \forall \mathbf{x} \in \Omega_{\mathcal{I}_\infty}, \end{cases} \quad (3.4)$$

where we have a given source term  $f(\mathbf{x})$  and Dirichlet volume constraint data  $g(\mathbf{x})$  defined for  $\mathbf{x} \in \Omega$  and  $\mathbf{x} \in \Omega_{\mathcal{I}_\infty}$ , respectively. The problem (3.4) is a nonlocal analog of the local Poisson problem for the PDE Laplacian  $\Delta$ . It is known (see, e.g., (Biccarri and Hernández-Santamaría 2018)) that as  $s \rightarrow 1^-$ , the solution of integral fractional diffusion model (3.4) strongly converges to the solution of the local diffusion problem in  $H^{1-\epsilon}(\Omega)$ .

A related operator on  $\Omega$  is the *regional fractional Laplacian* (Bogdan, Burdzy and Chen 2003, Chen and Kim 2002)

$$-(-\Delta)_{\text{regional}}^s u(\mathbf{x}) = C_{d,s} \int_{\Omega} \frac{u(\mathbf{y}) - u(\mathbf{x})}{|\mathbf{y} - \mathbf{x}|^{d+2s}} d\mathbf{y} \quad (3.5)$$

that is used in one of several approaches for generalizing the PDE Poisson problem with a homogeneous Neumann boundary condition to the fractional Laplacian case (Dipierro, Ros-Oton and Valdinoci 2017). Note that in (3.4) the operator has not changed, i.e., the operator defined in (3.1) is used; what has changed is that domain of the operator is changed from  $\mathbb{R}^d$  to the bounded domain  $\Omega$ . On the other hand, in using the operator in (3.5), not only is the domain changed in the same manner, but the operator itself has changed, i.e., (3.1) involves an integral over  $\mathbb{R}^d$  whereas (3.5) involves an integral over  $\Omega$ .

To discuss the variational form of the fractional Poisson problem (3.4), we use the standard fractional Sobolev space  $H^s(\mathbb{R}^d)$  defined via the Fourier transform as

$$H^s(\mathbb{R}^d) = \left\{ u \in L^2(\mathbb{R}^d) : \int_{\mathbb{R}^d} (1 + |\boldsymbol{\xi}|^{2s}) |\mathcal{F}u(\boldsymbol{\xi})|^2 d\boldsymbol{\xi} < \infty \right\}.$$

If  $\Omega \subset \mathbb{R}^d$  is a bounded domain, we define the Sobolev space  $H^s(\Omega)$  as (McLean 2000)

$$H^s(\Omega) := \{ u \in L^2(\Omega) : \|u\|_{H^s(\Omega)} < \infty \}$$

equipped with the norm

$$\|u\|_{H^s(\Omega)}^2 = |u|_{H^s(\Omega)}^2 + \|u\|_{L^2(\Omega)}^2,$$

where we have the seminorm

$$|u|_{H^s(\Omega)}^2 = \int_{\Omega} \int_{\Omega} \frac{(u(\mathbf{y}) - u(\mathbf{x}))^2}{|\mathbf{y} - \mathbf{x}|^{d+2s}} d\mathbf{y} d\mathbf{x}.$$

Moreover, when imposing a homogeneous Dirichlet volume constraints, e.g.,

$g = 0$  in (3.4), we use the space

$$H_c^s(\Omega) := \{u \in H^s(\mathbb{R}^d) : u = 0 \quad \forall \mathbf{x} \in \Omega_{\mathcal{I}_\infty}\}$$

that is equipped with the norm

$$\|u\|_{H_c^s(\Omega)}^2 = \|u\|_{H^s(\mathbb{R}^d)}^2 = \|u\|_{L^2(\Omega)}^2 + \|u\|_{H^s(\mathbb{R}^d)}^2.$$

For  $s > 1/2$ ,  $H_c^s(\Omega)$  coincides with the space  $H_0^s(\Omega)$  that is the closure of  $C_0^\infty(\Omega)$  with respect to the  $H^s(\Omega)$ -norm, whereas for  $s < 1/2$ ,  $H_c^s(\Omega)$  is identical to  $H^s(\Omega)$ . In the critical case  $s = 1/2$ ,  $H_c^s(\Omega) \subsetneq H_0^s(\Omega)$ . See, e.g., (McLean 2000, Chapter 3) for a detailed discussion.

A variational form of (3.4) is derived starting from the integration by parts formula (see (Dipierro et al. 2017) and also the nonlocal Green's first identity (1.22))

$$\begin{aligned} & \frac{1}{2} \int_{\Omega} \int_{\Omega} (u(\mathbf{y}) - u(\mathbf{x}))(v(\mathbf{y}) - v(\mathbf{x})) \gamma_s(\mathbf{x}, \mathbf{y}) d\mathbf{y} d\mathbf{x} \\ &= \int_{\Omega} ((-\Delta)^s u(\mathbf{x})) v(\mathbf{x}) d\mathbf{x} + \int_{\Omega_{\mathcal{I}_\infty}} (\mathcal{N}_s u(\mathbf{x})) v(\mathbf{x}) d\mathbf{x}, \end{aligned}$$

where, as in (1.12), we have the nonlocal Neumann operator given by

$$\mathcal{N}_s u(\mathbf{x}) = \int_{\Omega} (u(\mathbf{x}) - u(\mathbf{y})) \gamma_s(\mathbf{x}, \mathbf{y}) d\mathbf{y} \quad \forall \mathbf{x} \in \Omega_{\mathcal{I}_\infty}.$$

Substituting the volume constraint in (3.4) and  $v(\mathbf{x}) = 0$  on  $\Omega_{\mathcal{I}_\infty}$ , we then have the weak formulation

$$\begin{aligned} & \text{find } u(\mathbf{x}) \in H^s(\Omega) \text{ such that } u(\mathbf{x}) = g(\mathbf{x}) \quad \forall \mathbf{x} \in \Omega_{\mathcal{I}_\infty} \text{ and} \\ & \mathcal{A}_s(u, v) = \langle f, v \rangle - (g, v)_{\Omega_{\mathcal{I}_\infty}} \quad \forall v \in H_c^s(\Omega), \end{aligned} \tag{3.6}$$

where

$$\begin{aligned} \mathcal{A}_s(u, v) = & \underbrace{\frac{1}{2} \int_{\Omega} \int_{\Omega} (u(\mathbf{y}) - u(\mathbf{x}))(v(\mathbf{y}) - v(\mathbf{x})) \gamma_s(\mathbf{x}, \mathbf{y}) d\mathbf{y} d\mathbf{x}}_{\mathcal{A}_{\Omega, \Omega}(u, v)} \\ & + \underbrace{\int_{\Omega} u(\mathbf{x}) v(\mathbf{x}) \int_{\Omega_{\mathcal{I}_\infty}} \gamma_s(\mathbf{x}, \mathbf{y}) d\mathbf{y} d\mathbf{x}}_{\mathcal{A}_{\Omega, \Omega_{\mathcal{I}_\infty}}(u, v)} \end{aligned}$$

and

$$(g, v)_{\Omega, \Omega_{\mathcal{I}_\infty}} = \int_{\Omega} v(\mathbf{x}) \int_{\Omega_{\mathcal{I}_\infty}} g(\mathbf{y}) \gamma_s(\mathbf{x}, \mathbf{y}) d\mathbf{y} d\mathbf{x}. \tag{3.7}$$

The bilinear form  $\mathcal{A}_s(\cdot, \cdot)$  is  $H_c^s(\Omega)$ -coercive and continuous so that as long as the right-hand side of (3.6) is bounded, the well posedness of that problem

follows from the Lax-Milgram theorem. Note that the bilinear form  $\mathcal{A}_\Omega(\cdot, \cdot)$  can be seen to correspond to the regional fractional Laplacian.

Note that

$$\mathcal{A}_{\Omega, \Omega_{\mathcal{I}_\infty}}(u, v) = C_{d,s} \int_{\Omega} u(\mathbf{x})v(\mathbf{x}) \left( \int_{\Omega_{\mathcal{I}_\infty}} \frac{1}{|\mathbf{y} - \mathbf{x}|^{d+2s}} d\mathbf{y} \right) d\mathbf{x}.$$

The identity

$$\frac{1}{|\mathbf{y} - \mathbf{x}|^{d+2s}} = \frac{1}{2s} \nabla_{\mathbf{y}} \cdot \frac{\mathbf{y} - \mathbf{x}}{|\mathbf{y} - \mathbf{x}|^{d+2s}}$$

and Gauss' theorem results in

$$\mathcal{A}_{\Omega, \Omega_{\mathcal{I}_\infty}}(u, v) = \frac{C_{d,s}}{2s} \int_{\Omega} u(\mathbf{x})v(\mathbf{x}) \left( \int_{\partial\Omega} \frac{(\mathbf{y} - \mathbf{x}) \cdot \mathbf{n}_{\mathbf{y}}}{|\mathbf{y} - \mathbf{x}|^{d+2s}} d\mathbf{y} \right) d\mathbf{x},$$

where  $\mathbf{n}_{\mathbf{y}}$  denotes the unit outer normal to  $\partial\Omega$  at  $\mathbf{y}$ . We then have that

$$\mathcal{A}_s(u, v) = \mathcal{A}_{\Omega}(u, v) + \frac{C_{d,s}}{2s} \int_{\Omega} u(\mathbf{x})v(\mathbf{x}) \left( \int_{\partial\Omega} \frac{(\mathbf{y} - \mathbf{x}) \cdot \mathbf{n}_{\mathbf{y}}}{|\mathbf{y} - \mathbf{x}|^{d+2s}} d\mathbf{y} \right) d\mathbf{x} \quad (3.8)$$

so that an integral over the unbounded domain  $\Omega_{\mathcal{I}_\infty}$  can be avoided in any computation involving  $\mathcal{A}_s(u, v)$ . Of course, for a homogeneous volume constraint  $g(\mathbf{x}) = 0$  on  $\Omega_{\mathcal{I}_\infty}$ , the right-hand side in (3.6) also only involves integrals over  $\Omega$ . For  $g(\mathbf{x}) \neq 0$ , one does have to evaluate, for  $\mathbf{x} \in \Omega$ , the *data integral*  $\int_{\Omega_{\mathcal{I}_\infty}} g(\mathbf{y})\gamma_s(\mathbf{x}, \mathbf{y})d\mathbf{y}$  that, in principle, can be approximated using a quadrature rule.

Above we have incorporated the inhomogeneous volume constraint directly into the weak form. An alternative is to enforce that condition via Lagrange multipliers (Acosta, Borthagaray and Heuer 2019).

### 3.1.1. Truncated interaction domains

An alternative to the approach based on the bilinear form (3.8) is to *truncate the integration domain*  $\Omega_{\mathcal{I}_\infty}$  as is considered in (D'Elia and Gunzburger 2013). For  $\delta > \text{diam}(\Omega)$ , we pose the truncated problem

$$\begin{cases} (-\Delta)_\delta^s u = f & \forall \mathbf{x} \in \Omega \\ u = g & \forall \mathbf{x} \in \Omega_{\mathcal{I}_\delta}, \end{cases} \quad (3.9)$$

where

$$(-\Delta)_\delta^s u(\mathbf{x}) := \int_{\Omega \cup \Omega_{\mathcal{I}_\delta}} (u(\mathbf{x}) - u(\mathbf{y}))\gamma_s(\mathbf{x}, \mathbf{y}) d\mathbf{y}.$$

It is shown in (D'Elia and Gunzburger 2013, Burkovska and Gunzburger 2019b) that if  $u_\infty$  and  $u_\delta$  denote the solutions of (3.4) and (3.9), respectively, then

$$\|u_\delta - u_\infty\|_{H^s(\Omega)} \leq \frac{C}{\delta^{2s}} \quad \text{as } \delta \rightarrow \infty, \quad (3.10)$$

where  $C$  depends on norms of  $f$  and  $g$

**Remark 3.1.** Clearly, (3.10) implies that the solution of (3.9) can be viewed as an approximation of the solution of (3.4). However, (3.9) and its solution are useful in their own right. In (3.4), the horizon  $\delta$  is infinite, but, in practice, although  $\delta$  may be large, it is not likely to be infinite. In (3.9),  $\delta$  is assumed large but finite so that it may provide a better model for practical applications that feature large horizons. In this case, one can reverse roles and interpret the solution of (3.4) to be an approximation of the solution of (3.9), with now (3.10) telling us something about the error incurred by replacing the perhaps more useful model (3.9) by the much more studied model (3.4).  $\square$

### 3.2. Spectral fractional Laplacian models for diffusion on bounded domains

An alternate definition of a fractional-order Laplacian on a bounded domain  $\Omega$  makes use of spectral information about the PDE Laplacian. Here, we focus on the case of homogeneous constraints.

Let  $0 < \lambda_0 \leq \lambda_1 \leq \dots$  and  $\varphi_0, \varphi_1, \dots$  denote the eigenvalues and the corresponding eigenfunctions of the PDE Laplacian  $-\Delta$  with a homogeneous Dirichlet *boundary* condition, i.e., we have

$$\begin{cases} -\Delta \varphi_m(\mathbf{x}) = \lambda_m \varphi_m(\mathbf{x}) & \forall \mathbf{x} \in \Omega \\ \varphi_m(\mathbf{x}) = 0, & \forall \mathbf{x} \in \partial\Omega, \end{cases} \quad (3.11)$$

where the orthogonal eigenfunctions are normalized so that  $\|\varphi_m\|_{L^2(\Omega)} = 1$ . Then the eigenfunctions  $\{\varphi_m\}_{m=0}^\infty$  form a complete orthonormal basis for  $L^2(\Omega)$ . As a result, any function  $u \in L^2(\Omega)$  can be expanded as

$$u = \sum_{m=0}^{\infty} u_m \varphi_m \quad \text{with} \quad u_m = (u, \varphi_m),$$

where  $(\cdot, \cdot)$  denotes the inner product of  $L^2(\Omega)$ . We then have

$$(-\Delta)u(\mathbf{x}) = \sum_{m=0}^{\infty} u_m \lambda_m^2 \varphi_m(\mathbf{x})$$

and the *spectral fractional Laplacian* of order  $s \in (0, 1)$  with homogeneous boundary condition is given by

$$(-\Delta|_{\Omega,0})^s u(\mathbf{x}) = \sum_{m=0}^{\infty} u_m \lambda_m^s \varphi_m(\mathbf{x}).$$

As  $s \rightarrow 0$ , the identity operator is recovered, whereas the integer order Laplacian is recovered as  $s \rightarrow 1$ .



For a given source term  $f$ , the spectral fractional Laplacian Poisson problem for  $u(\mathbf{x})$ ,  $\mathbf{x} \in \Omega$ , is then given by

$$(-\Delta|_{\Omega,0})^s u(\mathbf{x}) = f(\mathbf{x}) \quad \forall \mathbf{x} \in \Omega. \quad (3.12)$$

Using the heat kernel  $p_{\Omega,0}(\mathbf{x}, \mathbf{y}, t)$ , the spectral fractional Laplacian can be rewritten (see, e.g., (Abatangelo and Dupaigne 2017)) in the form of the nonlocal operator

$$(-\Delta|_{\Omega,0})^s u(\mathbf{x}) = \int_{\Omega} \gamma_{\Omega,0;s}(\mathbf{x}, \mathbf{y}) (u(\mathbf{y}) - u(\mathbf{x})) d\mathbf{y} + \kappa_{\Omega,0;s}(\mathbf{x}) u(\mathbf{x}),$$

where

$$\begin{aligned} \gamma_{\Omega,0;s}(\mathbf{x}, \mathbf{y}) &= \frac{s}{\Gamma(1-s)} \int_0^\infty p_{\Omega,0}(t, \mathbf{x}, \mathbf{y}) \frac{1}{t^{1+s}} dt \\ \kappa_{\Omega,0;s}(\mathbf{x}) &= \frac{s}{\Gamma(1-s)} \int_0^\infty \left( 1 - \int_{\Omega} p_{\Omega,0}(t, \mathbf{x}, \mathbf{y}) d\mathbf{y} \right) \frac{1}{t^{1+s}} dt. \end{aligned}$$

If  $\Omega = \mathbb{R}^d$ , the integral and the spectral definitions of the fractional Laplacian coincide, but they are different for bounded domains (Servadei and Valdinoci 2014). For example, in the particular case of  $\Omega = \mathbb{R}_+^d$ , i.e., the half-plane, the kernel of the spectral fractional Laplacian is given by

$$\gamma_{\mathbb{R}_+^d,0;s}(\mathbf{x}, \mathbf{y}) = \gamma_s(\mathbf{x}, \mathbf{y}) - \gamma_s(\mathbf{x}, -\mathbf{x}) \neq \gamma_s(\mathbf{x}, \mathbf{y}) \quad \forall \mathbf{x}, \mathbf{y} \in \mathbb{R}_+^d.$$

Note that the spectral definition can allow for the treatment of non-homogeneous boundary conditions of various types; see, e.g., (Antil, Pfefferer and Rogovs 2018, Cusimano, del Teso, Gerardo-Giorda and Pagnini 2018).

### 3.3. Additional considerations about fractional Laplacian models

#### 3.3.1. Other integral representations of the fractional Laplacian

The *Dunford-Taylor integral* is a powerful tool in the numerical analysis of the fractional diffusion problem (Bonito and Pasciak 2015, Bonito and Pasciak 2017, Bonito, Lei and Pasciak 2019). In particular, the solution  $u$  of the Poisson problem (3.12) involving the spectral fractional Laplacian can be given the Dunford-Taylor representation

$$u = (-\Delta|_{\Omega,0})^s f = \frac{\sin(s\pi)}{\pi} \int_0^\infty \mu^{-s} (\mu - \Delta)^{-1} f d\mu.$$

A combination of using a sinc quadrature rule and a finite-element discretization of the reaction-diffusion-type term in the integrand was explored in (Bonito and Pasciak 2015, Bonito and Pasciak 2017).

Using similar techniques, the bilinear form  $\mathcal{A}_s(\cdot, \cdot)$  associated with the

integral fractional Laplacian can be rewritten as (Bonito et al. 2019)

$$\mathcal{A}_s(u, v) = \frac{2 \sin(s\pi)}{\pi} \int_0^\infty \int_\Omega ((-\Delta)(I - \mu^2 \Delta)^{-1} u(\mathbf{x})) v(\mathbf{x}) d\mathbf{x} d\mu. \quad (3.13)$$

### 3.3.2. Extension representations

An *extension representation* of the fractional Laplacian was introduced in (Molčanov and Ostrovskii 1969) and popularized by (Caffarelli and Silvestre 2007), where it is shown that the fractional Poisson problem (3.4) posed on  $\mathbb{R}^d$  can be recast as a Neumann-to-Dirichlet mapping over the extended domain  $\mathbb{R}^d \times [0, \infty)$ , i.e., we have

$$\begin{cases} -\nabla \cdot z^\beta \nabla U(\mathbf{x}, z) = 0 & \forall (\mathbf{x}, z) \in \mathbb{R}^d \times [0, \infty) \\ \frac{\partial U}{\partial \nu^\beta}(\mathbf{x}) = 2^{1-2s} \frac{\Gamma(1-s)}{\Gamma(s)} f(\mathbf{x}) & \forall \mathbf{x} \in \mathbb{R}^d, \end{cases} \quad (3.14)$$

where  $\beta = 1 - 2s$  and

$$\frac{\partial U}{\partial \nu^\beta}(\mathbf{x}) = - \lim_{y \rightarrow 0^+} z^\beta \frac{\partial U}{\partial z}(\mathbf{x}, y),$$

with the solution to (3.4) recovered by taking the trace of  $U$  on  $\mathbb{R}^d$ .

The spectral fractional Laplacian can be recovered, by restricting the extension domain from  $\mathbb{R}^d \times [0, \infty)$  to  $\Omega \times [0, \infty)$  and imposing a homogeneous Dirichlet boundary condition on the lateral surface (Stinga and Torrea 2010).

The apparent advantage of extension problem is that the nonlocal problem is replaced by a classical, integer-order local problem. This comes at the price of having to deal with a singular weight function and an additional spatial dimension.

### 3.3.3. Regularity of solutions

In the classical integer-order case, smoother domains and smoother right-hand sides result in smoother solutions of the Poisson problem; see, e.g. (?). A lifting property of this type does not hold for the fractional-order Poisson problems (3.4) and (3.12). The typical solution behavior of (3.4) close to the boundary can be characterized (see (Ros-Oton and Serra 2014)) as

$$u(\mathbf{x}) \approx \text{dist}(\mathbf{x}, \partial\Omega)^s. \quad (3.15)$$

The Sobolev regularity of the solution of (3.4) was studied in (Acosta, Bersetche and Borthagaray 2017) as a special case of a result in (Grubb 2015a). Suppose that  $\partial\Omega \in C^\infty$  and  $f \in H^r(\Omega)$  for  $r \geq -s$  and let  $u \in H_c^s(\Omega)$  denote the solution of the fractional Poisson problem (3.6). Then the regularity estimate

$$u \in \begin{cases} H^{2s+r}(\Omega) & \text{if } 0 < s+r < 1/2 \\ H^{s+1/2-\varepsilon}(\Omega) & \forall \varepsilon > 0 \text{ if } 1/2 \leq s+r \end{cases}$$

holds.

This result is extended to the case of non-homogeneous volume condition in (Acosta et al. 2019). Additional regularity results with respect to  $s$  and, for the truncated fractional Laplacian, with respect to  $\delta$ , are derived in (Burkovska and Gunzburger 2019b).

The solution of the spectral fractional Poisson problem (3.12) displays different properties. Its behavior close to the boundary is given by (see (Caffarelli and Stinga 2016))

$$u(\mathbf{x}) \approx \text{dist}(\mathbf{x}, \partial\Omega)^{\min\{2s, 1\}}, \quad s \neq 1/2.$$

It is shown in (Grubb 2015b) that if  $f \in H_c^r(\Omega)$ ,  $r \geq -s$ , then the weak solution of the spectral fractional Poisson problem (3.12) satisfies  $u \in H_c^{r+2s}(\Omega)$ .

More detailed regularity results for the spectral fractional Laplacian can be found in (Grubb 2015b).

### 3.3.4. Analytic solutions in one and two dimensions

Closed-form solutions of the fractional Poisson problem (3.4) posed on the unit ball are available; see (Dyda, Kuznetsov and Kwaśnicki 2016) for detailed derivations. These solutions are useful to have in hand, e.g., for verifying numerical results.

In  $d = 1$  dimension, for the source term

$$f_{k,0}^{1D} = 2^{2s} \Gamma(1+s)^2 \binom{s+k-1/2}{s} \binom{s+k}{s} P_k^{(s,-1/2)}(2x^2-1)$$

with  $k \geq 0$ , the solution is given by

$$u_{k,0}^{1D} = P_k^{(s,-1/2)}(2x^2-1) (1-x^2)_+^s,$$

where  $\binom{a}{b} = \frac{\Gamma(a+1)}{\Gamma(b+1)\Gamma(a-b+1)}$  denotes a generalized binomial coefficient,  $P_k^{(a,b)}$  denote the Jacobi polynomials, and  $a_+ = \max\{0, a\}$ . Moreover, for

$$f_{k,1}^{1D} = 2^{2s} \Gamma(1+s)^2 \binom{s+k+1/2}{s} \binom{s+k}{s} x P_k^{(s,1/2)}(2x^2-1)$$

with  $k \geq 0$ , the solution is given by

$$u_{k,1}^{1D} = x P_k^{(s,1/2)}(2x^2-1) (1-x^2)_+^s.$$

Turning to  $d = 2$  dimensions, for

$$f_{k,\ell}^{2D} = 2^{2s} \Gamma(1+s)^2 \binom{s+k+\ell}{s} \binom{s+k}{s} r^\ell \cos(\ell\varphi) P_k^{(s,\ell)}(2r^2-1)$$

with  $\ell, k \geq 0$  and  $(r, \varphi)$  denoting polar coordinates, the solution is given by

$$u_{k,\ell}^{2D} = r^\ell \cos(\ell\varphi) P_k^{(s,\ell)}(2r^2-1) (1-r^2)_+^s,$$

Two example solutions are shown in Figure 3.1. Observe that the solutions contains a term which behaves like  $\delta(\mathbf{x})^s$ , where  $\delta(\mathbf{x})$  is the distance from  $\mathbf{x} \in \Omega$  to the boundary.

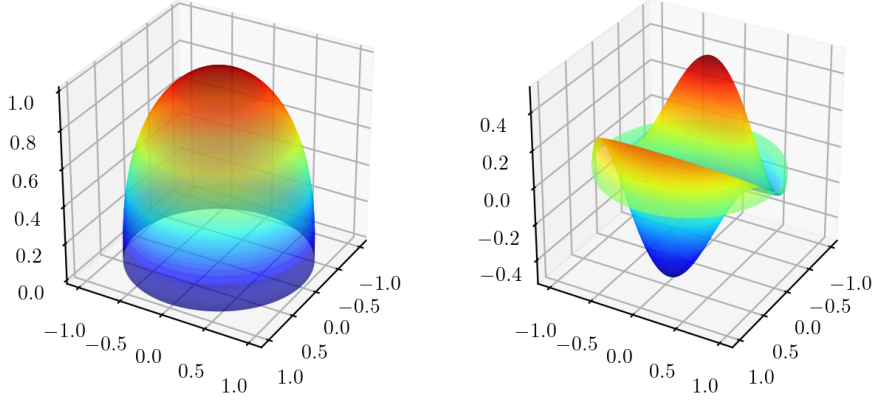


Figure 3.1. Analytic solutions  $u_{0,0}^{2D}$  for  $s = 0.4$  and  $u_{1,1}^{2D}$  for  $s = 0.6$ . The behavior (3.15) close to the boundary is apparent.

### 3.4. Inhomogeneous constitutive functions in fractional models

So far, in all of this section, only the fractional Laplacian and the various variants introduced have been considered which is analogous to considering local diffusion problems having a diffusivity that is not only constant, but is equal to one. Of course, in the local case, it is an easy matter to treat inhomogeneous diffusivities, i.e., one merely replaces  $\Delta u$  by  $\nabla \cdot (\mathbf{D} \nabla u)$ , where  $\mathbf{D}(\mathbf{x})$ , in general, denotes a inhomogeneous constitutive tensor. Using the nonlocal vector calculus, it is almost as easy to define integral fractional models in which the constitutive properties of the media considered are inhomogeneous, even if the nonlocal constitutive function is a tensor. Here, we only consider generalizations of the integral fractional Laplacian (3.1); generalizations of the other integral operators discussed in this section follow immediately from that for (3.1).

The inhomogeneous fractional Laplacian is simply defined by choosing the kernel in (3.1) to now be

$$\gamma_s(\mathbf{x}, \mathbf{y}) = C_{d,s} \frac{\theta_s(\mathbf{x}, \mathbf{y})}{|\mathbf{y} - \mathbf{x}|^{d+2s}} \quad \forall \mathbf{x}, \mathbf{y} \in \mathbb{R}^d, \quad (3.16)$$

where

$$\theta_s(\mathbf{x}, \mathbf{y}) := \frac{\mathbf{y} - \mathbf{x}}{|\mathbf{y} - \mathbf{x}|} \cdot \left( \Theta_s(\mathbf{x}, \mathbf{y}) \frac{\mathbf{y} - \mathbf{x}}{|\mathbf{y} - \mathbf{x}|} \right) \quad (3.17)$$

with  $\Theta_s(\mathbf{x}, \mathbf{y})$  denoting a constitutive tensor. Thus, we have defined the *inhomogeneous integral fractional Poisson operator*

$$(-\Delta)_{\Theta_s}^s u(\mathbf{x}) := \int_{\mathbb{R}^d} C_{d,s} \theta_s(\mathbf{x}, \mathbf{y}) \frac{u(\mathbf{x}) - u(\mathbf{y})}{|\mathbf{y} - \mathbf{x}|^{d+2s}} d\mathbf{y} \quad \forall \mathbf{x} \in \mathbb{R}^d. \quad (3.18)$$

Note that we could have arrived to (3.18) by defining

$$(-\Delta)_{\Theta_s}^s u(\mathbf{x}) := \mathcal{D}_s(\Theta_s \mathcal{D}_s^* u),$$

where  $\mathcal{D}_s$  and  $\mathcal{D}_s^*$  are defined by (1.13) and (1.15), respectively, with

$$\alpha_s(\mathbf{x}, \mathbf{y}) = \frac{\mathbf{y} - \mathbf{x}}{|\mathbf{y} - \mathbf{x}|} \sqrt{\frac{C_{d,s}}{|\mathbf{y} - \mathbf{x}|^{d+2s}}}. \quad (3.19)$$

If  $\Theta_s(\mathbf{x}, \mathbf{y}) = \Theta_s(|\mathbf{y} - \mathbf{x}|)$ , i.e.,  $\Theta_s$  is a *radial function*, then (3.1) is a model for a homogeneous medium, i.e., in this case, (3.1) is a fractional analog of the PDE  $-\nabla \cdot (\mathbf{D} \nabla u) = f$  in which  $\mathbf{D}$  is a constant tensor. If in addition  $\Theta_s$  is a scalar tensor, (3.1) is a fractional analog of the PDE  $-\kappa \Delta u = f$  in which  $\kappa$  is a constant. Thus, to obtain an inhomogeneous integral fractional model,  $\Theta_s(\mathbf{x}, \mathbf{y})$  cannot be a radial function. See Remark 2.3.

## PART TWO

### Numerical methods for nonlocal and fractional models

In this part, we consider the approximation, via finite element, finite difference, and spectral methods, of solutions of both weak and strong formulations of both nonlocal and fractional diffusion models. In so doing, we encounter, as we did in Part 1, problems posed on  $\mathbb{R}^d$  or on bounded domains  $\Omega \subset \mathbb{R}^d$  and also encounter problems for which the horizon  $\delta = \infty$  or  $\text{diam}(\Omega) < \delta < \infty$  or  $\delta < \text{diam}(\Omega)$ .

#### 4. Introductory remarks

In most cases we consider, two parameters will appear in the design of discretization algorithms, namely the horizon  $\delta$  and a discretization parameter such as a grid size parameter  $h$  for finite element and finite difference methods or the dimension  $N$  of a basis for spectral methods. The limiting behaviors of continuous and discretized models are thus of interest. Four types of limits can arise: for continuous, i.e., un-discretized, models,

- the limits  $\delta \rightarrow 0$  and  $\delta \rightarrow \infty$

and for discretized problems

- for fixed  $\delta$ , the limit  $h \rightarrow 0$  or  $N \rightarrow \infty$
- for fixed  $h$  or  $N$ , the limits  $\delta \rightarrow 0$  and  $\delta \rightarrow \infty$

- simultaneous limits such as both  $\delta \rightarrow 0$  and  $h \rightarrow 0$ .

For the second of these, one must be cognizant of how the constants appearing in error estimates depend on  $\delta$ , whereas for the third, the same can be said for the dependence of constants on  $h$  or  $N$ .

It turns out that for some algorithms, the order in which limits are taken matters, i.e., the limits obtained are different if the limits are taken in a different order, e.g.,  $\delta \rightarrow 0$  and then  $h \rightarrow 0$ , or  $h \rightarrow 0$  and then  $\delta \rightarrow 0$ , or if  $\delta$  and  $h$  are related in some way so that they simultaneously tend to zero. Presumably, at least one of the limits is “wrong” in some sense. Ideally, unless one is totally uninterested in limiting behaviors, one would like for the way in which limits are taken to not affect the limit obtained. In the remainder of our introductory remarks, we expand on this concept.

#### 4.1. Asymptotically compatible schemes

It is known in practice that to obtain consistency between nonlocal models and corresponding local PDE models, the mesh or quadrature point spacing may have to be reduced at a faster pace than the reduction of the horizon parameter (Bobaru, Yang, Alves, Silling, Askari and Xu 2009, Bobaru and Duangpanya 2010, Chen and Gunzburger 2011). Otherwise, there could potentially be complications, most notably inconsistent limiting solutions when the horizon parameter is coupled proportionally to the discretization parameter (Tian 2017, Tian and Du 2013, Tian and Du 2014, Tian and Du 2020). *Asymptotically compatible* (AC) schemes, motivated by the findings in (Tian and Du 2013) and formally introduced in (Tian and Du 2014), are numerical discretizations of nonlocal models that converge to nonlocal continuum models for a fixed horizon parameter and to the local discrete schemes as the horizon vanishes for both discrete schemes with a fixed numerical resolution and for continuum models with increasing numerical resolution.

Let  $h > 0$  denote a grid-size parameter (or particle spacing) and  $\delta$  denote the horizon parameter or even a more generic model parameter. Instead of  $h$ , we could use the dimension  $N$  of a spectral basis. The implications of the AC property are illustrated in Figure 4.1. There,  $u_\delta$  denotes the solution of the continuous nonlocal problem with  $\delta > 0$ ,  $u_0$  the solution of the corresponding continuous local problem,  $u_{\delta,h}$  the solution of the discretized nonlocal problem, and  $u_{0,h}$  the solution of the discretized local problem. Figure 4.1 is meant to illustrate the basic property of AC schemes, namely that for such schemes it does not matter in which order the limits are taken, or even if  $\delta$  and  $h$  are related in some way so that they simultaneously tend to zero.

Note that figures similar to Figure 4.1 can be drawn for  $N \rightarrow \infty$  and/or  $\delta \rightarrow \infty$ .

As seen from detailed studies given in (Tian and Du 2013), some popular

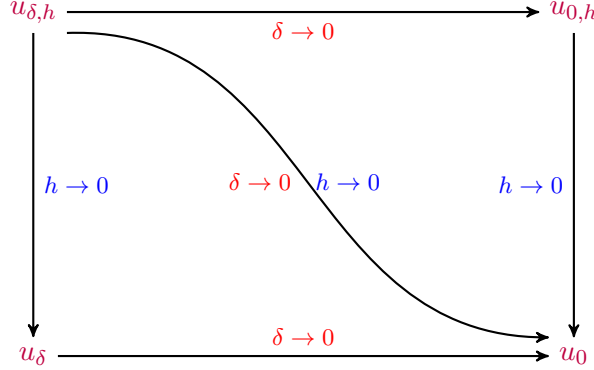


Figure 4.1. An illustrative diagram for AC schemes

discretization schemes for nonlocal peridynamics fail to be AC. In particular, if  $\delta$  is taken to be proportional to  $h$ , then as  $h \rightarrow 0$ , piecewise constant conforming finite element solutions actually converge to the incorrect limit, similarly to those based on simple Riemann sum quadrature approximations to nonlocal operators. Similar discussions can be found in (Bobaru et al. 2009, Chen and Gunzburger 2011) for diffusion models and (Seleson, Du and Parks 2016) for systems of peridynamic equations.

Asymptotically compatible (AC) schemes, being either conforming Galerkin-type approximations of weak forms (Chen and Gunzburger 2011, Tian and Du 2014, Xu, Gunzburger, Burkardt and Du 2016b), nonconforming discontinuous Galerkin approximations (Du, Ju, Lu and Tian 2019c, Du, Ju and Lu 2019b, Du and Yin 2019), or collocation or quadrature based approximations of strong forms (Du and Tian 2014, Seleson et al. 2016, Du et al. 2019d, Zhang, Gunzburger and Ju 2016a, Zhang, Gunzburger and Ju 2016b) offer the potential to solve for approximations of a model of interest with different choices of parameters to gain efficiency and to avoid the pitfall of reaching inconsistent limits.

## 5. Finite element methods for nonlocal models

Given weak formulations of nonlocal models, it is natural to consider finite element approximations (Chen and Gunzburger 2011, Tian and Du 2013, Tian and Du 2014, Xu, Gunzburger and Burkardt 2016a, Xu et al. 2016b, Tian and Du 2020, Du 2019, Jha and Lipton 2019a). To derive a finite element discretization, one possible way is to follow the same recipe as that used for the local PDE setting. We assume that  $\Omega \subset \mathbb{R}^d$  is polytopial so that the first step is to construct a regular subdivision of  $\Omega \cup \Omega_{\mathcal{I}_{\delta}}$  into finite elements, e.g., for  $d = 2$ , usually triangles or quadrilaterals. Based on the grid, one then defines a finite element space  $V^h(\Omega \cup \Omega_{\mathcal{I}_{\delta}})$ , usually consisting of piecewise polynomial functions with respect to the grid, and then chooses

a basis for that space containing functions whose support extends over a few contiguous elements. We do not dwell on the construction of finite element spaces because it is the same as that for the local PDE setting (Brenner and Scott 1994, Ciarlet 2002, Ern and Guermond 2004b), except perhaps that it is prudent to have the grid contain a regular subdivision of  $\Omega$  itself so that the boundary of  $\Omega$  is subdivided into  $(d-1)$ -dimensional faces. For *conforming finite element methods*, i.e., the finite element space  $V^h(\Omega \cup \Omega_{\mathcal{I}_\delta})$  is a subset of the energy space  $V(\Omega \cup \Omega_{\mathcal{I}_\delta})$  for the continuous problem, we define the constrained finite element space

$$V_c^h(\Omega \cup \Omega_{\mathcal{I}_\delta}) = \{v(\mathbf{x}) \in V^h(\Omega \cup \Omega_{\mathcal{I}_\delta}) : v(\mathbf{x}) = 0 \quad \forall \mathbf{x} \in \Omega_{\mathcal{I}_\delta}\}.$$

Note that  $V_c^h(\Omega \cup \Omega_{\mathcal{I}_\delta}) \subset V_c(\Omega \cup \Omega_{\mathcal{I}_\delta})$ . We denote by  $g_h(\mathbf{x})$  an approximation to  $g(\mathbf{x})$ , e.g.,  $g_h(\mathbf{x})$  could be the interpolant of  $g(\mathbf{x})$  in  $V_c^h(\Omega \cup \Omega_{\mathcal{I}_\delta})$  restricted to  $\Omega_{\mathcal{I}_\delta}$ , or, if  $g(\mathbf{x})$  is not smooth enough to have pointwise values, a least-square approximation could be used instead.

A conforming finite element approximation  $u_h(\mathbf{x}) \in V^h(\Omega \cup \Omega_{\mathcal{I}_\delta})$  of the solution of  $u(\mathbf{x}) \in V(\Omega \cup \Omega_{\mathcal{I}_\delta})$  of (2.9) is then determined by solving the following problem.

$$\begin{aligned} &\text{Given } \gamma_\delta(\mathbf{x}, \mathbf{y}) \text{ defined in (1.17) and given } f(\mathbf{x}) \in V_d(\Omega), \\ &\text{find } u_h(\mathbf{x}) \in V^h(\Omega \cup \Omega_{\mathcal{I}_\delta}) \text{ such that} \\ &\quad \begin{cases} \mathcal{A}_\delta(u_h, v_h) = \langle f, v_h \rangle & \forall v \in V_c^h(\Omega \cup \Omega_{\mathcal{I}_\delta}) \\ u_h(\mathbf{x}) = g_h(\mathbf{x}) & \forall \mathbf{x} \in \Omega_{\mathcal{I}_\delta}, \end{cases} \end{aligned} \quad (5.1)$$

where  $g_h(\mathbf{x})$  is defined as discussed above. Because the bilinear form  $\mathcal{A}_\delta(\cdot, \cdot)$  is continuous and coercive with respect to  $V_c(\Omega \cup \Omega_{\mathcal{I}_\delta})$ , it is likewise continuous and coercive with respect to  $V_c^h(\Omega \cup \Omega_{\mathcal{I}_\delta})$  so that the well posedness of the problem (5.1) follows immediately from the Lax-Milgram theorem. For problems involving singular nonlocal interaction kernels such as the fractional type given in Table 2.1, special numerical quadrature is needed for the evaluation of stiffness matrices. We refer to section 6.1 for related discussions.

**Remark 5.1.** *Discontinuous Galerkin methods in the nonlocal setting.* One of the major differences between finite element methods for local PDEs and nonlocal models occurs in the use of discontinuous Galerkin (DG) methods. For elliptic PDEs, DG methods are not conforming, i.e., a finite element space containing functions with jump discontinuities cannot be a subspace of the space  $H^1(\Omega)$  in which the PDE is well posed. As a result, the use of DG methods requires an accounting for fluxes across element faces; otherwise, elements would be uncoupled. On the other hand, for some kernel choices, finite element functions with jump discontinuities do belong to the energy space  $V(\Omega \cup \Omega_{\mathcal{I}_\delta})$  in which the nonlocal problem is well posed. This



is the case for integrable kernels and the fractional kernel with  $s < \frac{1}{2}$  as listed in Table 2.1. For such kernels, DG methods are conforming so that, at least for  $\delta > h$ , no explicit accounting for fluxes across element faces is needed. The coupling between elements is taken care of by nonlocality, i.e., even though the basis functions live only on single elements, any specific element is coupled to all other elements that overlap with the balls of radius  $\delta$  centered at the vertices of the element.  $\square$

### 5.1. Asymptotically compatible conforming finite element methods for nonlocal diffusion

To delve deeper into finite element methods for nonlocal diffusion with a finite range of interactions, we first specialize to a more specific setting. Consider the model given by (2.9) with  $g = 0$ . We also choose the kernel  $\gamma_\delta(\mathbf{x}, \mathbf{y})$  as a rescaled translation-invariant kernel, i.e.,

$$\gamma_\delta(\mathbf{x}, \mathbf{y}) = \frac{1}{\delta^{d+2}} \gamma\left(\frac{|\mathbf{y} - \mathbf{x}|}{\delta}\right) \quad (5.2)$$

for  $\delta \in (0, 1]$  and some kernel  $\gamma(|\cdot|)$  that is assumed to be radial, nonnegative, compactly supported in  $B_1(\mathbf{0})$  (the unit ball centered at the origin), and has a bounded second-order moment, i.e.,

$$\widehat{\gamma}(|\boldsymbol{\xi}|) = |\boldsymbol{\xi}|^2 \gamma(|\boldsymbol{\xi}|) \in L^1_{loc}(\mathbb{R}^d) \quad \text{and} \quad \int_{B_1(\mathbf{0})} \widehat{\gamma}(|\boldsymbol{\xi}|) d\boldsymbol{\xi} = d. \quad (5.3)$$

For kernels satisfying these conditions, we refer to the discussions in Section 2.2. For such kernels, we now denote the energy space  $V_{c,\delta}(\Omega \cup \Omega_{\mathcal{I}_\delta}) = V_c(\Omega \cup \Omega_{\mathcal{I}_\delta})$  as defined in (2.4) to highlight the dependence on  $\delta$ .

Now, for any fixed  $\delta \in (0, 1]$ , we introduce conforming finite element spaces  $\{V^{h,\delta}\} \subset V_{c,\delta}(\Omega \cup \Omega_{\mathcal{I}_\delta})$  associated with the triangulation  $\tau_h = \{K\}$  of the domain  $\Omega \cup \Omega_{\mathcal{I}_\delta}$  (or  $\Omega \cup \Omega_{\mathcal{I}_1}$  that contains the domain  $\Omega \cup \Omega_{\mathcal{I}_\delta}$  for any  $\delta < 1$ .) We set

$$V_{\delta,h} := \{v \in V_{c,\delta}(\Omega \cup \Omega_{\mathcal{I}_\delta}) : v|_K \in P_p(K) \quad \forall K \in \tau_h\},$$

where  $P_p(K)$  denotes the space of piecewise polynomials on  $K \in \tau_h$  of degree less than or equal to  $p$ . Again, for different  $\delta$ , in order to have the finite element functions defined on a common spatial domain, we also assume, as in the case for  $V_{c,\delta}(\Omega \cup \Omega_{\mathcal{I}_\delta})$ , that any element in  $V_{\delta,h}$  vanishes outside  $\Omega$ .

As  $h \rightarrow 0$ , we assume that  $\{V^{h,\delta}\}$  is dense in  $V_{c,\delta}(\Omega \cup \Omega_{\mathcal{I}_\delta})$ , i.e., for any  $v \in V_{c,\delta}(\Omega \cup \Omega_{\mathcal{I}_\delta})$ , there exists a sequence  $\{v_h \in V^{h,\delta}\}$  such that for a given  $\delta > 0$ ,

$$\|v_h - v\|_{V_{c,\delta}(\Omega \cup \Omega_{\mathcal{I}_\delta})} \rightarrow 0 \quad \text{as} \quad h \rightarrow 0. \quad (5.4)$$

These properties are easily satisfied by standard finite element spaces.

The Galerkin approximation is defined by replacing  $V_{c,\delta}(\Omega \cup \Omega_{\mathcal{I}_\delta})$  by  $V_{\delta,h}$

in (2.9):

$$\text{find } u_{h,\delta} \in V^{h,\delta} \text{ such that } \mathcal{A}_\delta(u_{h,\delta}, v_h) = \langle f, v_h \rangle \quad \forall v_h \in V^{h,\delta}. \quad (5.5)$$

The analysis of Galerkin approximations of parameterized nonlocal variational problems can be formulated within the general framework of AC schemes (Tian and Du 2014). Other than the necessary properties of functions and operators that guarantee  $u_\delta \rightarrow u_0$  as  $\delta \rightarrow 0$ , where  $u_0$  denotes the solution of the corresponding PDE, and standard density properties such as (5.4), one of the key ingredients for the asymptotic compatibility of the scheme is the *asymptotic density* property of the finite element space. Rather than a general definition, we provide a specific instance, adapted to the models studied here, as follows. A family of finite dimensional spaces  $\{V_{\delta,h} \subset V_{c,\delta}(\Omega \cup \Omega_{\mathcal{I}_\delta}), \delta \in (0,1), h \in (0,h_0]\}$  is *asymptotically dense* in  $H_0^1(\Omega)$ , if,  $\forall v \in H_0^1(\Omega)$ , there exists a sequence  $\{v_n \in V_{\delta_n,h_n}\}_{h_n \rightarrow 0, \delta_n \rightarrow 0}$  as  $n \rightarrow \infty$  such that

$$\|v - v_n\|_{H^1(\Omega)} \rightarrow 0 \quad \text{as } n \rightarrow \infty. \quad (5.6)$$

It has been rigorously shown in (Tian and Du 2014) that, for scalar nonlocal diffusion equations such as (2.9), all conforming Galerkin approximations of the nonlocal models containing continuous piecewise linear functions are automatically AC in any space dimension. This means that they can recover the correct local limit as long as both  $\delta$  and  $h$  are decreasing, even if the nonlocal parameter  $\delta$  is reduced at a much faster pace than the mesh spacing  $h$ . Even though the analysis of the above AC property is highly technical, an intuitive explanation is that even with  $h$  larger than  $\delta$ , the nonlocal features that ensure the correct local limit are still encoded in the stiffness matrices thanks to higher-order (than constant) basis functions. In fact, even though for the class of kernels we are considering, discontinuous piecewise constant finite element spaces are conforming, they do not generally result in AC approximations. This was first noticed numerically in (Chen and Gunzburger 2011).

For general nonlocal systems in any dimension, in (Tian and Du 2014, Tian and Du 2020) it is shown that as long as the condition  $h = o(\delta)$  is met as  $\delta \rightarrow 0$ , then one obtains the correct local limit even for discontinuous piecewise constant finite element approximations when they are of the conforming type. Practically speaking, this implies that a mild growth of the bandwidth in the finite element stiffness matrix is needed as the mesh is refined in order to recover the correct local limit for piecewise constant finite element schemes. In fact, it has been shown (Tian and Du 2013, Du and Tian 2015) that if a constant bandwidth is kept as the mesh is refined, the approximations may converge to an incorrect local limit.

Naturally, schemes using higher-order basis functions tend to provide

higher-order accuracy in the nonlocal setting as well, should the solutions enjoy sufficient regularity. At the moment, the theory on AC schemes does not offer any estimate of the order of convergence with respect to different couplings of  $h$  and  $\delta$ . Preliminary numerical experiments in (Tian and Du 2014) offer some insight about the balance of modeling and discretization errors, but additional theoretical analyses need to be carried out, except for the case of Fourier spectral approximations of nonlocal models with periodic boundary conditions for which precise error estimates can be found in (Du and Yang 2016a, Du and Yang 2017, Slevinsky, Montanelli and Du 2018).

### 5.2. Nonconforming and DG FEMs for nonlocal models with sufficiently singular kernels

The framework of AC schemes is very general. For example, the theory also guided the development of nonconforming discontinuous Galerkin (DG) approximations (Tian and Du 2015) for nonlocal diffusion and nonlocal peridynamic models with sufficiently singular interaction kernels. Consider the scalar model given by (2.9) with  $g = 0$ . If the nonlocal interaction kernel satisfies

$$\int_{|\mathbf{x}| < \epsilon} |\mathbf{x}| \gamma_\delta(|\mathbf{x}|) d\mathbf{x} = \infty \quad \forall \epsilon \in (0, \epsilon_0], \quad (5.7)$$

then, it may be the case that discontinuous finite element solutions do not belong to the associated energy space and alternative formulations have to be developed. For technical reasons, in (Tian and Du 2015), it is also assumed that

$$\lim_{\epsilon \rightarrow 0} \epsilon^2 \left( \int_{|\mathbf{x}| < \epsilon} |\mathbf{x}|^2 \gamma_\delta(|\mathbf{x}|) d\mathbf{x} \right)^{-1} = 0. \quad (5.8)$$

Note that for kernels  $\gamma_\delta(r)$  that behave like  $1/r^{d+2s}$  as  $r \rightarrow 0$  with  $s \in (1/2, 1)$ , conditions (5.7) and (5.8) are satisfied.

The paper (Tian and Du 2015) introduces a nonconforming DG scheme based on the removal of the singularity in the nonlocal interaction kernel in a sufficiently small neighborhood of the origin parameterized by a cut-off level  $n$ . In other words,  $\gamma_\delta(r)$  in (2.9) is replaced by

$$\gamma_\delta^n(r) := \begin{cases} \gamma_\delta(r) & \text{if } \gamma_\delta(r) \leq n \\ n & \text{if } \gamma_\delta(r) > n. \end{cases} \quad (5.9)$$

For nonlocal problems with the regularized kernel  $\gamma_\delta^n(r)$ , discontinuous element spaces, such as conventional discontinuous finite element spaces, can be used as conforming Galerkin approximations, leading to a discrete solution  $u_{h,\delta,n}$ . Naturally, there are other ways to define the cut-off. The essential requirement is that the resulting modified kernel is integrable (for a given  $n$ ) and it converges pointwise to the original kernel.

The goal is then to demonstrate that  $u_{h,\delta,n}$  converges to the solution  $u_\delta$  of the original continuous nonlocal model with a singular kernel as  $n \rightarrow \infty$  and  $h \rightarrow 0$ . The convergence theory can be established by generalizing the relevant compactness results given in (Bourgain, Brezis and Mironescu 2001) as  $n \rightarrow \infty$  for a given  $\delta > 0$ . Indeed, the following generalization is made in (Tian and Du 2015).

*Compactness results.* Given the kernels  $\gamma_\delta^n$  and  $\gamma_\delta$  and the corresponding energy spaces  $V_{c,\delta}^n(\Omega \cup \Omega_{\mathcal{I}_\delta})$  and  $V_{c,\delta}(\Omega \cup \Omega_{\mathcal{I}_\delta})$ , assume that the energy norms of  $\{v_n \in V_{c,\delta}^n(\Omega \cup \Omega_{\mathcal{I}_\delta})\}$  have the uniform bound

$$\sup_n \int_{\Omega \cup \Omega_{\mathcal{I}_\delta}} \int_{\Omega \cup \Omega_{\mathcal{I}_\delta}} \gamma_\delta^n(|\mathbf{y} - \mathbf{x}|) (v_n(\mathbf{y}) - v_n(\mathbf{x}))^2 d\mathbf{y} d\mathbf{x} \leq C_0.$$

Then,  $\{v_n\}$  is relatively compact in  $L^2(\Omega \cup \Omega_{\mathcal{I}_\delta})$  and any limit function  $v$  belongs to  $V_{c,\delta}(\Omega \cup \Omega_{\mathcal{I}_\delta})$  with

$$\int_{\Omega \cup \Omega_{\mathcal{I}_\delta}} \int_{\Omega \cup \Omega_{\mathcal{I}_\delta}} \gamma_\delta(|\mathbf{y} - \mathbf{x}|) (v(\mathbf{y}) - v(\mathbf{x}))^2 d\mathbf{x} d\mathbf{y} \leq C_0. \quad (5.10)$$

The classical Bourgain-Brezis-Mironescu compactness result established in (Bourgain et al. 2001) can be seen as the local limit of the new compactness result for nonlocal spaces in (Tian and Du 2015) with a finite  $\delta$ . By applying the framework of asymptotically compatible discretization (Tian and Du 2014, Tian and Du 2020) reviewed earlier with respect to the mesh parameter  $h$  and the cut-off level  $n$ , we can obtain the convergence of  $u_{h,\delta,n}$  to  $u_\delta$  unconditionally as  $n \rightarrow \infty$  and  $h \rightarrow 0$  if the underlying finite element space contains the continuous piecewise linear finite element space. Moreover, in this case, if  $n \rightarrow \infty$ , we expect that for any given  $\delta$  and  $h$ ,  $u_{h,\delta,n} \rightarrow u_{h,\delta}$  as  $n \rightarrow \infty$ , where  $u_{h,\delta}$  denotes the conforming finite element approximation of  $u_\delta$  in the space  $V_{\delta,h} \cap V_{c,\delta}(\Omega \cup \Omega_{\mathcal{I}_\delta})$ .

If piecewise constant finite elements are used, a conditional convergence theorem has been established in (Tian and Du 2015), provided the definition of the cut-off is suitably modified. For instance, consider a kernel of the type

$$\frac{\gamma_\star}{|\mathbf{y} - \mathbf{x}|^{d+2s}} \leq \gamma_\delta(|\mathbf{x} - \mathbf{y}|) \leq \frac{\gamma^\star}{|\mathbf{y} - \mathbf{x}|^{d+2s}} \quad \text{for } \mathbf{x}, \mathbf{y} \in \Omega \cup \Omega_{\mathcal{I}_\delta}, \quad (5.11)$$

for some  $s \in (1/2, 1)$  and positive constants  $\gamma_\star$  and  $\gamma^\star$ . Then, one may let

$$\gamma_\delta^n(r) := \begin{cases} \gamma_\delta(r) & \text{for } r \geq 1/n \\ \gamma_\delta(1/n) & \text{for } 0 < r < 1/n. \end{cases} \quad (5.12)$$

For the approximate solution  $u_{h,\delta,n}$  defined as the Galerkin approximation to the nonlocal problem with kernel  $\gamma_\delta^n$  using piecewise constants, we have that  $\|u_{h,\delta,n} - u_\delta\|_{L^2} \rightarrow 0$  if  $h = o(1/n)$  as  $n \rightarrow \infty$ .

We note that the nonconforming approximations discussed in (Tian and Du 2015) in the local limit do not yield a standard nonconforming finite element approximation nor a DG approximation to the local problem. One may construct other alternative formulations that can give rise to the conventional nonconforming and DG discretization of local PDEs, see, e.g., (Du et al. 2019c) for a study based on the DG with penalty formulation.

### 5.3. Adaptive mesh refinement for nonlocal models

Due to, e.g., reduced sparsity, nonlocal models generally incur greater computational costs than do their local PDE-based counterparts. Thus, designing effective adaptive methodologies is important and is an area worthy of much attention. At the moment, the work has been limited to nonlocal models with a finite range of interactions.

The paper (Du, Ju, Tian and Zhou 2013b) contains an a posteriori error analysis of conforming finite element methods for solving linear nonlocal diffusion and peridynamic models. The approach adopted is a residual type error estimator in the  $L^2$  norm, e.g., of the form  $\|-\mathcal{L}_\delta(u_{\delta,h}) - f\|_{L^2}$  that remains well-defined and can be easily computed for integrable kernels from element-wise contributions without worrying about flux jumps across element boundaries. This is in sharp contrast to the case of second-order elliptic PDEs. The theory of a posteriori error analysis has been rigorously derived for nonlocal volume constrained problems associated with scalar equations. The reliability and efficiency of the estimators are proven, and relationships between nonlocal and classical local a posteriori error estimates are also studied.

In (Du, Tian and Zhao 2013c), a convergent adaptive finite element algorithm for the numerical solution of scalar nonlocal models has also been developed. For problems involving certain non-integrable kernel functions, the convergence of the adaptive algorithm is rigorously derived with the help of several basic ingredients, such as an upper bound on the estimator, the estimator reduction, and the orthogonality property. How these estimators and methods work in the local limit and for general time-dependent and nonlinear peridynamic models remains to be investigated.

Concerning nonlocal problems having solutions with jump discontinuities, an adaptive finite element method is given in (Xu et al. 2016a). There, an algorithm is developed that first detects the location of the discontinuity and then refines the grid near the discontinuity. To preserve the  $h^2$  accuracy possible with the use of piecewise-linear elements even when the exact solution contains jump discontinuities at unknown locations, the elements surrounding the discontinuity should have thickness of  $\mathcal{O}(h^4)$  across the discontinuity. This was already observed for the one-dimensional case in (Chen and Gunzburger 2011, Xu et al. 2016b). In higher dimensions, a naive re-

finement strategy that results in small, well-shaped elements in the vicinity of a  $(d - 1)$ -dimensional surface can thus result in an excessive number of degrees of freedom. The adaptive refinement strategy of (Xu et al. 2016a) instead results in elongated elements having thickness  $\mathcal{O}(h^4)$  across the discontinuity, but length  $\mathcal{O}(h)$  along the discontinuity, as illustrated in Figure 5.1. The presence of elongated elements is not harmful to the error because of the anisotropic behavior of the solution, i.e., it is smooth along the discontinuity but discontinuous across the discontinuity. Whereas robust meshing algorithms for this types of anisotropic refinement and accurate predictions of solution jump discontinuities remain computationally challenging in multispace dimensions, the numerical examples in (Xu et al. 2016a) illustrate that the adaptive strategy developed there does indeed result in  $h^2$  convergence, as is also the case for the one-dimensional numerical results in (Chen and Gunzburger 2011, Xu et al. 2016b).

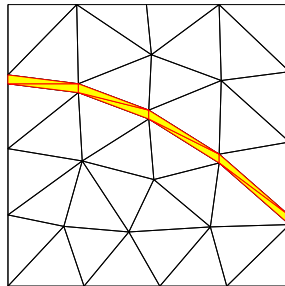


Figure 5.1. An coarse-grid illustration of a mesh resulting from the adaptive strategy discussed in the section. The elongated yellow elements surround the discontinuity in the solution.

Another useful feature of the adaptive strategy developed in (Xu et al. 2016a) is that the transition between the elongated elements along discontinuities and well-shaped elements with sides of length  $\mathcal{O}(h)$  away from the discontinuity can be abrupt, i.e., there is no need to have a transition zone in which elements gradually grow in size. This is also illustrated in Figure 5.1. This feature is already present in the methods developed in (Chen and Gunzburger 2011, Xu et al. 2016b) for the one-dimensional case. The importance of this feature is that it also helps to keep down the number of degrees of freedom.

The next means of savings in the number of degrees of freedom is to use discontinuous basis functions only in the elongated elements, and continuous basis functions in elements in which the exact solution is smooth. The final means is to switch from the nonlocal model to the corresponding PDE model in all elements that do not interact with the elongated elements that

surround the discontinuity, i.e., all elements whose vertices are at distance greater than  $\delta$  from the vertices of the elongated elements.

The four degrees of freedom-saving features (i.e., elongated elements, abrupt grid transitions, the use of discontinuous basis function only in the elongated elements, and the switch to a local PDE model away from the discontinuity), result in tremendous savings in the number of degrees of freedom. In fact, the resulting number of degrees of freedom is comparable to that for a local PDE model using a regular grid of elements having sides of  $\mathcal{O}(h)$ . Moreover, the relative savings become greater as the grid size is reduced and as the dimension  $d$  is increased. See (Xu et al. 2016a) for several numerical illustrations supporting these conclusions,

With regard to more general coupling strategies of local and nonlocal models for computational effectiveness, relevant works are discussed in a recent review on the subject (Du 2019). AC schemes have also been studied in the context of multiscale problems modeled by local-nonlocal coupling formulations with a spatially heterogeneous horizon (Du and Tian 2018, Tao, Tian and Du 2019), based on a new trace theorem for nonlocal function spaces that provides a stronger version of the classical local counterparts (Tian and Du 2017).

#### 5.4. *Approximations of fractional models as limit of nonlocal models with a finite range of interactions*

One of the key messages we want to get across is to show that many popularly studied fractional PDEs are either specialized nonlocal models or can be treated as limiting cases.

Naturally, for fractional differential operators defined in integral form, by truncating the fractional kernel in the fractional operators to a finite range measured by the horizon parameter  $\delta$ , we end up with a nonlocal model parameterized by  $\delta$ . Hence, we see from Section 3.1.1 that on the continuum level, the fractional models may then be viewed as the infinite horizon limit of nonlocal models with a finite  $\delta$ , after a suitable scaling of the kernel.

In (D’Elia and Gunzburger 2013, Burkovska and Gunzburger 2019b), it is shown that as  $\delta \rightarrow \infty$ , the Galerkin approximations of the nonlocal model with the parameter  $\delta$  can converge to the solution of the fractional equations, provided  $h$  is taken to be sufficiently small. One can actually apply the framework of the AC schemes to show that all conforming Galerkin approximations are AC in the limit  $\delta \rightarrow 0$  (Tian, Du and Gunzburger 2016). That is, the discretization of fractional equations associated with the fractional Laplacian can be viewed as the global (with an infinite nonlocal horizon parameter) limit of nonlocal models with properly scaled fractional type

nonlocal interaction kernels (Tian et al. 2016). Moreover, the convergence does not require the dependence of  $h$  on  $\delta$ .

Let us give an illustration of the work presented in (Tian et al. 2016). Consider the volume constrained problems defined for the fractional Laplacian in  $\Omega$  with homogeneous Dirichlet condition in  $\Omega_{\mathcal{I}_\infty} = \mathbb{R}^d \setminus \Omega$ . By truncations of both the spatial domain and the range of nonlocal interactions, we may end up with a class of parametrized problems

$$\begin{cases} -\mathcal{L}_\delta u(\mathbf{x}) = -2 \int_{\mathbb{R}^d} (u(\mathbf{y}) - u(\mathbf{x})) \gamma_\delta(|\mathbf{y} - \mathbf{x}|) d\mathbf{y} = f & \forall \mathbf{x} \in \Omega \\ u = 0 & \forall \mathbf{x} \in \Omega_{\mathcal{I}_\delta}. \end{cases} \quad (5.13)$$

with

$$\gamma_\delta(|\mathbf{y} - \mathbf{x}|) = \begin{cases} \frac{C_{d,s}}{|\mathbf{y} - \mathbf{x}|^{d+2s}} & \mathbf{y} \in B_\delta(\mathbf{x}) \\ 0 & \mathbf{y} \in \mathbb{R}^d \setminus B_\delta(\mathbf{x}). \end{cases} \quad (5.14)$$

Here, the constant  $C_{d,s}$  is given as in (3.2) so that  $\mathcal{L}_\infty = (-\Delta)^s$  as in (3.1).

Let  $h$  denote the discretization parameter associated with Galerkin approximations of (5.13). For example,  $h$  could be the mesh parameter for the finite element discretization or the reciprocal of the number of basis functions in spectral approximations. We can then apply the AC framework to obtain the convergence of the Galerkin approximations of (5.13) to the solution of the fractional equation as  $h \rightarrow 0$  and  $\delta \rightarrow \infty$  as long as the finite dimensional approximations spaces are subspaces of the underlying energy space, i.e., as long as we adopt conforming discretizations.

As pointed out in (Tian et al. 2016, Tian and Du 2020), analyses of the fractional and local limits ( $\delta \rightarrow \infty$  and  $\delta \rightarrow 0$  respectively) of nonlocal models parameterized by a finite  $\delta$  and with fractional-type kernels demonstrate that nonlocal models are more general than their fractional and local counterparts and they also serve as a bridge between fractional and local models, see Figure 5.2 and, again, Figure 4.1 and similar diagrams given in (Du 2019, Tian and Du 2020). For AC schemes, the bridging roles of nonlocal diffusion with a finite range of nonlocal interactions, presented in above at the continuum level, remain valid on the discrete level.

## 6. Finite element methods for the integral fractional Laplacian

Henceforth, let  $\Omega$  denote a polygon, let  $\mathcal{T}_h$  denote a family of shape-regular and locally quasi-uniform triangulations of  $\Omega$  (Ciarlet 2002, Brenner and Scott 1994, Ern and Guermond 2004a), and let

$$\partial\mathcal{T}_h := \{\text{edge } e : \exists K \in \mathcal{T}_h \text{ such that } e \subset \partial K \cap \partial\Omega\}$$



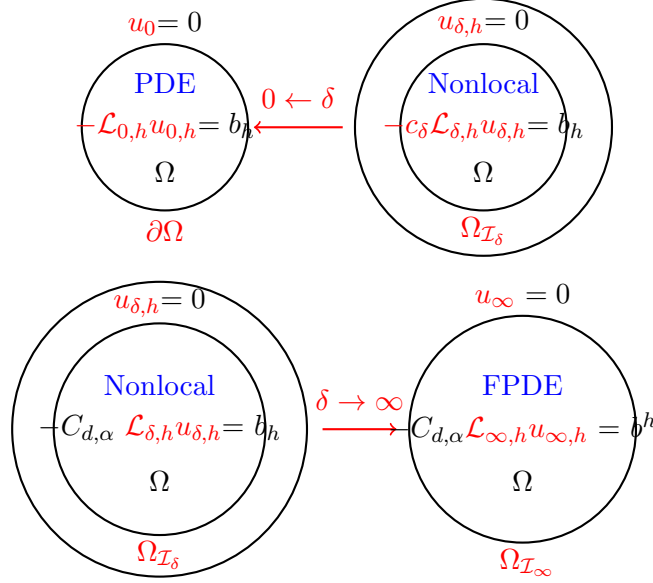


Figure 5.2. Partial differential equations (PDEs) as the local limit ( $\delta \rightarrow 0$ ) and fractional PDEs (FPDEs) as the global limit ( $\delta \rightarrow \infty$ ) of nonlocal models with a finite range parameterized by  $\delta$ .

denote the “trace” of the interior mesh. Let  $\mathcal{Z}_h$  denote the set of vertices of  $\mathcal{T}_h$ ,  $h_K$  denote the diameter of the element  $K \in \mathcal{T}_h$ , and  $h_e$  denote the diameter of  $e \in \partial\mathcal{T}_h$ . Moreover, let

$$h := \max_{K \in \mathcal{T}_h} h_K, \quad h_{\min} := \min_{K \in \mathcal{T}_h} h_K, \quad \text{and} \quad h_{\partial} := \max_{e \in \partial\mathcal{T}_h} h_e.$$

Note that  $h_{\partial}$  denotes the maximum size of all elements  $K$  whose patch  $S_K$  touches the boundary. Let  $\varphi_i$  denote the usual piecewise linear Lagrange basis function associated with a node  $\mathbf{z}_i \in \mathcal{Z}_h$ , satisfying  $\varphi_i(\mathbf{z}_j) = \delta_{ij}$  for  $\mathbf{z}_j \in \mathcal{Z}_h$ , and let  $X_h := \text{span}\{\varphi_i : \mathbf{z}_i \in \mathcal{Z}_h\}$ . The finite element subspace  $V_h \subset H_c^s(\Omega)$  is given by  $V_h = X_h$  when  $s < 1/2$  and by

$$V_h = \{v_h \in X_h : v_h = 0 \text{ on } \partial\Omega\} = \text{span}\{\varphi_i : \mathbf{z}_i \notin \partial\Omega\}$$

when  $s \geq 1/2$ . The corresponding cardinality  $N_h$  of  $V_h$  is equal to the number of nodes in  $\mathcal{Z}_h$  when  $s < 1/2$  and otherwise is the number of interior nodes in  $\Omega$ .

Now, let  $u_h$  denote the solution of the finite element discrete problem given by

$$\text{find } u_h \in V_h \text{ such that } \mathcal{A}(u, v) = \langle f, v \rangle \quad \forall v \in V_h,$$

where the bilinear form and right-hand side are defined in the usual manner. The following error estimates are derived in (Acosta and Borthagaray 2017).

If  $u \in H^t(\Omega) \cap H_{\text{loc}}^\ell(\Omega)$ , for  $t, \ell \in (1/2, 2]$  and  $0 < s \leq t \leq \ell$ , i.e. if  $u$  has Sobolev regularity  $t$  and interior regularity  $\ell$ , then

$$\|u - u_h\|_{H_c^s(\Omega)} \leq C(h^{\ell-s} |u|_{H_{\text{loc}}^\ell(\Omega)} + h_\partial^{t-s} |u|_{H^t(\Omega)}). \quad (6.1)$$

In particular, if the family of triangulations  $\mathcal{T}_h$  is globally quasi-uniform, and if  $u \in H^t(\Omega)$  for  $t \in (1/2, 2]$  and if  $0 < s \leq t$ , then

$$\|u - u_h\|_{H_c^s(\Omega)} \leq Ch^{t-s} |u|_{H^t(\Omega)}. \quad (6.2)$$

The estimate (6.2) implies that for  $u \in H^2(\Omega)$ , the expected rate of convergence on a globally quasi-uniform mesh is  $h^{2-s} = \mathcal{O}(N_h^{(s-2)/d})$ . Because the solutions of (3.4) generally have limited regularity up to the boundary (see Section 3.3.3), using a mesh that is more refined close to the boundary with  $h_\partial \ll h$  is advisable. Whereas using such a mesh can restore the optimal rate of convergence  $\mathcal{O}(N_h^{(s-2)/d})$  in  $d = 1$  dimensions, this does not hold for higher dimensional problems, where shape regularity of the elements becomes the limiting factor. Therefore, we can expect no more than  $\mathcal{O}(N_h^{-1/2+\varepsilon})$  rate of convergence in  $d = 2$  dimensions.

Whereas it may be possible to construct an appropriately graded mesh for simple geometries, the general case will require adaptively refined meshes to resolve the boundary singularity. A posteriori error estimators for the integral fractional Laplacian have been developed in (Nochetto, von Petersdorff and Zhang 2010, Faustmann, Melenk, Parvizi and Praetorius 2019, Ainsworth and Glusa 2017).

### 6.1. Quadrature rules

The fractional Poisson equation (3.4) leads to a dense linear algebraic system

$$\mathbf{A}_s \vec{u} = \vec{f}, \quad (6.3)$$

in which the entries in the matrix  $\mathbf{A}_s = \{\mathcal{A}_s(\varphi_i, \varphi_j)\}_{ij}$  involve singular integrals. In order to compute these entries, we decompose the integrals into contributions between pairs of elements  $K, \hat{K} \in \mathcal{T}_h$  and between pairs consisting of elements  $K \in \mathcal{T}_h$  and external edges  $e \in \partial\mathcal{T}_h$  as follows:

$$\mathcal{A}_s(\varphi_i, \varphi_j) = \sum_K \sum_{\hat{K}} \mathcal{A}_s^{K \times \hat{K}}(\varphi_i, \varphi_j) + \sum_K \sum_e \mathcal{A}_s^{K \times e}(\varphi_i, \varphi_j).$$

The individual contributions  $\mathcal{A}_s^{K \times \hat{K}}$  and  $\mathcal{A}_s^{K \times e}$  are given by:

$$\begin{aligned} \mathcal{A}_s^{K \times \hat{K}}(\varphi_i, \varphi_j) &= \frac{C(d, s)}{2} \int_K d\mathbf{x} \int_{\hat{K}} d\mathbf{y} \frac{(\varphi_i(\mathbf{x}) - \varphi_i(\mathbf{y}))(\varphi_j(\mathbf{x}) - \varphi_j(\mathbf{y}))}{|\mathbf{x} - \mathbf{y}|^{d+2s}} \\ \mathcal{A}_s^{K \times e}(\varphi_i, \varphi_j) &= \frac{C(d, s)}{2s} \int_K d\mathbf{x} \int_e d\mathbf{y} \frac{\varphi_i(\mathbf{x}) \varphi_j(\mathbf{y}) \vec{n}_e \cdot (\mathbf{x} - \mathbf{y})}{|\mathbf{x} - \mathbf{y}|^{d+2s}}. \end{aligned}$$

Contributions from non-disjoint pairs of elements (see Figure 6.1) are not directly amenable to numerical quadrature, due to their singular nature. Fortunately, these can be treated by adapting techniques used in the boundary element method (BEM) literature to address similar issues arising from singular kernels (Sauter and Schwab 2010).

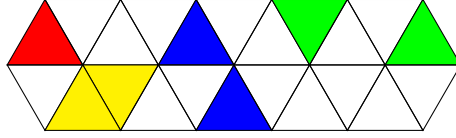


Figure 6.1. Classes of element pairs configurations that need to be handled: pairs of identical elements (*red*), element pairs with common edge (*yellow*), with common vertex (*blue*) and separated element pairs (*green*).

However, the fractional Laplacian does pose new difficulties beyond those addressed by the BEM literature, but which can be treated as described in (Ainsworth and Glusa 2018b, Acosta et al. 2017). In particular, in (Ainsworth and Glusa 2018b, Ainsworth and Glusa 2017), non-uniform order Gauss-type quadrature rules are developed. Alternatively, an approach proposed in (Chernov, von Petersdorff and Schwab 2011) could be taken. It allows for transforming quadrature rules given on the unit hypercube  $[0, 1]^{2d}$  to any pair of elements  $K \times \hat{K}$ . Here, the singularity is taken into account through the choice of the weight in the quadrature rules.

In (Ainsworth and Glusa 2017), the following result is given. Denote the quadrature approximation to the bilinear form  $\mathcal{A}_s(\cdot, \cdot)$  by  $\mathcal{A}_s^Q(\cdot, \cdot)$ . Then, for given  $\beta > 0$ , quadrature rules can be chosen such that the consistency error due to quadrature is bounded by

$$|\mathcal{A}_s(u, v) - \mathcal{A}_s^Q(u, v)| \leq CN_h^{-\beta} \|u\|_{L^2(\Omega)} \|v\|_{L^2(\Omega)} \quad \forall u, v \in V_h.$$

A brief discussion about solvers and condition numbers for finite element discretizations of the integral fractional Laplacian is given in 12.2.

## 7. Finite element methods for the spectral fractional Laplacian

The extension problem (3.14) has been extensively used to solve equations involving the spectral fractional Laplacian. For a bounded domain, the extension problem is posed on  $\Omega_z = \Omega \times [0, \infty)$  and takes the form

$$\begin{cases} -\nabla \cdot z^\beta \nabla U(\mathbf{x}, z) = 0 & \forall (\mathbf{x}, z) \in \Omega_z \\ U(\mathbf{x}, z) = 0, & \forall (\mathbf{x}, z) \in \partial_L \Omega_z \\ \frac{\partial U}{\partial n^\beta}(\mathbf{x}) = d_s f(\mathbf{x}) & \forall \mathbf{x} \in \Omega, \end{cases} \quad (7.1)$$

where  $d_s$  is the constant given in (3.14) and where  $\partial_L \Omega_z := \partial \Omega \times [0, \infty)$  denotes the lateral surface of the semi-infinite cylinder. The solution  $u$  to the spectral fractional Poisson problem (3.12) is then recovered by taking the trace on  $\Omega$ , i.e.  $u = \text{trace}_\Omega U$ .

We define the solution space  $\mathcal{H}_\beta^1(\Omega_z)$  on the semi-infinite cylinder  $\Omega_z$  as

$$\mathcal{H}_\beta^1(\Omega_z) = \{V \in H_{z\beta}^1(\Omega_z) : V = 0 \text{ on } \partial_L \Omega_z\},$$

with norm  $\|V\|_{\mathcal{H}_\beta^1} = |V|_{H_{z\beta}^1}$ . The weak form of the extension problem is then given by

$$\begin{aligned} &\text{find } U \in \mathcal{H}_\beta^1(\Omega_z) \text{ such that} \\ &\int_{\Omega_z} z^\beta \nabla U \cdot \nabla V = d_s \langle f, \text{tr}_\Omega V \rangle \quad \forall V \in \mathcal{H}_\beta^1(\Omega_z). \end{aligned} \quad (7.2)$$

In the literature, the fact that the domain is unbounded in the  $z$ -direction has been handled in different ways. One class of methods exploits the fact that truncation of the domain to  $\Omega_{z_{trun}} := \Omega \times [0, z_{trun}]$  can be shown to be exponentially converging in  $z_{trun}$ , and then discretizes the domain  $\Omega_{z_{trun}}$  using finite elements. A second class uses a hybrid approach and discretizes using finite elements in the  $\mathbf{x}$ -direction and a suitable spectral method in the  $z$ -direction. We will describe both these methods below.

### 7.1. Truncation in the extended direction

The truncation approach was pioneered in (Nochetto, Otárola and Salgado 2015). A first result shows that truncation of the semi-infinite cylinder  $\Omega_z$  only leads to an exponentially small error.

Let  $U \in \mathcal{H}_\beta^1$  denote the solution of (7.2) and  $U_{z_{trun}}$  the extension by zero to  $\Omega_z$  of the solution to (7.2) posed on the truncated domain  $\Omega_{z_{trun}}$ ,  $z_{trun} \geq 1$ , with a homogeneous Dirichlet condition enforced at  $z = z_{trun}$ . Then

$$\|U - U_{z_{trun}}\|_{\mathcal{H}_\beta^1(\Omega_z)} \leq C e^{-\sqrt{\lambda_0} z_{trun}/4} \|f\|_{H^{-s}(\Omega)},$$

where  $\lambda_0$  is the smallest eigenvalue of the integer-order Laplacian as given by (3.11).

Now, let  $\mathcal{T}_h$  denote a quasi-uniform mesh of  $\Omega$  with mesh size  $h$  and define a graded mesh  $\mathcal{T}_{z_{trun}}$  of the interval  $[0, z_{trun}]$  by

$$z_k = (k/M)^\gamma z_{trun}, \quad k = 0, \dots, M,$$

with  $M \sim h^{-1}$  and  $\gamma > 3/(1 - \beta)$ . Then, define a mesh  $\mathcal{T}$  on the extended domain  $\Omega_{z_{trun}}$  as the tensor product of  $\mathcal{T}_h$  and  $\mathcal{T}_{z_{trun}}$ , and let  $V_h$  denote the space of piecewise  $\mathbb{Q}_1$  finite element functions on  $\mathcal{T}$ . Let  $N = \dim V_h$  be the overall number of degrees of freedom and choose the truncation to be  $z_{trun} \sim |\log N|$ . Then the following convergence result holds.

Let  $f \in H_c^{1-s}(\Omega)$ ,  $U \in \mathcal{H}_\beta^1(\Omega_z)$  the solution of (7.2), and  $U_h \in V_h$  the solution of the restriction of (7.2) to  $V_h$ . Moreover, let  $u = \text{trace}_\Omega U$  denote the solution to the spectral fractional-order Poisson problem (3.12), and  $u_h = \text{trace}_\Omega U_h$  its discrete approximation. Then

$$\begin{aligned} \|u - u_h\|_{H_c^s(\Omega)} &\leq C \|U - U_h\|_{\mathcal{H}_\beta^1(\Omega_z)} \\ &\leq C |\log h|^s h \|f\|_{H_c^{1-s}(\Omega)} \\ &\leq C |\log N|^s N^{-1/(d+1)} \|f\|_{H_c^{1-s}(\Omega)}. \end{aligned}$$

As observed in (Nochetto et al. 2015), this shows that the result is optimal in terms of regularity, but sub-optimal in terms of complexity. This shortcoming can be addressed using sparse grids (Banjai, Melenk, Nochetto, Otárola, Salgado and Schwab 2019) or  $hp$ -finite elements (Meidner, Pfefferer, Schürholz and Vexler 2018).

### 7.2. Spectral method in the extended direction

A different approach was taken in (Ainsworth and Glusa 2018a). Instead of truncating the domain, a spectral method is used for the extended direction, based on the observation that the eigenfunctions of the extension problem (7.1) are given by

$$\varphi_m(\mathbf{x})\psi_m(y), \quad m \in \mathbb{N},$$

where

$$\psi_m(y) = c_s \left( \lambda_m^{1/2} y \right)^s K_s \left( \lambda_m^{1/2} y \right), \quad (7.3)$$

with  $c_s = 2^{1-s}/\Gamma(s)$  and  $(\varphi_m, \lambda_m)$  are the eigenpairs of (3.11).

This motivates the choices

$$\begin{aligned} V_h &= \{v_h \in H_0^1(\Omega) : v_h|_K \in \mathbb{P}_k(K) \ \forall K \in \mathcal{T}_h\}, \\ V_{h,M} &= \left\{ V_{h,M} = \sum_{m=0}^{M-1} v_{h,m}(\mathbf{x}) \hat{\psi}_m(y) : v_{h,m} \in V_h \right\} \subset \mathcal{H}_\beta^1(\Omega_z), \end{aligned}$$

where

$$\hat{\psi}_m(y) := c_s \left( \hat{\lambda}_m^{1/2} y \right)^s K_s \left( \hat{\lambda}_m^{1/2} y \right). \quad (7.4)$$

are defined using suitable approximations  $\hat{\lambda}_m$  instead of the true eigenvalues  $\lambda_m$ .

It turns out that using the asymptotic law for the eigenvalues of the Laplacian and using a coarse finite element approximation give sufficiently good approximations  $\hat{\lambda}_m$ . Moreover, by decimation, only  $|\log h|^p$  for some  $p > 0$  eigenvalue approximations are required. Overall, this results in the following error estimate.

Let  $f \in H_c^r(\Omega)$ ,  $r \geq -s$ ,  $U \in \mathcal{H}_\beta^1(\Omega_z)$  the solution of (7.2) and  $U_h \in V_h$  the solution of the restriction of (7.2) to  $V_h$ . Moreover, let  $u = \text{trace}_\Omega U$  by the solution to the spectral fractional-order Poisson problem (3.12), and  $u_h = \text{trace}_\Omega U_h$  its discrete approximation. Then

$$\begin{aligned} \|u - u_h\|_{H_c^s(\Omega)} &\leq C \|U - U_{h,M}\|_{\mathcal{H}_\beta^1(\Omega_z)} \\ &\leq C \|f\|_{H_c^r(\Omega)} h^{\min\{k, r+s\}} \sqrt{|\log h|} \\ &= C \|f\|_{H_c^r(\Omega)} N^{-\min\{k, r+s\}/d} |\log N|^p. \end{aligned}$$

**Remark 7.1.** *Solution of the linear system.* Provided that the discretization of the extension problem (7.1) displays a tensor structure, the solution of the arising linear system reduces to a sequence of discretized integer-order reaction-diffusion-type problems. These problems are readily solved using classical iterative linear solvers such as conjugate gradient and multi-grid; see e.g. (Chen, Nochetto, Otárola and Salgado 2016a, Ainsworth and Glusa 2018a).  $\square$

## 8. Spectral-Galerkin methods for nonlocal diffusion

Compared with its fractional counterparts discussed in Section 9, algorithms and numerical analyses of spectral method for nonlocal diffusion have been much less studied. Here, we simply consider a Fourier spectral-Galerkin method developed in (Du and Yang 2016a, Du and Yang 2017).

For simplicity, we focus on the one-dimensional periodic nonlocal diffusion problem given by

$$-(\mathcal{L}_\delta u)(x) = f(x) \quad \forall x \in (-\pi, \pi) \quad (8.1)$$

with periodic boundary condition, where we express the nonlocal operator  $\mathcal{L}_\delta$  in the equivalent form

$$(\mathcal{L}_\delta u)(x) = 2 \int_{|z| \leq \delta} \gamma_\delta(z) (u(x+z) - u(x)) dz, \quad (8.2)$$

where  $f(x) \in L_{per}^2[-\pi, \pi]$ , where  $L_{per}^2[-\pi, \pi]$  denotes the space of periodic functions in  $L^2[-\pi, \pi]$  having zero mean. As always,  $\delta$  denotes the horizon. Here, the kernel function  $\gamma_\delta(z)$  is a nonnegative, radial function such that

$$\gamma_\delta(z) = \frac{1}{\delta^3} \gamma\left(\frac{|z|}{\delta}\right) \quad \forall z \in [-\delta, \delta], \quad (8.3)$$

where  $\gamma = \gamma(\xi)$  denotes a nonnegative, non-increasing function having compact support in  $[0, 1]$  and has a bounded second moment, i.e.,

$$2 \int_0^1 \gamma(\xi) \xi^2 d\xi = 1. \quad (8.4)$$

The scalings used in (8.3) insure that as the horizon  $\delta$  tends to zero, the nonlocal operator  $\mathcal{L}_\delta$  reduces to the PDE Laplacian, i.e.,  $d^2/dx^2$  in one dimension.

For any positive integer  $n$ ,  $e^{inx}$  is an eigenfunction of  $\mathcal{L}_\delta$  under periodic boundary conditions with the corresponding eigenvalues<sup>2</sup>

$$\lambda_{n,\delta} = 4 \int_0^\delta \gamma_\delta(z)(\cos(nz) - 1)dz. \quad (8.5)$$

Let  $X_N^0 := \text{span}\{e^{inx}\}_{n=1,2,\dots,N}$  and let

$$v_N(x) = \sum_{n=1}^N \widehat{v}_n e^{inx} \in X_N^0$$

for any set of constants  $\{\widehat{v}_n\}$ . Note that because, for any integer  $n > 0$ ,  $e^{inx}$  has zero mean with respect to any interval of length  $2\pi$ , so does  $v_N(x)$ . We have that

$$-\mathcal{L}_\delta v_N = \sum_{n=1}^N \lambda_{n,\delta} \widehat{v}_n e^{inx} \quad \text{for } \delta \geq 0.$$

The Fourier spectral-Galerkin scheme of (Du and Yang 2016a, Du and Yang 2017) is given as follows:

given  $f(x) \in L^2_{\text{per}}[-\pi, \pi]$ , seek  $u_{N,\delta}(x) \in X_N^0$  such that

$$(-\mathcal{L}_\delta u_{N,\delta}, v_N) = (f, v_N) \quad \forall v_N \in X_N^0$$

or, equivalently, (8.6)

$$u_{N,\delta} = -\mathcal{L}_\delta^{-1} P_N f = \sum_{n=1}^N \lambda_{n,\delta}^{-1} \widehat{f}_n e^{inx},$$

where here  $(\cdot, \cdot)$  denotes the standard  $L^2(-\pi, \pi)$  inner product and  $P_N$  denotes the standard spectral Fourier projection onto  $X_N := \text{span}\{e^{inx}\}_{n=0,1,\dots,N}$  of an element in  $L^2[-\pi, \pi]$ .

It was proved in (Du and Yang 2016a, Lemma 1) that the numerical scheme (8.6) is asymptotically compatible. In particular, it was proved that

$$\|u_{N,\delta} - u_{N,0}\|_{L^2(-\pi,\pi)} \leq C\delta^2 \|P_N f\|_{L^2(-\pi,\pi)}, \quad (8.7)$$

where the constant  $C$  is independent of  $N$  and  $\delta$ . Here,  $u_{N,0}$  denotes the Fourier spectral solution in  $X_N^0$  of the local diffusion problem

$$-\mathcal{L}_0 u(x) := -u_{xx}(x) = f(x) \quad \forall x \in (-\pi, \pi) \quad (8.8)$$

<sup>2</sup> Note that  $-d^2/dx^2$  has the same eigenfunctions  $e^{inx}$  as does  $-\mathcal{L}_\delta$  and has the eigenvalues  $n^2$ . Note that, in the limit  $\delta \rightarrow 0$ ,  $\lambda_{n,\delta} \rightarrow \lambda_{n,0} := n^2$ .

with the periodic boundary condition. The proof of the estimate (8.7) follows from the error representation

$$\|u_{N,\delta} - u_{N,0}\|_{L^2(-\pi,\pi)}^2 = \sum_{n=1}^N \left| \frac{1}{\lambda_{n,\delta}} - \frac{1}{\lambda_{n,0}} \right|^2 |\widehat{f}_n|^2$$

and a careful analysis on the asymptotic behavior of  $\lambda_{n,\delta}$ .

Let  $u_0(\mathbf{x})$  denote the exact solution of the local problem (8.8). Then, using standard error estimation theories for local models, it is easy to show that  $u_{N,0}$  converges in  $L^2$ -sense to  $u_0$  at least quadratically with respect to  $1/N$ , provided that  $f \in L^2(-\pi, \pi)$ . As a result, we arrive at

$$\|u_N^\delta - u^0\|_{L^2(-\pi,\pi)} \leq C(\delta^2 + N^{-2})\|f\|_{L^2(-\pi,\pi)}, \quad (8.9)$$

with a generic constant  $C$  independent of  $\delta$ ,  $N$ ,  $f$ ,  $u_0$ , and  $u_\delta$ , where  $u_\delta$  denotes the exact solution of (8.1). This estimate indicates that the Fourier spectral method of (Du and Yang 2016a, Du and Yang 2017) is asymptotically compatible. Moreover, we obtain a uniform error estimate in the sense that the estimates hold for any sufficiently small  $\delta$  and any sufficiently large  $N$  without any restriction on the relative sizes of  $\delta$  and  $N$ .

These one-dimensional results can be easily extended to higher-dimensional nonlocal diffusion problems in rectangular and rectangular parallelepiped domains with periodic boundary conditions. See (Du and Yang 2017) for discussions about two and three-dimensional problem. Furthermore, the analysis was extended to the nonlocal Allen-Cahn equations (Du and Yang 2016a, Section 4).

The eigenvalues  $\lambda_{n,\delta}$  defined by (8.5) cannot, in general, be determined analytically. Thus, when implementing the scheme given in (8.6), those eigenvalues  $\lambda_{n,\delta}$  have to be estimated. The numerical evaluation of the integral in (8.5) is challenging because  $\cos(nz)$  is highly oscillatory for large  $n$ . As an example, we focus on a kernel that is singular at the origin, namely,

$$\gamma_\delta(z) = \frac{C_\beta}{\delta^{3-\beta}|z|^\beta} \quad \forall z \in [-\delta, 0) \cup (0, \delta] \quad \text{and for } \beta \in (0, 3). \quad (8.10)$$

Then, by Taylor expansion, we have that

$$\begin{aligned} \lambda_{n,\delta} &= \frac{2(3-\beta)}{\delta^2} \int_0^1 r^{-\beta} (\cos(n\delta r) - 1) dr \\ &= \frac{2(3-\beta)}{\delta^2} \sum_{k=1}^{\infty} \frac{(-1)^k |n\delta|^{2k}}{(2k)!(2k+1-\alpha)} := \frac{2(3-\beta)}{\delta^2} K(n\delta). \end{aligned} \quad (8.11)$$

Therefore, it suffices to compute  $K(n\delta)$  accurately. In (Du and Yang 2017), a hybrid algorithm is given for computing  $K(n\delta)$ . If  $n\delta$  is “small,” then the series in (8.11) converges fast so that one may approximate  $K(n\delta)$  by using a truncation of that series. On the other hand, for  $n\delta$  “large,” it is observed



in (Du and Yang 2017) that  $K(n\delta)$  is a solution of the ordinary differential equation

$$K'(z) = \frac{z-1}{z}K(z) + \frac{\cos(z)-1}{z} \quad \text{on } (0, n\delta] \quad (8.12)$$

evaluated at  $z = n\delta$ . For a starting condition,  $K(1)$  may be used; it can be computed using a truncation of the series in (8.11). As a result,  $K(n\delta)$  can be accurately evaluated for large  $n\delta$  by using, e.g., a high-order Runge-Kutta method.

In (Slevinsky et al. 2018), a Fourier spectral method was proposed to solve nonlocal diffusion models on the unit sphere  $\mathcal{S}^2 \subset \mathbb{R}^3$ , where the nonlocal Laplace-Beltrami operator is defined by

$$\mathcal{L}_\delta u(x) = 2 \int_{\mathcal{S}^2} (u(x+z) - u(x)) \gamma_\delta(z) d\nu(z), \quad (8.13)$$

where  $\nu$  denotes the standard measure on  $\mathcal{S}^2$ . The basic idea is to apply spherical harmonics (Atkinson and Han 2012):

$$Y_l^m(x) = Y_l^m(\theta, \varphi) = \frac{e^{im\varphi}}{\sqrt{2\pi}} i^{m+|m|} \sqrt{\left(l + \frac{1}{2}\right) \frac{(l-m)!}{(l+m)!}} P_l^m(\cos \theta)$$

with  $l \geq 0$  and  $-l \leq m \leq l$ , for which it is shown that they are the eigenfunctions of the nonlocal Laplace-Beltrami operator. Here  $(\theta, \varphi)$  is the spherical coordinate of  $x \in \mathbb{S}^2$  and  $P_l$  denotes the associated Legendre polynomials. Specifically, there holds  $\mathcal{L}_\delta Y_l^m(x) = \lambda_\delta(l) Y_l^m(x)$  with

$$\lambda_\delta(l) = 4\pi \int_{-1}^1 (P_l(y) - 1) \gamma_\delta(\sqrt{2(1-y)}) dy.$$

To compute the eigenvalue  $\lambda_\delta(l)$ , one evaluates an integral which is highly oscillatory due to the Legendre polynomials. Slevinsky et. al (Slevinsky et al. 2018) proposed a numerical scheme by using a modified Clenshaw-Curtis quadrature rule with the computation complexity  $O(l^2)$  per eigenvalue  $\lambda_\delta(l)$ . For sufficiently large  $l$ , they applied Szegő's asymptotic formula for Legendre polynomials, which reduces the complexity to  $O(l \log l)$  per eigenvalue. Then, a fast spherical harmonic transform (Slevinsky n.d.) was applied to accelerate synthesis and analysis of the series expansion in spherical harmonics.

**Remark 8.1.** *Extension to phase-field methods.* The study of spectral approximation to nonlocal problems has been extended to nonlinear models such as phase field equations (Du and Yang 2016b, Du, Ju, Li and Qiao 2018b). While the conventional phase field (diffuse interface) models take

on a free energy of the type (Du and Feng 2020)

$$E^0(u) = \int_{\Omega} \left( \frac{\epsilon}{2} |\nabla u(x)|^2 + \frac{1}{4\epsilon} (u(x) - 1)^2 \right) dx. \quad (8.14)$$

The nonlocal version of the free energy can be written as (Du and Yang 2016b)

$$E^\delta(u) = \int_{\Omega} \int_{\Omega} \left( \frac{\epsilon}{2} \gamma_\delta(|s|) \frac{(u(x+s) - u(x))^2}{2} ds + \frac{1}{4\epsilon} (u(x) - 1)^2 \right) dx, \quad (8.15)$$

which recovers  $E^0$  as its Gamma limit for  $\delta \rightarrow 0$ .

A nonlocal Allen-Cahn equation can be defined as the  $L^2$  gradient flow of the energy in (8.15). The convergence of AC spectral approximations for problems defined on periodic domains has been established in (Du and Yang 2016b). With the assumption on smooth minimizers, spectral accuracy can be assured. In the case nonlocal interaction kernels do not have sufficiently strong singularities, the minimizers of the nonlocal free energy (subject to a total mass condition) may develop a discontinuous profile, in contrast to the conventional diffuse interface models with smooth phase field functions. Yet, the convergence of spectral approximations can be assured even for such cases. We note that historically, (8.14) is often derived from a nonlocal form (8.15) via the *Landau expansion*; see the additional discussions on this perspective given in (Du 2019). Naturally, one may also consider the  $H^{-1}$  gradient flow of the nonlocal energy or gradient flows with respect to a nonlocal space embedded between  $H^{-1}$  and  $L^2$ ; some related numerical analysis can be found in (Li, Qiao and Wang 2019, Ainsworth and Mao 2017).  $\square$

**Remark 8.2.** Nonlocal diffusion allows for singular solutions, which pose new challenges in the design of numerical discretizations. Whereas spectral methods are shown to possess many good properties such as asymptotic compatibility and are able to capture the discontinuities in solutions, spurious Gibbs phenomena do appear. Given the development of spectral methods in the context of PDEs that are effective in singularity detection and in high-order recovery of solution information near and away from singularities (see, e.g., (Tadmor 2007)), it is natural to pursue further studies on how to adopt and extend those techniques to nonlocal models.

Furthermore, the algorithms introduced in this section focus on periodic boundary conditions and allows for the derivation of uniform convergence rates with respect to both  $\delta$  and  $N$ ; see, e.g., (8.9). The extension to other types of boundary conditions, e.g., Dirichlet or Neumann volume constraints, remains an open problem. The main difficulty stems from the lack of a closed expression for the eigenvalues analogous to the expression given in (8.5).

Hence, the difference  $\lambda_{n,\delta}^{-1} - \lambda_{0,\delta}^{-1}$  is difficult to estimate. An investigation of the AC property of spectral method in such settings is also warranted.  $\square$

## 9. Spectral-Galerkin methods for fractional diffusion

In this section, we consider spectral methods for determining approximate solutions of fractional diffusion problems. We first address the fractional Poisson problem posed on  $\Omega = \mathbb{R}^d$ . In this case, the solution decays slowly with algebraic rates as  $|\mathbf{x}| \rightarrow \infty$ , even if the source term is compactly supported. As a result, some traditional discretization strategies used for the local PDE diffusion problem are not applicable here. Subsequently, we consider fractional diffusion in a bounded domain  $\Omega$  for which the solution possesses a weakly singular layer near the boundary  $\partial\Omega$ , even if the source term is smooth. This property engenders many challenges in the development and analysis of numerical schemes. Compared to, say, finite difference and finite element methods, spectral methods with specially constructed basis functions may approximate the solution of fractional diffusion problems on bounded domains with higher accuracy.

### 9.1. Spectral-Galerkin methods in unbounded domains

For  $s \in (0, 1)$ , we consider the fractional diffusion problem in  $\Omega = \mathbb{R}^d$  given by

$$\begin{cases} (-\Delta)^s u(\mathbf{x}) + cu(\mathbf{x}) = f(\mathbf{x}) & \forall \mathbf{x} \in \mathbb{R}^d \\ u(\mathbf{x}) \rightarrow 0 & \text{as } |\mathbf{x}| \rightarrow \infty, \end{cases} \quad (9.1)$$

where  $c$  denotes a given positive constant and  $f$  denotes a given source term. A weak formulation of the problem (9.1) is given as follows:

$$\begin{aligned} & \text{given a positive constant } c \text{ and } f \in H^{-s}(\mathbb{R}^d), \\ & \text{seek } u \in H^s(\mathbb{R}^d) \text{ such that} \\ & A_s(u, v) = (f, v) \quad \forall v \in H^s(\mathbb{R}^d), \end{aligned} \quad (9.2)$$

where, for all  $u, v \in H^s(\mathbb{R}^d)$ ,

$$\mathcal{A}_s(u, v) = \frac{C_{d,s}}{2} \int_{\mathbb{R}^d} \int_{\mathbb{R}^d} \frac{(u(\mathbf{y}) - u(\mathbf{x}))(v(\mathbf{y}) - v(\mathbf{x}))}{|\mathbf{y} - \mathbf{x}|^{d+2s}} d\mathbf{y} d\mathbf{x} + c(u, v)$$

with  $C_{d,s}$  is defined in (3.2). The well posedness of the problem (9.2) follows directly from the Lax-Milgram theorem.

Several successful strategies have been developed for determining approximations of solutions of local PDE diffusion problems posed on  $\mathbb{R}^d$ ; see, e.g., the survey paper (Shen and Wang 2009) and the references cited therein. One way is to truncate the domain  $\mathbb{R}^d$ , provided that the solution decays

rapidly. However, it is known that solution of the fractional diffusion equation decays slowly with a power law at infinity so that the naive truncation approach results in a relatively large error due to domain truncation<sup>3</sup>. Another approach is to design an artificial boundary condition imposed on the boundary of a truncated domain that results in the same solution within a bounded region; the use of this approach remains largely an open question in the fractional case. A third approach, which is the approach used here, does not involve domain truncation, but instead approximates the solution in terms of orthogonal functions that potentially can well approximate the solution in the unbounded domain.

For simplicity, we restrict our discussion to the one-dimensional case, i.e.,  $d = 1$ ; higher-dimensional cases can be treated in a similar manner by using tensor products of one-dimensional orthogonal polynomials.

#### 9.1.1. Approximation by Hermite polynomials

The orthonormal Hermite polynomials  $\{H_n(x)\}$  are defined by the three-term recurrence relation (Abramowitz and Stegun 1972, Mao and Shen 2017)

$$\begin{aligned} H_0 &= \pi^{-\frac{1}{4}}, & H_1(x) &= \sqrt{2}\pi^{-\frac{1}{4}}x, \\ H_{n+1} &= x\sqrt{\frac{2}{n+1}}H_n(x) - \sqrt{\frac{n}{n+1}}H_{n-1}(x) \quad \text{for } n = 1, 2, \dots \end{aligned}$$

It is well-known that those polynomials form an orthonormal basis in the weighted space  $L_w^2(\mathbb{R})$ , where the weight function is given by  $w(x) = e^{-x^2}$ . Let  $V_N^H$  denote the space spanned by the Hermite polynomials of degree less than or equal to  $N$ , and let

$$X_N^H = \{v : \sqrt{w(x)}u(x) \quad \forall u \in V_N^H\}.$$

We define the  $L_w^2(\mathbb{R})$ -projection operator  $Q_N^H : L_w^2(\mathbb{R}) \rightarrow X_N^H$  by

$$\int_{\mathbb{R}} u(x)v_N(x)w(x)dx = \int_{\mathbb{R}} (Q_N^H u)(x)v_N(x)w(x)dx \quad \forall v_N \in X_N^H.$$

We also define the modified operator  $\hat{Q}_N^H : L^2(\mathbb{R}) \rightarrow X_N^H$  by

$$\hat{Q}_N^H u = w^{\frac{1}{2}}Q_N^H(uw^{-\frac{1}{2}}) \quad \forall u \in L^2(\mathbb{R}).$$

Then, we have the approximation property

$$\|\hat{Q}_N^H u - u\|_{H^s(\mathbb{R})} \leq CN^{(\ell-m)/2}\|u\|_{\hat{H}^m(\mathbb{R})} \quad \forall s \in [0, m], \quad (9.3)$$

<sup>3</sup> However, see Remark 3.1 where it is pointed out that truncated domains may be of interest in their own right.

where  $C > 0$  does not depend on  $u$  or  $N$  and where the modified Sobolev space  $\hat{H}^m(\mathbb{R})$  comes equipped with the norm and seminorm

$$\|u\|_{\hat{H}^m(\mathbb{R})}^2 = \sum_{0 \leq k \leq m} \left\| \left( \frac{d}{dx} + x \right)^k u \right\|_{L^2(\mathbb{R})}^2 \quad \text{and} \quad |u|_{\hat{H}^m(\mathbb{R})} = \left\| \left( \frac{d}{dx} + x \right)^m u \right\|_{L^2(\mathbb{R})}^2,$$

respectively.

The Hermite-Galerkin discretization of the fractional diffusion problem (9.1) is then given as follows:

$$\begin{aligned} &\text{given a positive constant } c \text{ and } f \in H^{-s}(\mathbb{R}^d), \\ &\text{seek } u_N(x) \in X_N^H \text{ such that} \\ &\mathcal{A}_s(u_N, v_N) = (I_N^H f, v_N) \quad \forall v_N \in X_N^H, \end{aligned} \tag{9.4}$$

where  $I_N^H : C(\mathbb{R}) \rightarrow X_N$  denotes the Gauss-Hermite interpolation operator with respect to the Gauss-Hermite points (Shen, Tang and Wang 2011). Then, the standard energy estimate along with the approximation property (9.3) result in the error estimate

$$\|u - u_N\|_{H^s(\mathbb{R})} \leq CN^{s-m} |u|_{\hat{H}^m(\mathbb{R})} + CN^{1/6-\ell/2} |f|_{\hat{H}^\ell(\mathbb{R})}, \tag{9.5}$$

provided that  $u \in \hat{H}^m(\mathbb{R})$  and  $f \in \hat{H}^\ell(\mathbb{R})$ , where again  $C > 0$  does not depend on  $u$ ,  $f$ , or  $N$ . This estimate indicates that the numerical solution fails to converge exponentially, because either  $u$  and or  $f$  will decay algebraically as  $x \rightarrow \infty$ ; cf. (Mao and Shen 2017, Section 5).

The Hermite-Galerkin discretization (9.4) is simple to implement because the mass matrix is diagonal, while the stiffness matrix can be computed efficiently using the Fourier transform. An implementation of the Hermite-Galerkin method (9.4) using Fourier transforms is provided in (Mao and Shen 2017). See also (Mao and Shen 2017, Tang, Yuan and Zhou 2018) for related Hermite collocation methods, whose error estimate also depend on the Fourier transform of the solution  $u$  and the source term  $f$ .

### 9.1.2. Approximation by modified Gegenbauer polynomials

In (Tang, Wang, Yuan and Zhou 2019), the approach taken in Section 9.1.1 is extended to approximations in which the basis is constructed by using Gegenbauer polynomials that are modified using a nonlinear singular mapping. The resulting basis has proven to be better suited for approximating functions with algebraic decay rates (see, e.g., (Boyd 1987, Boyd 2001)) when compared to a classical basis based on orthogonal polynomials such as Hermite or Laguerre polynomials.

The Gegenbauer polynomials, denoted by  $G_n^\lambda(t)$  with  $t \in (-1, 1)$  and scal-

ing parameter  $\lambda > -1/2$ , are defined by the three-term recurrence relation

$$\begin{aligned} G_0^\lambda(t) &= 1, & G_n^\lambda(t) &= 2\lambda t, \\ nG_n^\lambda(t) &= 2t(n + \lambda - 1)G_{n-1}^\lambda(t) - (n + 2\lambda - 2)G_{n-2}^\lambda(t), & n &= 2, 3, \dots \end{aligned}$$

The Gegenbauer polynomials are orthogonal with respect to the weight function  $w_\lambda(t) = (1-t^2)^{\lambda-1/2}$ , and they are closely related to the hypergeometric functions (Gradshteyn and Ryzhik 2007, P. 1000) that are widely used for the analysis of fractional differential equations; see, e.g., (Ervin, Heuer and Roop 2018).

We seek approximate solutions in the space

$$X_N^G = \text{span}\{R_n^\lambda(x) : n = 0, 1, \dots, N\},$$

where the mapped Gegenbauer functions  $R_n^\lambda(x)$  are defined by

$$R_n^\lambda(x) := (1+x^2)^{-\frac{\lambda+1}{2}} G_n^\lambda\left(\frac{x}{\sqrt{1+x^2}}\right) \quad \forall x \in \mathbb{R}.$$

The  $L^2(\mathbb{R})$ -orthogonal projection operator  $Q_N^G : L^2(\mathbb{R}) \rightarrow X_N^G$  is defined by

$$\int_{\mathbb{R}} u(x)v_N(x)dx = \int_{\mathbb{R}} Q_N^G u(x)v_N(x)dx \quad \forall v_N \in X_N^G.$$

Next, let  $B_m^G(\mathbb{R})$  denote the weighted Sobolev space defined by the norm and seminorm

$$\begin{aligned} \|u\|_{B_m^G(\mathbb{R})}^2 &= \sum_{0 \leq k \leq m} \left\| (1+x^2)^{\frac{1}{4}-\frac{\lambda+m}{2}} \left( (1+x^2)^{\frac{3}{2}} \frac{d}{dx} \right)^k ((1+x^2)^{\frac{\lambda+1}{2}} u) \right\|_{L^2(\mathbb{R})}^2 \\ |u|_{B_m^G(\mathbb{R})} &= \left\| (1+x^2)^{\frac{1}{4}-\frac{\lambda+m}{2}} \left( (1+x^2)^{\frac{3}{2}} \frac{d}{dx} \right)^m ((1+x^2)^{\frac{\lambda+1}{2}} u) \right\|_{L^2(\mathbb{R})}^2, \end{aligned}$$

respectively. Then, for any  $u \in H^s(\mathbb{R}) \cap B_m^G(\mathbb{R})$  with integer  $1 \leq m \leq N+1$ ,  $s \in (0, 1)$ , and  $\lambda > -1/2$ , we have the approximation property

$$\|Q_N^G u - u\|_{H^s(\mathbb{R})} \leq C N^{s-m} |u|_{B_m^G(\mathbb{R})},$$

where  $C > 0$  does not depend on  $N$  and  $u$ .

The mapped Gegenbauer-Galerkin discretization of the fractional diffusion problem (9.1) is given as follows:

$$\begin{aligned} &\text{given a positive constant } c \text{ and } f \in H^{-s}(\mathbb{R}^d), \\ &\text{seek } u_N(x) \in X_N^G \text{ such that} \\ &\mathcal{A}_s(u_N, v_N) = (I_N^G f, v_N) \quad \forall v_N \in X_N^G, \end{aligned}$$

where  $I_N^G : C(\mathbb{R}) \rightarrow X_N^G$  denotes the mapped Gegenbauer-Gauss interpolation operator based on the Gegenbauer-Gauss quadrature points (Shen et al. 2011, Chapter 3). We then have, for any  $u \in H^s(\mathbb{R}) \cap B_m^G(\mathbb{R})$  and

$f \in B_\ell^G(\mathbb{R})$  with integers  $1 \leq m, \ell \leq N+1$  and  $\lambda > -1/2$ , the error estimate

$$\|u - u_N\|_{H^s(\mathbb{R})} \leq CN^{s-m}|u|_{B_m^G(\mathbb{R})} + CN^{-\ell}|f|_{B_\ell^G(\mathbb{R})}, \quad (9.6)$$

where  $C$  denotes a positive constant having value independent of  $N$ ,  $u$ , and  $f$ . The proof relies on the standard energy estimate as well as the approximation properties of  $Q_N^G$  and  $I_N^G$ . Compared to the Hermite-Galerkin spectral method of Section (9.1.1), we have that  $(-\Delta)^s R_n^\lambda(x)$  is not as compact as for the Hermite polynomials, but can be easily approximated by a finite series of hypergeometric functions.

### 9.1.3. Approximation by modified Chebyshev polynomials

It is noteworthy that  $|\xi|^{2s}$ , the symbol of Fourier transform of the fractional Laplacian, is non-separable so that direct extensions to higher dimensions of methods developed for the one-dimensional setting can be very complicated. To overcome this computational difficulty, in (Sheng, Shen, Tang, Wang and Yuan 2019), a reformulation of the weak formulation (9.2) by the Dunford-Taylor formula (see (Bonito et al. 2019, Theorem 4.1) and also Section (3.3.1)) is proposed and a spectral-Galerkin method is constructed having Fourier-like bi-orthogonal mapped Chebyshev polynomials as basis functions. This method leads to a diagonalized system that can be efficiently solved via the fast Fourier transform (FFT), and the approach can be easily extended to higher-dimensional problems via tensor products of the basis functions.

For any  $u, v \in H^s(\mathbb{R})$ , by the Dunford-Taylor formula, we have (see (3.13))

$$\begin{aligned} & \frac{C_{d,s}}{2} \int_{\mathbb{R}^d} \int_{\mathbb{R}^d} \frac{(u(\mathbf{y}) - u(\mathbf{x}))(v(\mathbf{y}) - v(\mathbf{x}))}{|\mathbf{y} - \mathbf{x}|^{d+2s}} d\mathbf{y} d\mathbf{x} \\ &= \frac{2 \sin(\pi s)}{\pi} \int_0^\infty t^{1-2s} \int_{\mathbb{R}^d} ((-\Delta)(I - t^2 \Delta)^{-1} u)(\mathbf{x}) v(\mathbf{x}) d\mathbf{x} dt, \end{aligned}$$

where here  $I$  denotes the identity operator. Letting  $w(\mathbf{x}) := (I - t^2 \Delta)^{-1} u(\mathbf{x})$ , we can rewrite the weak formulation (9.2) as: seek  $u \in H^s(\mathbb{R}^d)$  such that for all  $v \in H^s(\mathbb{R}^d)$

$$\mathcal{A}_s(u, v) = \frac{2 \sin(\pi s)}{\pi} \int_0^\infty t^{-1-2s} (u - w, v) dt + c(u, v) = (f, v), \quad (9.7)$$

where  $w = w(\mathbf{x}; u, t) \in H^1(\mathbb{R}^d)$  is, for any  $t > 0$ , the solution of

$$t^2(\nabla w, \nabla \psi) + (w, \psi) = (u, \psi) \quad \forall \psi \in H^1(\mathbb{R}^d). \quad (9.8)$$

The spectral-Galerkin approximation to (9.7)-(9.8) is then given as fol-

lows: find  $u_N \in X_N$  such that

$$\begin{aligned} \mathcal{A}_s(u_N, v_N) &= \frac{2 \sin(\pi s)}{\pi} \int_0^\infty t^{-1-2s} (u_N - w_N, v_N) dt + c(u_N, v_N) \\ &= (I_N f, v_N) \quad \forall v_N \in X_N^C, \end{aligned} \quad (9.9)$$

where  $w_N(\mathbf{x}; u_N, t) \in X_N^C$  is, for any  $t > 0$ , the solution of

$$t^2(\nabla w_N, \nabla \psi) + (w_N, \psi) = (u_N, \psi) \quad \forall \psi \in X_N^C. \quad (9.10)$$

To solve the numerical scheme (9.9)-(9.10), in (Sheng et al. 2019) a basis of Fourier-like mapped Chebyshev polynomials are used. Recall that the classical Chebyshev polynomials are defined by, for  $n = 0, 1, \dots$ ,

$$T_n(y) = \cos(n \arccos(y)) \quad \text{with } y \in (-1, 1).$$

Then, we define the mapped Chebyshev polynomials by

$$R_n(x) := (1 + x^2)^{-\frac{1}{2}} T_n\left(\frac{x}{\sqrt{1 + x^2}}\right), \quad x \in \mathbb{R}. \quad (9.11)$$

It is well known that the mapped Chebyshev functions are orthonormal in  $L^2(\mathbb{R})$  but are not orthogonal in  $H^1(\mathbb{R}^d)$ . Following the spirit of (Shen and Wang 2009), in (Sheng et al. 2019), the approximation space is defined by  $X_N^C = \text{span}\{R_n : n = 0, 1, \dots, N\}$  for which a Fourier-like basis that is bi-orthogonal can be constructed, i.e., the basis functions are orthogonal with respect to both the  $L^2$ - and  $H^1$ -inner products. As a result, (9.10) is diagonalizable as is (9.9), and hence they can be efficiently solved by an FFT related to Chebyshev polynomials.

The integration in terms of  $t$  in (9.9) can be evaluated exactly by using a sinc quadrature scheme (Bonito et al. 2019) whose computational cost is negligible compared with that of an FFT. Furthermore, this fast algorithm can be easily applied in higher-dimensional settings by using tensor products of the one-dimensional basis functions. The resulting complexity of solving (9.9) is then of  $\mathcal{O}(N(\log_2 N)^d)$ , where  $N$  is the number of degree of freedom along each coordinate direction. The relevant error estimate is similar to that in (9.6) with  $\lambda = 0$ .

**Remark 9.1.** Although the solution to the fractional diffusion problem (9.1) has a simple and closed form in the Fourier domain, all existing spectral methods fail to achieve an exponential convergence rate. This is because the solution generally decays at an algebraic rate at infinity, even if the source term is smooth and compactly supported. The proposed Hermite and the mapped rational/Chebyshev polynomials can only approximate exponentially decaying functions with spectral accuracy. How one designs a spectral method that accurately captures the algebraic decaying behavior of the solution to (9.1) remains a largely open problem.



All the estimates stated in this subsection are derived with respect to the energy norm, e.g.,  $H^s(\mathbb{R}^d)$ . There is, of course, interest in obtaining higher approximation rates with respect to the  $L^2(\mathbb{R}^d)$  norm. However, the approximation properties of orthogonal polynomials are derived in weighted Sobolev spaces, so that the usual duality arguments are not directly applicable here. Thus, optimal  $L^2(\mathbb{R}^d)$ -norm error estimates are still not well understood and warrant further investigation.  $\square$

### 9.2. Spectral-Galerkin methods in bounded domains

Now we turn to fractional diffusion in a bounded domain. Owing to the low regularity of the solution of the underlying problems involving the fractional Laplacian (see, e.g., (Ervin et al. 2018, Grubb 2015c, Ros-Oton and Serra 2014)), classical spectral methods cannot approximate the solution very well. In this section, we focus on the particular fractional Poisson problem (3.4) with  $g(\mathbf{x}) = 0$ , i.e., on the problem

$$\begin{cases} (-\Delta)^s u = f & \forall \mathbf{x} \in \Omega \\ u = 0 & \forall \mathbf{x} \in \Omega_{\infty} = \mathbb{R}^d \setminus \Omega, \end{cases} \quad (9.12)$$

where  $f(\mathbf{x})$  is a smooth function and  $\Omega$  is a bounded domain with a smooth boundary.

In (Mao, Chen and Shen 2016), the one-dimensional setting is considered with  $\Omega = (-1, 1)$  and  $s \in (1/2, 1)$ . In this case, the fractional Laplacian is equivalent to the *Riesz-fractional differential derivative* that is defined by, for  $u \in C_c^\infty(-1, 1)$ ,

$$-D^{2s}u(x) := -\frac{1}{2\cos((1-s)\pi)} \frac{d^2}{dx^2} \int_{-1}^1 |x-t|^{1-2s} u(t) dt = (-\Delta)^s u(x).$$

Then, the problem (9.12) is equivalent to the two-point boundary value problem: find the function  $u$  satisfying

$$\begin{aligned} -D^{2s}u(x) &= f(x) \quad \forall x \in (-1, 1), \\ u(0) &= u(1) = 0. \end{aligned} \quad (9.13)$$

The discussion in (Mao et al. 2016) is motivated by the observation that

$$(-\Delta)^s \{(1-x^2)_+^s P_n^{s,s}(x)\} = \frac{\Gamma(2s+n+1)}{\Gamma(n+1)} P_n^{s,s}(x), \quad (9.14)$$

where  $P_n^{a,b}$  with  $a, b > -1$  denotes the classical Jacobi polynomials that are orthogonal with respect to the weight function  $w^{a,b}(x) = (1-x)^a(1+x)^b$ . This implies that if the source term  $f(x)$  can be expanded in terms of the Jacobi polynomials  $P_n^{s,s}(x)$ , then the solution of the fractional diffusion problem (9.12) is a series in  $(1-x^2)_+^s P_n^{s,s}(x)$ .

By choosing the test space  $V_N = \text{span}\{P_n^{s,s}(x) : n = 0, \dots, N\}$  and the trial space  $X_N = \text{span}\{(1-x^2)_+^s P_n^{s,s}(x) : n = 0, \dots, N\}$ , a Petrov-Galerkin spectral method is given as follows: find  $u_N \in X_N$  such that, for all  $v_N \in V_N$ ,

$$\int_{-1}^1 (-\Delta)^s u_N(x) v_N(x) (1-x^2)^s dx = \int_{-1}^1 f(x) v_N(x) (1-x^2)^s dx.$$

Using the relation (9.14) and the approximation property of Jacobi polynomials (Shen et al. 2011, Thm. 3.35), the following error estimate in the weighted  $L^2$ -norm is derived in (Mao et al. 2016, Theorem 5):

$$\|u_N - u\|_{B_{-s}^0} \leq CN^{-2s-m} \|f\|_{B_s^m} \quad \text{for any integer } m \geq 0,$$

where the norm  $\|\cdot\|_{B_\lambda^m}$  is defined by

$$\|v\|_{B_\lambda^m}^2 = \sum_{j=0}^m \int_{-1}^1 |v^{(j)}|^2 (1-x^2)^{j+\lambda} dx.$$

In case that  $m$  is not an integer, the space  $B_\lambda^m$  is defined by interpolation (Guo and Wang 2004). The argument also applies to the case that  $s \in (0, 1/2]$  and  $\Omega$  is multi-interval (Acosta, Borthagaray, Bruno and Maas 2018).

The above estimate indicates the exponential convergence under the assumption that the source term  $f$  is smooth. The results in (Mao et al. 2016) extend the studies on spectral methods for solving one-sided fractional equations found in (Chen, Shen and Wang 2016b, Zayernouri and Karniadakis 2014, Zayernouri, Ainsworth and Karniadakis 2015b); see also (Mao and Karniadakis 2018, Samiee, Zayernouri and Meerschaert 2019a, Samiee, Zayernouri and Meerschaert 2019b) for general two-sided fractional equations, (Zayernouri, Ainsworth and Karniadakis 2015a) for tempered fractional diffusion equations, and (Deng, Zhang and Zhao 2019) for the study of super-convergence points.

A similar analysis may be extended to higher-dimensional cases. In (Xu and Darve 2018b), a spectral method is studied for solving the fractional Poisson problem (9.13) with  $\Omega = B_1(\mathbf{0}) \subset \mathbb{R}^d$ ,  $d = 2, 3$ , i.e., the unit ball in two or three dimension. The basic idea is to construct a spectral basis by using Jacobi polynomials and spherical harmonic polynomials (Dyda, Kuznetsov and Kwaśnicki 2017). In particular, spherical harmonic polynomials of degree  $\ell \geq 0$  form a finite dimensional space, having dimension

$$M_{d,\ell} = \frac{d+2\ell-2}{d+\ell-2} \binom{d+\ell-2}{\ell}.$$

For each  $\ell$ , we fix a linear basis for this space, denoted by  $V_{\ell,m}$  with  $m = 1, \dots, M_{d,\ell}$  that is orthonormal with respect to the surface measure on the

unit sphere. Then, the functions

$$\phi_{\ell,m,n}(\mathbf{x}) = V_{\ell,m}(\mathbf{x}) P_n^{s, \frac{d}{2} + \ell - 1}(2|\mathbf{x}|^2 - 1) \quad \text{with } \ell \geq 0, n \geq 0, 0 \leq m \leq M_{d,\ell},$$

form an orthogonal basis in  $L_w^2(\Omega)$  with respect to the weight function  $w(x) = (1 - |\mathbf{x}|^2)^s$  (Dyda et al. 2017). Analogous to (9.14), we have that

$$(-\Delta)^s((1 - |\mathbf{x}|^2)_+^s \phi_{\ell,m,n}) = \frac{2^{2s} \Gamma(s + n + 1) \Gamma(\frac{d}{2} + \ell + s + n)}{n! \Gamma(\frac{d}{2} + n)} \phi_{\ell,m,n}(\mathbf{x}).$$

Then, in (Xu and Darve 2018b), fast and accurate spectral methods were developed and analyzed based on this property and the approximation property of the Jacobi polynomials.

Unfortunately, the above argument heavily relies on the relation (9.14) so that, due to the singular behavior of the solution near the boundary, it cannot be directly applied to the fractional diffusion with lower-order terms. In (Zhang 2019), the regularity of the one-dimension fractional diffusion-reaction model

$$\begin{aligned} (-\Delta)^s u(x) + cu(x) &= f(x) \quad \forall x \in (-1, 1) \\ u(x) &= 0 \quad \forall x \in \mathbb{R} \setminus (-1, 1) \end{aligned} \quad (9.15)$$

with the constant  $s \in (0, 1)$  and  $c > 0$  is studied. In particular, it was proved there that  $(1 - x^2)^{-s}u$  belongs to  $B_s^{(2s \wedge m) + 2s}$  if  $f \in B_s^m$ . Moreover, the regularity index could be slightly improved, i.e.,

$$(1 - x^2)^{-s}u \in B_{s-1}^{(6s-\epsilon) \wedge (1+4s)} \quad \text{provided that } f \in B_{s-1}^m \quad \text{for large } m.$$

The convergence rate of the spectral method certainly deteriorates accordingly, due to a lack of sufficient solution regularity. See also (Mao and Shen 2018) for a spectral element method based on geometric meshes.

**Remark 9.2.** In one dimension, the fractional Poisson problem without lower-order terms has been comprehensively studied. The analysis of the regularity and numerical approximations rely crucially on the simple relation (9.14) which indicates that the Jacobi polynomials are suitable to approximate the solution. This is largely the main reason why problems without lower-order terms dominate the study of spectral methods for fractional diffusion. Thus, it is of significant interest to develop proper techniques for rigorously handling convection and reaction terms.

The numerical analysis of higher-dimensional fractional problems is a non-trivial endeavor. One reason is the difficulty of designing spectral methods for irregular domains. Another is due to the unclear regularity theory of (9.12) in higher-dimensional domains, even for convex polygonal domains. Therefore, it is of substantial interest to analyze spectral methods for solving fractional diffusion problems in bounded domains in higher dimensions.

Many theoretical questions, e.g., regularity in suitable spaces, appropriate selection of basis functions, and optimal convergence rates, remain largely open problems.  $\square$

## 10. Finite difference methods for the strong form of nonlocal diffusion

The AC property was first demonstrated for quadrature-based finite difference discretizations of nonlocal models in (Tian and Du 2013). Additional observations can be found in (Du and Tian 2015). In (Du, Tao, Tian and Yang 2016b), an AC quadrature difference discretization was also studied together with superconvergent nonlocal gradient recovery. In (Du et al. 2019d), quadrature rules are considered for scalar models in multidimensional spaces, resulting in AC schemes. The key to obtain AC non-variational methods in these work is to guarantee the uniform truncation errors of the numerical schemes independent of the parameter  $\delta$ . Numerical methods for the strong form of nonlocal diffusion are analyzed under the standard framework of truncation error analysis and numerical stability. Quadrature-based finite difference schemes for nonlocal diffusion equation are introduced in (Du et al. 2019d, Tian and Du 2013), and a reproducing kernel (RK) collocation method is studied in (Leng, Tian, Trask and Foster 2019). Note that although (Trask, You, Yu and Parks 2019) is referred to as an AC meshfree scheme, the numerical scheme presented there only converges to the corresponding local solution, but not to the nonlocal solution with a fixed  $\delta$ .

We denote a uniform Cartesian grid on  $\mathbb{R}^d$  as

$$\mathcal{T}_h := \{\mathbf{x}_j = h\mathbf{j} : \mathbf{j} \in \mathbb{Z}^d\}.$$

We can then rewrite the nonlocal diffusion operator at any node  $\mathbf{x}_i \in \mathcal{T}_h \cap \Omega$  as

$$\mathcal{L}_\delta u(\mathbf{x}_i) = 2 \int_{\mathcal{B}_\delta(\mathbf{0})} \frac{u(\mathbf{z} + \mathbf{x}_i) - u(\mathbf{x}_i)}{W(\mathbf{z})} W(\mathbf{z}) \gamma_\delta(|\mathbf{z}|) d\mathbf{z},$$

where  $W(\mathbf{z})$  is a weight function that is crucial to guarantee the AC property. One-dimensional problems are considered in (Tian and Du 2013) with the weight function  $W(z) = |z|$  used for  $z \in \mathbb{R}$ . In the multi-dimensional case considered in (Du et al. 2019d), the weight function  $W(\mathbf{z}) = |\mathbf{z}|^2/|\mathbf{z}|_1$  is chosen, where  $|\cdot|_1$  denotes the  $\ell_1$  norm in the  $d$ -dimensional vector space whereas  $|\cdot|$  denotes the standard Euclidean norm. The finite difference scheme on the Cartesian grid is then given by

$$\mathcal{L}_{\delta,h} u(\mathbf{x}_i) = 2 \int_{\mathcal{B}_\delta(\mathbf{0})} \mathcal{I}_h \left( \frac{u(\mathbf{z} + \mathbf{x}_i) - u(\mathbf{x}_i)}{W(\mathbf{z})} \right) W(\mathbf{z}) \gamma_\delta(|\mathbf{z}|) d\mathbf{z}, \quad (10.1)$$

where  $\mathcal{I}_h(\cdot)$  denotes the piecewise  $d$ -multilinear interpolation operator in  $\mathbf{z}$  associated with the grid  $\mathcal{T}_h$ .

There are two major features of the finite difference scheme (10.1). The first is a uniform consistency result. In this regard, the following result about what we refer to as *quadratic exactness* is proved in (Du et al. 2019d); it is a nonlocal analog of its local counterpart. That is, the fact that the centered difference approximation to the Laplacian is exact for quadratic polynomials, holds as well in the nonlocal case.

*Quadratic exactness.* For any quadratic polynomial in  $\mathbb{R}^d$  given as  $u(\mathbf{x}) = \mathbf{x} \otimes \mathbf{x} : M$ , where  $M = (m_{kj})$  denotes a constant matrix and  $\otimes$  denotes the tensor product, we have

$$\mathcal{L}_{\delta,h}u(\mathbf{x}_i) = \mathcal{L}_\delta u(\mathbf{x}_i) = \sum_k m_{kk} \quad \forall \mathbf{i}. \quad (10.2)$$

Quadratic exactness plays a vital role in the analysis of the AC property of quadrature-based finite difference schemes. It leads to the *uniform consistency result* that says that (10.1) is an  $O(h^2)$  approximation of the nonlocal diffusion operator independent of the parameter  $\delta$ , which means that the truncation error is independent of  $\delta$  for small  $\delta$ .

*Uniform truncation error.* Assume that  $u \in C^4(\overline{\Omega_\delta})$ . Then, for all  $\mathbf{x}_i \in \mathcal{T}_h \cap \Omega$ , we have that

$$|\mathcal{L}_{\delta,h}u(\mathbf{x}_i) - \mathcal{L}_\delta u(\mathbf{x}_i)| \leq C|D^4u|_\infty h^2, \quad (10.3)$$

where  $C$  denotes a constant independent of  $\delta$  and  $h$ .

With this observation, it then follows that  $u_{\delta,h}$  approximates  $u_0$  at the rate  $O(h^2 + \delta^2)$ , once numerical stability is established.

Another major feature of (10.1) is that it satisfies a discrete maximum principle, thus it is a stable numerical scheme. In fact, (10.1) can be rewritten as

$$\mathcal{L}_{\delta,h}u(\mathbf{x}_i) = \sum_{\mathbf{x}_j \in B_\delta(\mathbf{x}_i)} a_{i,j} (u(\mathbf{x}_j) - u(\mathbf{x}_i)), \quad (10.4)$$

where each  $a_{i,j}$  is a nonnegative number given by

$$a_{i,j} = \frac{2}{W(h(\mathbf{j} - \mathbf{i}))} \int_{B_\delta(\mathbf{0})} \varphi_j(\mathbf{z} + h\mathbf{i}) W(\mathbf{z}) \gamma_\delta(|\mathbf{z}|) d\mathbf{z}, \quad (10.5)$$

with  $\varphi_j$  being the piecewise multilinear basis function centered at  $\mathbf{x}_j = h\mathbf{j}$ ;  $\varphi_j$  satisfies  $\varphi_j(\mathbf{x}_i) = 0$  when  $\mathbf{i} \neq \mathbf{j}$  and  $\varphi_j(\mathbf{x}_j) = 1$ . The discrete maximum principle of (10.4) can then be easily seen from the fact  $a_{i,j} \geq 0$  for each  $\mathbf{i}$  and  $\mathbf{j}$ .

Equation (10.4) gives a second-order accurate AC finite difference scheme on uniform Cartesian grids. Higher-order finite difference schemes may also be constructed. However, the discrete maximum principle is not satisfied for higher-order methods because  $a_{i,j}$  could be negative for higher-order interpolants. In this case, one needs new techniques to study the stability of

numerical schemes, which is still an open problem except for some specialized kernels; see (Leng et al. 2019).

We note that there have been other works concerning AC schemes for nonlocal models based on the strong form. For example, AC schemes have been studied for coupled local and nonlocal models in (Du, Zhang and Zheng 2018*d*, You, Yu and Kamensky 2019, Tao et al. 2019). Implementation techniques and numerical experiments of AC schemes for problems defined in infinite domains have been presented in (Du, Han, Zheng and Zhang 2018*a*, Zhang, Yang, Zhang and Du 2017, Du et al. 2018*d*) via the development of nonlocal artificial boundary conditions. In these works, time dependent nonlocal models are considered. Similar studies have also been made for models that are nonlocal in time and space models (Chen, Du, Li and Zhou 2017) which are generalizations of models developed in (Du, Yang and Zhou 2017*b*). The latter work only considered nonlocal memory/history effects in time but the spatial interactions remained local. The former work also replaced the local spatial differential operators by nonlocal operators.

AC difference approximations of nonlinear models have also been investigated, including approximations of nonlocal hyperbolic conservation laws. From a modeling perspective, one can argue that conservation laws in integral forms may be particularly more natural than their local counterpart, especially in the presence of singular solution behaviors. Important physics might be lost in the local formulation, thus additional assumptions such as entropy conditions have to be re-introduced to maintain validity. On the other hand, it is possible to introduce nonlocal conservation laws for which appropriate entropy conditions are automatically satisfied (Du, Huang and LeFloch 2017*a*), thus retaining important physical features in the modeling process that are missing from local models. The model in (Du et al. 2017*a*) also improves the model studied in (Du, Kamm, Lehoucq and Parks 2012*b*). With AC discretization (Du and Huang 2017), the numerical convergence has been demonstrated with or without singular solutions.

We also mention some other works concerning difference approximations of nonlocal models, e.g., (Jha and Lipton 2019*b*) studied the discretization of peridynamic models involving bond-softening. Concerning the consistency between the approximations of nonlocal models and their local limits, one can also find comparisons in (Bobaru et al. 2009, Seleson et al. 2016).

In (Leng et al. 2019), the strong form of nonlocal diffusion operators is discretized by using the reproducing kernel particle method (RKPM) (Liu, Jun and Zhang 1995). The work shows the consistency and stability of the linear RK collocation scheme on quasi-uniform Cartesian grids. Define a quasi-uniform Cartesian grid on  $\mathbb{R}^d$  as

$$\mathcal{T}_h = \{\mathbf{x}_j := \mathbf{h} \odot \mathbf{j} : \mathbf{j} \in \mathbb{Z}^d\},$$

where  $\mathbf{h}$  denotes a vector in  $\mathbb{R}^d$  and  $\odot$  denotes component-wise multiplication

of vectors. We also assume that  $\mathbf{h} = h\bar{\mathbf{h}}$ , where  $h \in \mathbb{R}$  and  $\bar{\mathbf{h}}$  is a fixed unit vector in  $\mathbb{R}^d$ , so that the convergence rate will again be given in terms of  $h \in \mathbb{R}$ . RKPM provides a systematic means for generating basis functions from scattered particles such that polynomials can be exactly represented up to a certain order. Here we assume that the RK basis functions  $\{\Psi_{\mathbf{j}}(\mathbf{x})\}_{\mathbf{j} \in \mathbb{Z}^d}$  are generated with respect to the quasi-uniform Cartesian grid  $\mathcal{T}_{\mathbf{h}}$ . Then, the RK interpolation of any continuous function  $u$  is defined as

$$(\mathcal{R}_h u)(\mathbf{x}) := \sum_{\mathbf{j} \in \mathbb{Z}^d} \Psi_{\mathbf{j}}(\mathbf{x}) u(\mathbf{x}_{\mathbf{j}}).$$

In (Leng et al. 2019), the RK basis functions given by

$$\Psi_{\mathbf{j}}(\mathbf{x}) := \prod_{k=1}^d \varphi\left(\frac{[\mathbf{x}]_k - [\mathbf{x}_{\mathbf{j}}]_k}{[\mathbf{a}]_k}\right) \quad (10.6)$$

are considered, where  $[\mathbf{x}]_k$  denotes the  $k$ -th component of the vector  $\mathbf{x} \in \mathbb{R}^d$ . The vector  $\mathbf{a} \in \mathbb{R}^d$  is assumed to satisfy  $\mathbf{a} = m\mathbf{h}$  with  $m > 0$  being an even number. The function  $\varphi$  is the cubic B-spline given by

$$\varphi(x) = \begin{cases} \frac{2}{3} - 4|x|^2 + 4|x|^3 & 0 \leq |x| \leq \frac{1}{2} \\ \frac{4}{3}(1 - |x|)^3 & \frac{1}{2} \leq |x| \leq 1 \\ 0 & \text{otherwise.} \end{cases}$$

Those assumptions allow the RK approximation  $\mathcal{R}_h u$  to represent multilinear polynomials exactly, and a special synchronized convergence property is satisfied (Li and Liu 1996).

With the RK interpolation operator  $\mathcal{R}_h$  defined, the RK collocation scheme is then defined as

$$\mathcal{L}_{\delta,h} u(\mathbf{x}_i) = \mathcal{L}_{\delta}(\mathcal{R}_h u)(\mathbf{x}_i), \quad (10.7)$$

for any  $\mathbf{x}_i \in \mathcal{T}_{\mathbf{h}} \cap \Omega$ . One nice property about the interpolation operator  $\mathcal{R}_h$  defined above is that although it only reproduces multilinear polynomials exactly, it shifts quadratic polynomials by a constant, so that  $\mathcal{L}_{\delta,h}$  defined in (10.7) actually satisfies the quadratic exactness result given earlier. This property and the synchronized convergence property become the crucial reasons that render the scheme (10.7) to be AC. Indeed, (Leng et al. 2019) shows that the collocation scheme (10.7) satisfies the same uniform consistency result presented previously. The stability of the scheme, however, is a more tricky issue. In fact, all RK collocation schemes fail to satisfy the discrete maximum principle. But the linear RK basis function  $\Psi_{\mathbf{0}}$  given by (10.6) has a special property that its Fourier transform, given

by

$$\widehat{\Psi}_0(\boldsymbol{\xi}) = \prod_{k=1}^d [\mathbf{a}]_k \cdot \widehat{\varphi}([\mathbf{a}]_k [\boldsymbol{\xi}]_k) = \prod_{k=1}^d \frac{[\mathbf{a}]_k}{2} \left( \frac{\sin([\mathbf{a}]_k [\boldsymbol{\xi}]_k / 4)}{([\mathbf{a}]_k [\boldsymbol{\xi}]_k / 4)} \right)^4. \quad (10.8)$$

is always nonnegative. This result is a key observation used in (Leng et al. 2019) to show that the strong form discretization (10.7) is comparable in terms of Fourier symbols with the Galerkin approximation (5.5) with  $V_{\delta,h}$  being the span of RK basis functions (10.6). This immediately implies the stability of the scheme (10.7), because the standard Galerkin approximation is naturally stable. Stability issues again prevent us from discussing higher-order RK collocation methods because the higher-order RK basis functions fail to have purely nonnegative Fourier transforms such as one shown in (10.8). More careful investigations are needed for the stability analysis of higher-order methods. As a last comment, we note that the analysis in (Leng et al. 2019) is extended, in (Leng, Tian, Trask and Foster 2020), to the peridynamics Navier system.

## 11. Numerical methods for the strong form of fractional diffusion

In contrast to Sections 6, 7, and 9 in which the discretization of a weak formulation of a fractional diffusion model was studied, in this section we consider discretizations of a strong formulation. We consider three such approaches: quadrature-rule based finite difference methods, Monte Carlo methods, and radial basis function methods.

### 11.1. Quadrature-rule based finite difference methods

The most used class of methods for discretizing fractional diffusion models in bounded domains is quadrature-rule based finite difference methods, where their popularity stems from their simplicity. These method directly discretize the integral fractional Laplacian that features a singular, non-integrable integrand. A common approach to deal with the difficulties that singular integrals pose is to split the integral into the sum of two integrals, one isolating the singular part for which some care should be exercised, the other one having a smooth integrand so that standard quadrature rules can be used to obtain accurate approximations. This approach, which we report on here, was used in (Huang and Oberman 2014) to develop a quadrature-based finite difference scheme for approximately solving the fractional diffusion problem in one dimension.



We have the one-dimensional fractional equation and volume constraint

$$\begin{aligned} (-\Delta)^s u(x) &= C_{1,s} \int_{-\infty}^{\infty} \frac{u(x+z) - u(x)}{|z|^{1+2s}} dy = f(x) \quad \forall x \in \Omega \\ u(x) &= 0 \quad \forall x \in \Omega_{\mathcal{I}_{\infty}} \end{aligned} \quad (11.1)$$

with  $s \in (0, 1)$ ,  $\Omega = (-L, L)$  with  $L > 0$ , and  $\Omega_{\mathcal{I}_{\infty}} = \mathbb{R} \setminus \Omega$ . To discretize the problem, for a chosen integer  $N$ , let  $h = 2L/N$  denote the uniform mesh size and let  $x_j = -L + jh$ ,  $j = 0, 1, \dots, N$ , denote the grid points. In (Huang and Oberman 2014), the fractional equation in (11.1) is evaluated at the grid points  $x_j$  and then split into two integrals, i.e., we have that for  $j = 0, \dots, N$ ,

$$\begin{aligned} (-\Delta)^s u(x_j) &= C_{1,s} \int_{-\infty}^{\infty} \frac{u(x_j+z) - u(x_j)}{|z|^{1+2s}} dy \\ &= \underbrace{C_{1,s} \int_{|z| < h} \frac{u(x_j+z) - u(x_j)}{|z|^{1+2s}} dy}_{I_1} \\ &\quad + \underbrace{C_{1,s} \int_{|z| > h} \frac{u(x_j+z) - u(x_j)}{|z|^{1+2s}} dy}_{I_2}. \end{aligned} \quad (11.2)$$

For small  $h$  and  $u \in C^4(\mathbb{R})$ , the use of Taylor series results in

$$I_1 = -\frac{C_{1,s} h^{2-2s}}{2-2s} u''(x_j) + O(h^{4-\alpha}).$$

Then, approximating the second derivative by the standard central difference quotient results in

$$I_1 = -\frac{C_{1,s}}{2-2s} \left( \frac{u(x_{j+1}) - 2u(x_j) + u(x_{j-1}))}{h^{2s}} \right) + O(h^{4-2s}). \quad (11.3)$$

The second term  $I_2$  in (11.2) has a regular integrand so that term can be well approximated using standard quadrature rules. As an example, let  $I_h^k$  denote the Lagrange interpolation operator for piecewise polynomials of order less than or equal to  $k$ . Then,

$$I_2 = C_{1,s} \int_{|y| > h} \frac{u(x_j) - (I_h^k u)(x_j - y)}{|y|^{1+2s}} dy + R_h(x_j). \quad (11.4)$$

In the case that  $u \in W^{k+1,\infty}(\mathbb{R})$ , the truncation error  $R_h(x_j)$  can be bounded

by

$$\begin{aligned} |R_h(x_j)| &= C_{1,s} \left| \int_{|y|>h} \frac{(I_h^k u)(x_j - y) - u(x_j - y)}{|y|^{1+2s}} dy \right| \\ &\leq C_{1,s} \|u - I_h^k u\|_{L^\infty(\mathbb{R})} \int_{|y|>h} |y|^{-1-2s} dy \leq ch^{k+1-2s} \|u\|_{W^{k+1,\infty}(\mathbb{R})}. \end{aligned} \quad (11.5)$$

Then (11.3) and (11.4) result in a discrete approximation of the fractional Laplacian:

$$(-\Delta)^s u(x_j) = D_h u(x_j) + O(h^{\min(4,k+1)-2s}), \quad (11.6)$$

where the discrete operator  $D_h$  is defined by

$$\begin{aligned} D_h u(x_j) &:= -\frac{c_{1,s}}{2-2s} \frac{-u(x_{j-1}) + 2u(x_j) - u(x_{j+1}))}{h^{2s}} \\ &\quad + c_{1,s} \int_{|y|>h} \frac{u(x_j) - (I_h^k u)(x_j - y)}{|y|^{1+2s}} dy. \end{aligned} \quad (11.7)$$

As a result, the corresponding quadrature-based finite difference scheme is given as follows: find  $U_j$ ,  $j \in \mathbb{A} = \{1, \dots, N-1\}$ , such that

$$D_h U_j = f(x_j) \quad \text{with} \quad U_j = 0 \quad \forall j \in \mathbb{Z} \setminus \mathbb{A}. \quad (11.8)$$

A maximum principle for the above scheme (and hence its stability) was proved in (Huang and Oberman 2014) for  $k = 1$  and  $2$  by using a barrier function method, and therefore the error estimate follows immediately.

The extension of the above arguments to the multi-dimensional case is non-trivial. In (Minden and Ying 2018), the discretization of the fractional Laplacian in two and three dimension is discussed. The basic idea is to use a “window” function  $w(z) := w(|z|)$  such that  $1 - w(z) = O(|z|^p)$  as  $z \rightarrow 0$  for some positive integer  $p$ . Then, the following splitting is applied:

$$\begin{aligned} &(-\Delta)^s u(x_j) \\ &= C_{d,s} \int_{\mathbb{R}^d} \frac{u(x) - u(y) + w(|x-y|) \sum_{1 \leq |\beta| \leq 3} D^\beta u(x) (y-x)^\beta / |\beta|!}{|x-y|^{d+2s}} dy \\ &\quad - C_{d,s} \int_{\mathbb{R}^d} \frac{w(|x-y|) \sum_{1 \leq |\beta| \leq 3} D^\beta u(x) (y-x)^\beta / |\beta|!}{|x-y|^{d+2s}} dy. \end{aligned}$$

Note that the second term is regular and thus can be easily approximated by standard quadrature rules. On the other hand, by using a window function, the first term can be evaluated by the trapezoidal rule. If the grid is uniform, then the resulting scheme provides a discrete operator that is translation invariant and therefore an FFT can be used (Minden and Ying 2018, Section 3) for efficient solution.

In (Duo, van Wyk and Zhang 2018, Duo and Zhang 2019), another splitting approach is suggested, namely

$$\frac{u(x) - u(y)}{|x - y|^{d+2s}} = \left(|x - y|^{-d+\beta-2s}\right) \left((u(x) - u(y))|x - y|^{-\beta}\right)$$

for an appropriate parameter  $\beta \in (2s, 2)$ . The first term is singular but can be evaluated analytically whereas the second term is regular so it can be approximated using, e.g., the trapezoidal rule.

The discrete systems obtained by the quadrature-based finite difference methods introduced above can be Toeplitz-like, which can be tackled by using an FFT, but only for shift-invariant discretizations that usually require the use of uniform grids. As we mentioned in Section 3.3.3, the solution of the fractional Poisson equation (11.1) is weakly singular near the boundary, and hence graded meshes are preferred. In this case, discretization results in dense and unstructured matrices, and hence the storage complexity will be  $O(N^2)$  whereas the computational complexity will be  $O(N^3)$ . One promising strategy for efficiently solving the nonlocal problem (11.1) with unstructured meshes is to apply hierarchical matrices so that only linear storage and computational complexity are required; see (Xu and Darve 2018a).

In one dimension, the problem (11.1) is closely related to the fractional boundary problem involving the Riemann-Liouville fractional derivative or Riesz derivative (Podlubny 1999, Ortigueira 2006). For such problems, many finite difference methods have been studied (Meerschaert and Tadjeran 2004, Tadjeran, Meerschaert and Scheffler 2006, Çelik and Duman 2012, Meerschaert and Tadjeran 2006, Chen and Deng 2014, Ding, Li and Chen 2015) and fast algorithms (Pan, Ng and Wang 2016, Wang and Basu 2012, Wang and Du 2013, Wang and Du 2014, Zhang, Sun and Pang 2015, Lei and Sun 2013). See also the comprehensive survey (Li and Chen 2018) and the monograph (Karniadakis 2019) for details about these kind of models and their numerical approximation.

### 11.2. Monte Carlo method by Feynman-Kac formula

Since its formulation in (Kac 1949), the Feynman-Kac formula has been a powerful tool for both theoretical reformulations and practical simulations of local PDEs. The link it establishes between PDEs and related stochastic processes can be exploited to develop Monte Carlo methods that are effective, especially for the numerical simulation of high-dimensional problems (Curtiss 1950, Muller 1956, Sabelfeld and Simonov 1994, Yan, Cai and Zeng 2013).

In (Kyprianou, Osójnik and Shardlow 2018), a Monte Carlo algorithm is developed for approximately solving the fractional Poisson problem with

inhomogeneous volume constraints given by

$$\begin{aligned} (-\Delta)^s u(\mathbf{x}) &= f(\mathbf{x}) & \forall \mathbf{x} \in \Omega \\ u(\mathbf{x}) &= g(\mathbf{x}) & \forall \mathbf{x} \in \Omega_{\mathcal{I}_\infty}. \end{aligned} \quad (11.9)$$

The solution representation of (11.9) has been extensively studied from both the analytical and probabilistic perspectives; see e.g. (Bogdan and Byczkowski 1999, Bucur 2016, Ros-Oton 2016, Kyprianou et al. 2018). In particular, we assume that  $\Omega$  is bounded, that  $f \in C^{2s+\epsilon}(\overline{\Omega})$  for some  $\epsilon > 0$ , and that  $g$  is a continuous function belonging to  $L^1_{2s}(\mathbb{R}^d \setminus \Omega)$ , e.g.,

$$\int_{\mathbb{R}^d \setminus \Omega} \frac{|g(\mathbf{x})|}{1 + |\mathbf{x}|^{2s+d}} dx < \infty.$$

Then, the solution of the fractional Poisson problem (11.9) has the probabilistic representation (Kyprianou et al. 2018, Theorem 6.1)

$$u(\mathbf{x}) = \mathbb{E}_{\mathbf{x}}[g(X_{\sigma_\Omega})] + \mathbb{E}_{\mathbf{x}}\left[\int_0^{\sigma_\Omega} f(X_s) ds\right], \quad (11.10)$$

with  $\mathbb{E}_{\mathbf{x}}(\cdot)$  denoting the expected value and where  $X = (X_t, t \geq 0)$  is an isotropic  $\alpha$ -stable Lévy process with index  $\alpha = 2s$  and  $\sigma_\Omega = \inf\{t > 0 : X_t \notin \Omega\}$  is the first exit time of  $X_t$  from  $\Omega$ . In particular, let  $B(0, 1) \subset \mathbb{R}^d$  be a unit ball centred at the origin, and then for  $|y| > 1$  there holds (Blumenthal, Gettoor and Ray 1961, Theorem A)

$$\mathbb{P}_0(X_{\sigma_{B(0,1)}} \in d\mathbf{y}) = \frac{\Gamma(d/2) \sin(\pi\alpha/2)}{\pi^{d/2+1}} |1 - |\mathbf{y}|^2|^{-\alpha/2} |\mathbf{y}|^{-d} d\mathbf{y}. \quad (11.11)$$

This gives the distribution of the stable process that begins from the origin when it first exits the unit ball.

The formula (11.10) is a nonlocal analogue to the Feynman-Kac formula of the classical Laplacian, but the role of  $d$ -dimensional Brownian motion is replaced by an isotropic  $\alpha$ -stable Lévy process in  $\mathbb{R}^d$ . One significant difference to the Brownian motion is that the  $\alpha$ -stable Lévy process will exit the domain by a jump rather than hitting the boundary.

Then, the solution to (11.9) can be computed numerically by applying a Monte-Carlo sampling method, based on the Feynman-Kac formula (11.10). That is to say, if  $(X_t^i, t \leq \sigma_\Omega^i)$  are *i.i.d* copies of  $(X_t, t \leq \sigma_\Omega)$  issued from  $x \in \Omega$ , then by the law of large numbers, there holds that

$$u(x) = \lim_{n \rightarrow \infty} \frac{1}{n} \sum_{i=1}^n \left( g(X_{\sigma_\Omega^i}^i) + \int_0^{\sigma_\Omega^i} f(X_s^i) ds \right), \quad (11.12)$$

where sample paths of the stable process could be constructed by (11.11). However, the direct application of a Monte Carlo method based on the Feynman-Kac formula is inefficient, because the evaluation of  $u(x)$  requires

the simulation of a very large number of paths of  $X_t$ , beginning from the single point  $x \in \Omega$ .

One way to speed things up is to apply the *walk-on-spheres* strategy (WOS), that was first established in (Muller 1956) for the Laplace equation and then adopted in (Kyprianou et al. 2018) for the fractional Laplace equation. The WOS method does not require a complete simulation of the entire path and takes advantage of the distributional symmetry of the stochastic process  $X_t$ . Next, we briefly discuss the WOS method for solving the fractional diffusion problem (11.9) within a convex domain  $\Omega \subset \mathbb{R}^d$ ,  $d \geq 2$ .

With an arbitrary  $\mathbf{x} \in \Omega$ , we let  $\boldsymbol{\rho}_0 = \mathbf{x}$  and define  $r_1$  to be the radius of the largest sphere inscribed in  $\Omega$  that is centered at  $\boldsymbol{\rho}_0$ . Then, we set  $B_1 = \{\mathbf{x} \in \mathbb{R}^d: |\mathbf{x} - \boldsymbol{\rho}_0| < r_1\}$  and select  $\boldsymbol{\rho}_1$  according to  $X_{\sigma_{B_1}}$  under  $\mathbb{P}_{\boldsymbol{\rho}_0}$  which is known from (11.11). Repeating the argument, we construct a sequence  $\{\boldsymbol{\rho}_n\}_{n \geq 1}$  inductively. The algorithm ends at the random index  $N = \min\{n \geq 0: \boldsymbol{\rho}_n \notin \Omega\}$ . As a result, the Feynman-Kac formula (11.12) can be replaced by (Kyprianou et al. 2018, Corollary 6.4)

$$u(\mathbf{x}) = \mathbb{E}_x[g(\boldsymbol{\rho}_N)] + \mathbb{E}_x \left[ \sum_{n=0}^{N-1} r_n^\alpha \int_{|\mathbf{y}| < 1} f(\boldsymbol{\rho}_n + r_n \mathbf{y}) V_1(0, d\mathbf{y}) \right]$$

where  $V_1(0, d\mathbf{y})$  denotes the expected occupation measure of the stable process prior to exiting a unit ball centered at the origin, which is given for  $|\mathbf{y}| < 1$  by (Blumenthal et al. 1961, Corollary 4)

$$V_1(0, d\mathbf{y}) = 2^{-\alpha} \pi^{-d/2} \frac{\Gamma(d/2)}{\Gamma(s)^2} |\mathbf{y}|^{2s-d} \left( \int_0^{|\mathbf{y}|^{-2}-1} (u+1)^{-d/2} u^{s-1} du \right) d\mathbf{y}.$$

We refer interested readers to (Kyprianou et al. 2018) for more details about convergence analysis, discussion of nonconvex domain and implementation of WOS.

A multilevel Monte Carlo method based on the WOS algorithm was proposed in (Shardlow 2019) for efficiently computing the solution for the entire domain  $\Omega$ . In (Shardlow 2019, Section 5), comparisons are drawn between the multilevel WOS Monte Carlo method and the adaptive finite element method of (Ainsworth and Glusa 2017).

### 11.3. Radial basis function methods

The development, analysis and implementation of mesh-free methods using radial basis functions (RBFs) has been studied thoroughly for the integer order (local) PDEs; see (Buhmann 2000, Buhmann 2003) and the references cited therein. Compared to finite difference methods, the RBF method is seemingly easier to implement for approximately solving the nonlocal prob-

lem (11.1), especially in high dimension, because only minor modifications to existing algorithms for local PDEs are needed.

However, studies of RBF methods for fractional diffusion model is fairly scarce. In (Rosenfeld, Rosenfeld and Dixon 2019), RBF interpolants are used to approximate the fractional Laplacian of a given function through a mesh-free pseudo-spectral method. Specifically, they used the compactly supported Wendland functions  $\Phi(\mathbf{x}) = \phi_{d,k}(|\mathbf{x}|)$  defined in (Wendland 1995, Wendland 2005), where  $k$  is a smoothness parameter. With the collection of points  $X = \{\mathbf{x}_1, \mathbf{x}_2, \dots, \mathbf{x}_m\} \subset \Omega$ , the mesh size  $h$  of  $X$  is defined by

$$h_X = \sup_{\mathbf{x} \in \Omega} \min_{\mathbf{x}_j \in X} \|\mathbf{x} - \mathbf{x}_j\|_2.$$

Then, for any function  $f \in N_\Phi(\mathbb{R}^d)$ , where  $N_\Phi(\mathbb{R}^d)$  denotes the native space of the RBFs (Wendland 2005), the interpolant of  $f$  is defined by

$$I_X f(\mathbf{x}) = \sum_{j=1}^n w_j \Phi(\mathbf{x} - \mathbf{x}_j) \quad \text{such that} \quad I_X f(\mathbf{z}) = f(\mathbf{z}) \quad \forall \mathbf{z} \in X.$$

Suppose that  $\Phi \in C^{2k}(\mathbb{R}^d)$  is symmetric and strictly positive definite, and  $f \in N_\Phi(\mathbb{R}^d)$  is compactly supported. Then, by estimating the inverse Fourier transform, the following interpolation error result is proved in (Rosenfeld et al. 2019, Proposition 3.2):

$$|(-\Delta)^s(I_X f)(x) - (-\Delta)^s f(x)| \leq \left( ch_X^{k-2\beta} \|f\|_{N_\Phi(\mathbb{R}^d)} + E \right),$$

where the parameter  $\beta \in \mathbb{N}$  satisfies  $2\beta < k$  and  $2\beta - 2s > n$ . Here,  $E$  denotes the residual error that can be further bounded by applying a smooth cut-off function (Rosenfeld et al. 2019, Theorem 3.1). Numerical experiments showed no measurable difference in the resulting estimations when using the cutoff function as compared to when the cutoff function is not used (Rosenfeld et al. 2019, Section 4.1). However, the optimal convergence rate of the method without cutoff functions still remains an open question.

The above interpolation property inspires the future study of collocation methods (or Galerkin methods) using RBFs for approximately solving the fractional diffusion problem (11.1). Many interesting questions, e.g., the selection of proper RBFs, stability of numerical methods, optimal convergence rates, and adaptive algorithms are largely open and warrant further investigation. In addition, for high-dimensional problems, an additional challenge stems from the computation of the fractional Laplacian of the basis functions, which requires fast and accurate numerical approximation. See also (Lehoucq and Rowe 2016, Lehoucq, Narcowich, Rowe and Ward 2018) for a Galerkin method using RBFs for solving nonlocal diffusion with integrable kernel functions and (Pang, Chen and Fu 2015, Sun, Liu, Zhang, Pang and

Garrard 2017) for collocation methods using RBFs for solving fractional diffusion with Riemann-Liouville type fractional derivatives.

## 12. Conditioning and fast solvers

The effectiveness of nonlocal modeling and simulations relies on effectively solving the algebraic systems resulting from the discretization of nonlocal models. Thus, a good theoretical understanding of the conditioning of the stiffness matrices for nonlocal problems is important. Results in this direction has been provided, using the Fourier analysis of the point spectrum for nonlocal operators, as given in (Zhou and Du 2010); see also (Aksoylu and Mengesha 2010, Aksoylu and Parks 2011, Aksoylu and Unlu 2014, Du et al. 2012a, Seleson, Parks, Gunzburger and Lehoucq 2009) for additional discussions.

It is well-known a typical local diffusion model yields a condition number of  $\mathcal{O}(h^{-2})$  for a discretization having a meshing parameter  $h$ . The corresponding nonlocal models have condition numbers that depend, in general, on both  $\delta$  and  $h$ . For example, in (Du and Zhou 2017), sharp lower and upper bounds are given for the condition number of the stiffness matrix corresponding to a finite element discretization of a nonlocal diffusion operator based on a quasi-uniform regular triangulation. Typically, if a fractional type translation invariant kernel such as those satisfying (5.11) is used to describe nonlocal interactions, the condition number of the resulting discretized nonlocal diffusion model of  $\mathcal{O}(h^{-2s}\delta^{2s-2})$ , where, as always  $\delta$  denotes the size of the horizon parameter. In practice, both  $h$  and  $\delta$  could be small parameters so that the view that nonlocal models yield better conditioned systems than do their local counterpart should be carefully guarded. Additional detailed estimates on the conditioning of nonlocal stiffness matrixes can be found in (Aksoylu and Unlu 2014).

For effective algebraic solvers of the resulting linear system, we refer to studies on the use of Toeplitz (Wang and Tian 2012, Vollmann and Schulz 2019) and multigrid solvers (Du and Zhou 2017).

### 12.1. Fast algorithm for kernels with non-smooth truncation

In (Tian and Engquist 2019), methods based on fast multipole methods (FMMs) and hierarchical matrix techniques are developed. A key observation in (Tian and Engquist 2019) is that the non-smooth transition of the kernel function typically used in peridynamics and nonlocal diffusion models affects the effectiveness of many standard fast solvers that are based on the compression of far field interactions. A typical kernel  $\gamma$  used in practice, shown in the left plot of Figure 12.1, has a singularity at origin and its nonlocal interaction is truncated at a finite distance. The kernel is then decomposed into two parts,  $\gamma_1$  and  $\gamma_2$ , as illustrated in the middle and the

right plots in Figure 12.1. The first part ( $\gamma_1$ ) is smooth away from origin so that fast solvers using FMMS or hierarchical matrix techniques for the compression of far field interactions can be successfully applied. The second part ( $\gamma_2$ ) is smooth inside the support of its support. In (Tian and Engquist 2019), a FMM-type algorithm for the fast evaluation of nonlocal operators with such a kernel function is developed. The key idea is to compress the nonlocal interaction away from boundary of the support. This idea is depicted in Figure 12.2, where the geometric boundary of the interaction kernel centered at a certain point is finely resolved by small boxes whereas away from the boundary, large boxes are used because there the kernel function is smooth. Because the number of small boxes needed to resolve co-dimension 1 surfaces increases with dimension, the complexity of the algorithm also increases with dimension. It is shown in (Tian and Engquist 2019) that the optimal complexity  $O(N \log N)$  can be achieved for  $N$  unknowns in one dimension. In higher dimensions there is algebraic complexity  $O(N^{2-1/d})$ , where  $d$  is the spatial dimension of the problem.

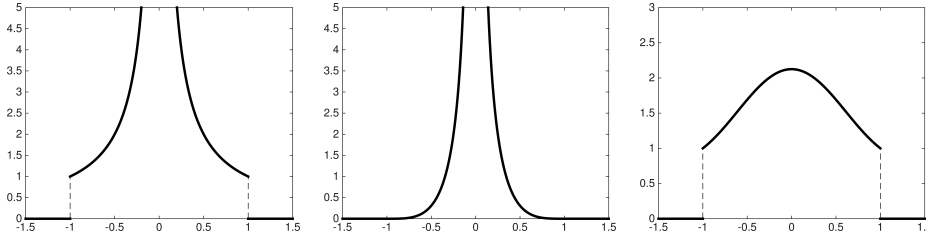


Figure 12.1. The kernel  $\gamma(x)$  (left) splits into  $\gamma_1(x)$  (middle) and  $\gamma_2(x)$  (right).

### 12.2. Conditioning and solvers for finite element discretizations of the integral fractional Laplacian model

In (Ainsworth, McLean and Tran 1999), the following results are given for the stiffness matrices resulting from finite element methods for the integral fractional Laplacian model.

For  $s < d/2$  and a family of shape regular triangulations  $\mathcal{T}_h$  with minimal and maximal element size  $h_{\min}$  and  $h$ , the spectrum of the stiffness matrix  $\mathbf{A}_s$  satisfies

$$cN_h^{-2s/d}h_{\min}^{d-2s}\mathbf{I} \leq \mathbf{A}_s \leq Ch^{d-2s}\mathbf{I}$$

and

$$cN_h^{-2s/d}\mathbf{I} \leq (\mathbf{D}^s)^{-1/2}\mathbf{A}_s(\mathbf{D}^s)^{-1/2} \leq C\mathbf{I},$$

where  $\mathbf{D}^s$  denotes the diagonal part of  $\mathbf{A}_s$ . Moreover, the condition number



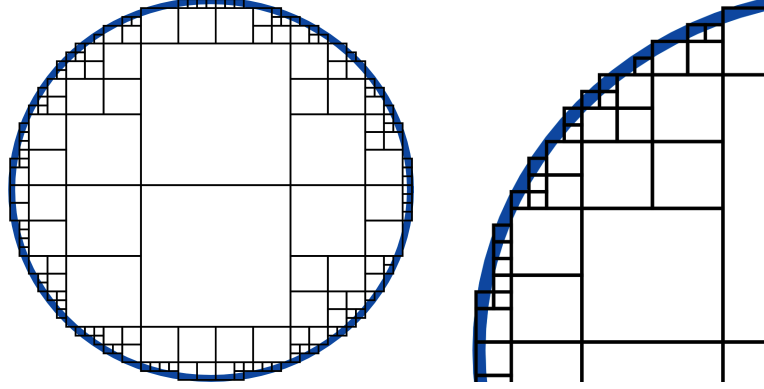


Figure 12.2. The circular region represent the interaction region corresponding to a point located at its center. The decomposition of the circular region into hierarchical boxes is illustrated, with the right plot begin a zoom in of the left one..

of the stiffness matrix satisfies

$$\kappa(\mathbf{A}_s) = C \left( \frac{h}{h_{\min}} \right)^{d-2s} N_h^{2s/d} \quad \text{and} \quad \kappa\left((\mathbf{D}^s)^{-1} \mathbf{A}_s\right) = C N_h^{2s/d}.$$

If an implicit time-stepping scheme is used for the solution of the fractional-order heat equation (18.4), systems having matrices of the form

$$\mathbf{M} + \Delta t \mathbf{A}_s$$

need to be solved, where  $\mathbf{M}$  denotes the usual finite element mass matrix. In (Ainsworth and Glusa 2017), the following result about the condition number of  $\mathbf{M} + \Delta t \mathbf{A}_s$  is given.

For a shape regular and globally quasi-uniform family of triangulations  $\mathcal{T}_h$  and for a time step  $\Delta t \leq 1$ ,

$$\kappa(\mathbf{M} + \Delta t \mathbf{A}_s) \leq C \left( 1 + \frac{\Delta t}{h^{2s}} \right).$$

More generally, for a family of triangulations that is only locally quasi-uniform and  $\Delta t \leq h_{\min}^{2s} N_h^{2s/d}$ , it holds that

$$\kappa(\mathbf{M} + \Delta t \mathbf{A}_s) \leq C \left( \frac{h}{h_{\min}} \right)^d \left( 1 + \frac{\Delta t}{h^{2s}} \right). \quad (12.1)$$

If  $\mathbf{D}^0$  is taken to be the diagonal part of the mass matrix and  $\Delta t \leq h^{2s} N_h^{2s/d}$ , then

$$\kappa\left((\mathbf{D}^0)^{-1} (\mathbf{M} + \Delta t \mathbf{A}_s)\right) \leq C \left( 1 + \frac{\Delta t}{h_{\min}^{2s}} \right). \quad (12.2)$$

These results show that for small fractional order  $s$  if the time step  $\Delta t$  is chosen small enough with respect to the mesh size, the conjugate gradient method with diagonal preconditioning will converge in a fixed number of steps. For larger fractional orders or for the steady-state problem, the number of iterations depends on the problem size. It has been shown that by applying a multigrid solver, one can restore a uniform bound on the number of iterations; see (Sauter and Schwab 2010, Hackbusch 1985, Hackbusch 1994, Ainsworth and McLean 2003, Ainsworth and Glusa 2018b, Ainsworth and Glusa 2017).

We also observe that the system matrix  $\mathbf{A}_s$  is entirely dense, owing to the nonlocal interactions. This means that for the efficient solution, efficient techniques for computing matrix-vector products with  $\mathbf{A}_s$  need to be used. In the literature, fast transforms and matrix compression (Ainsworth and Glusa 2018b, Ainsworth and Glusa 2017) have been explored. The drawback of the former is their limitation to uniform meshes, whereas the latter are more difficult to implement. Both approaches lead to quasi-optimal complexity, i.e.  $\mathcal{O}(N_h \log N_h)$  operations to solve the system.

We note that a brief discussion about solvers for extended fractional Laplacian problems is given in Remark 7.1.

## PART THREE

### Selected extensions

So far in the article, we have mostly focused on steady-state nonlocal diffusion models, including fractional models. In this part, we provide brief accounts about the extension of the models we have considered to other settings, about additional approaches for obtaining approximate solutions of the models, and about a few applications of the models.

### 13. Weakly coercive indefinite, and non-self-adjoint problems

The discussion about discretization schemes given in Part 2 dealt with problems that fall into the category of what are known as *Rayleigh-Ritz* or *strongly coercive* problems. As such, the Lax-Milgram theorem is a fundamental tool in proving well posedness of both continuous and discrete problems. In this section, we consider more general settings involving indefinite and non-self-adjoint problems, settings for which the Lax-Milgram theorem cannot be applied.

### 13.1. Indefinite and non-self-adjoint problems

Instead of the symmetric and coercive bilinear form (2.10) (see also (21.2)), we now consider bilinear forms that have neither of these properties. As such, the bilinear forms considered in this section can be used in many settings that cannot be treated using the bilinear form (2.10). The discussion here largely follows the formulations given in (Tian and Du 2020) for a more general class of parameterized problems.

The bilinear form  $\mathcal{B}_\delta(\cdot, \cdot)$  is defined on a trial space  $V_\delta$  and test space  $W_\delta$  and satisfies the following requirements.

- (i)  $\mathcal{B}_\delta$  is *bounded*: there exists a constant  $C_b > 0$  independent of  $\delta$  such that

$$\mathcal{B}_\delta(u, v) \leq C_b \|u\|_{V_\delta} \|v\|_{W_\delta} \quad \forall u \in V_\delta, v \in W_\delta.$$

- (ii) *Inf-sup condition*: there exists a constant  $C_c > 0$  independent of  $\delta$  such that

$$\inf_{u \in V_\delta} \sup_{v \in W_\delta} \frac{\mathcal{B}_\delta(u, v)}{\|u\|_{V_\delta} \|v\|_{W_\delta}} \geq C_c > 0.$$

- (iii) If  $\mathcal{B}_\delta(u, v) = 0$  for all  $u \in V_\delta$ , then  $v = 0$ .

These conditions, as first shown in (Necas 2016, Necas 1967), guarantee that the problem

$$\text{find } u(\mathbf{x}) \in V_\delta \text{ such that } \mathcal{B}_\delta(u, v) = \langle f, v \rangle \quad \forall v \in W_\delta \quad (13.1)$$

is well posed, provided that the linear functional on the right-hand side is bounded. Note that there are no symmetry or self-adjoint conditions placed on the bilinear form in (13.1). Note also that the discrete inf-sup condition is automatically satisfied in the case of coercive self-adjoint problems with  $V_{\delta,h} = W_{\delta,h}$ . Otherwise, it has to be verified for the chosen finite element spaces and the problem under consideration. Problems such as (13.1) that feature different test and trial spaces are often referred to as *Petrov-Galerkin* formulations. If  $W_\delta = V_\delta$ , then (13.1) is often referred to as a *weakly-coercive* formulation.

Conforming discretizations are defined, as introduced in (Tian and Du 2020) for the parameterized setting under consideration here, by choosing approximation subspaces  $V_{\delta,h} \subset V_\delta$  and  $W_{\delta,h} \subset W_\delta$  satisfying the following requirements.

1. For a given  $\delta \in (0, \delta_0)$ , the family  $\{W_{\delta,h}, h \in (0, h_0]\}$  of discrete subspaces of  $W_\delta$  is dense in  $W_\delta$  as  $h \rightarrow 0$ .
2. *Discrete inf-sup condition*: there exists a constant  $\tilde{C}_c > 0$ , independent of  $\delta$  and  $h$ , such that

$$\inf_{u \in V_{\delta,h}} \sup_{v \in W_{\delta,h}} \frac{\mathcal{B}_\delta(u, v)}{\|u\|_{V_\delta} \|v\|_{W_\delta}} \geq \tilde{C}_c > 0.$$

These conditions, as first shown in (Babuska 1971, Babuska and Aziz 1972), guarantee that for a given  $\delta \in (0, \delta_0)$  the problem

$$\text{find } u(\mathbf{x}) \in V_{\delta,h} \text{ such that } \mathcal{B}_\delta(u, v) = \langle f, v \rangle \quad \forall v \in W_{\delta,h} \quad (13.2)$$

is well posed. Note that the independence of the constants  $C_b, C_c$  and  $\tilde{C}_c$  on the parameter  $\delta$  is not required if one is only interested in solving the problem for a fixed  $\delta$ , as in the original theory of (Babuska 1971, Babuska and Aziz 1972). It is imposed here for the study of asymptotic compatibility discussed next in section 13.2 (Tian and Du 2020).

The problem (13.1) includes several important settings such as nonlocal mixed finite element methods (see Section 13.3) and nonlocal convection-diffusion problems (see Section 14), nonlocal diffusion models and bond based peridynamic models involving both attractive and repulsive interactions (Mengesha and Du 2013), and nonlocal systems such as the nonlocal Stokes equation introduced in (Du and Tian 2019, Lee and Du 2019b).

### 13.2. Asymptotically compatible schemes

The discrete problem (13.2) involves the horizon parameter  $\delta$  and the grid-size parameter  $h$  so that the asymptotic compatibility of particular choices of finite element spaces should be questioned. An study of this question is given in (Tian and Du 2020) based on an extension of the original AC framework presented in (Tian and Du 2014). The latter deals with only symmetric and coercive bilinear forms of the types similar to (2.10) and (21.2).

Concerning the discrete approximations, in addition to the requirements (1) and (2) listed in Section 13.1, we impose the following requirement (Tian and Du 2020).

3. The family of discrete subspaces of  $\{W_{\delta,h}\}$  is *asymptotically dense* in  $W_0$  as  $\delta \rightarrow 0$  and  $h \rightarrow 0$ , in the sense of the definition (5.6). Here,  $W_0$  refers to the energy space for the original continuum local PDE problem corresponding to (13.1) and (13.2).

Now any scheme that satisfies requirements (1), (2), and (3) is provably an AC scheme (Tian and Du 2020).

### 13.3. Mixed finite element methods

PDE equations such as  $-\nabla \cdot (\mathbf{D}\nabla u)$  are often derived by first postulating a balance law  $\nabla \cdot \mathbf{w} = f$  and choosing a constitutive (Darcy, Fick, Fourier, Ohm, etc.) law  $\mathbf{w} = -\mathbf{D}\nabla u$ . In some settings, there are advantages to directly solving the two first-order equations instead of the single second-order equation, perhaps the most important and useful being that well posedness

can be proved for  $u \in L^2(\Omega)$  instead of  $H^1(\Omega)$  as is the case for the second-order equation. On the other hand, there are problems that are most often posed as a mixed formulation, the most common being the Stokes equations for incompressible flows.

One can mimic the local setting by recasting the problem (1.5) with  $\mathcal{L}_\delta u = -\mathcal{D}_\delta \cdot (\mathcal{D}_\delta^* u)$  in  $\Omega$  and with, say,  $u = 0$  on  $\Omega_{\mathcal{I}_\delta}$ , into the equivalent mixed formulation

$$\mathcal{D}_\delta \boldsymbol{\nu}(\mathbf{x}, \mathbf{y}) = f(\mathbf{x}) \quad \text{and} \quad \boldsymbol{\nu}(\mathbf{x}, \mathbf{y}) = \mathcal{D}_\delta^* u \quad \forall \mathbf{x} \in \Omega \quad (13.3)$$

along with  $u(\mathbf{x}) = 0$  for all  $\mathbf{x} \in \Omega_{\mathcal{I}_\delta}$ .

$$\begin{cases} (\boldsymbol{\nu}(\mathbf{x}, \mathbf{y}), \boldsymbol{\mu}(\mathbf{x}, \mathbf{y})) - (\mathcal{D}_\delta \boldsymbol{\mu}(\mathbf{x}, \mathbf{y}), u(\mathbf{x})) = 0 & \forall \boldsymbol{\mu}(\mathbf{x}, \mathbf{y}) \in \Omega \\ (\mathcal{D}_\delta \boldsymbol{\nu}(\mathbf{x}, \mathbf{y}), v(\mathbf{x})) = (f(\mathbf{x}), v(\mathbf{x})) & \forall v \in \Omega \end{cases} \quad (13.4)$$

along with  $u(\mathbf{x}) = 0$  for all  $\mathbf{x} \in \Omega_{\mathcal{I}_\delta}$ , where  $(\cdot, \cdot)$  denotes  $L^2$  inner products and the pairs  $\boldsymbol{\nu}, \boldsymbol{\mu}$  and  $u, v$  belong to appropriate function spaces.

The problem (13.4) can be treated as an example of the problem (13.1) with the bilinear form

$$\begin{aligned} \mathcal{B}_\delta((\boldsymbol{\nu}, u), (\boldsymbol{\mu}, v)) &= (\boldsymbol{\nu}(\mathbf{x}, \mathbf{y}), \boldsymbol{\mu}(\mathbf{x}, \mathbf{y})) - (\mathcal{D}_\delta \boldsymbol{\mu}(\mathbf{x}, \mathbf{y}), u(\mathbf{x})) \\ &\quad + (\mathcal{D}_\delta \boldsymbol{\nu}(\mathbf{x}, \mathbf{y}), v(\mathbf{x})). \end{aligned}$$

Finite element discretizations of nonlocal models based on mixed formulations can be found in (Du, Ju and Lu 2019a, Du et al. 2019b) for integrable nonlocal interaction kernels that recover the local Discontinuous Galerkin (LDG) discretization of the local PDE problem as  $\delta \rightarrow 0$ . The nonlocal Stokes model is another example that can be formulated as a system in mixed form; see the discussions in (Du and Tian 2019, Lee and Du 2019b) in which spectral and finite difference approximations have also been analyzed in a periodic boundary condition setting.

## 14. Nonlocal convection-diffusion problems

In this section we consider nonlocal analogs of the local convection-diffusion (also referred to as advection-diffusion) problem

$$\begin{cases} -\nabla \cdot (\mathbf{D} \nabla u) + \nabla \cdot (\mathbf{U} u) = f & \forall \mathbf{x} \in \Omega \\ u = 0 & \forall \mathbf{x} \in \partial\Omega, \end{cases} \quad (14.1)$$

where  $\mathbf{U}(\mathbf{x})$  denotes a given velocity field and  $\mathbf{D}(\mathbf{x})$  denotes a given symmetric, positive definite matrix. The most common approach towards defining a nonlocal convection-diffusion model is to replace the second-order diffusion term in (14.1) by a nonlocal analog  $-\mathcal{L}u$  but to keep the convection term as it is in (14.1). Such classical convection–nonlocal diffusion problems have been investigated for fractional models, including their connection to Lévy jump processes; see, e.g., (Meerschaert and Sikorskii 2012).

However, we consider fully nonlocal analogs of (14.1) in which the convection term in (14.1) is also replaced by a nonlocal analog. As a result, the nonlocal convection-diffusion models we consider feature non-symmetric kernels  $\gamma_\delta(\mathbf{x}, \mathbf{y})$ , so that they also can be viewed as modeling non-symmetric diffusion. Among other description of non-symmetric diffusion that are not necessarily related to stochastic processes, we mention (Baeumer and Meerschaert 2010, Meerschaert, Benson and Bäumer 1999, Meerschaert and Sikorskii 2012) where the equations are set either in free space or in bounded domains, (Ervin and Roop 2007) where the same problem is treated in a variational setting, in (Felsinger, Kassmann and Voigt 2015) where a variational formulation of non-symmetric diffusion for integrable and non-integrable kernels is analyzed, and in (Andreu, Mazón, Rossi and Toledo 2010) where the strong form of non-symmetric diffusion equations for integrable, positive, and translation invariant kernels is considered.

Based on (D'Elia, Du, Gunzburger and Lehoucq 2017), we consider the most general form of a nonlocal analog of (14.1), treating the two nonlocal terms as separate phenomena. Note that (D'Elia et al. 2017) is a generalization of (Du, Huang and Lehoucq 2014) to a more general class of kernels.

#### 14.1. Non-symmetric kernels and nonlocal convection-diffusion operators

Let  $\mathcal{L}_{cd,\delta}$  denote the nonlocal convection-diffusion operator defined as

$$-\mathcal{L}_{cd,\delta}u(\mathbf{x}) := \mathcal{D}_{d,\delta_d}(\Theta\mathcal{D}_{d,\delta_d}^*u)(\mathbf{x}) + \mathcal{D}_{c,\delta_c}(\mu u)(\mathbf{x}), \quad (14.2)$$

where  $\mathcal{D}_{d,\delta_d}$  and  $\mathcal{D}_{c,\delta_c}$  are nonlocal divergence operators associated with the anti-symmetric functions  $\alpha_d(\mathbf{x}, \mathbf{y})$  and  $\alpha_c(\mathbf{x}, \mathbf{y})$  and where  $\mu(\mathbf{x}, \mathbf{y}) = \mu(\mathbf{y}, \mathbf{x})$  is a given function. Note that we allow for different horizons and different kernel functions for the diffusion and convection terms. We refer to the second-order tensor  $\Theta(\mathbf{x}, \mathbf{y})$  as the nonlocal diffusion tensor (see Section 1.1) and to the vector  $\mu(\mathbf{x}, \mathbf{y})$  as the nonlocal convection “velocity.” Specifically, from (1.17), we have

$$\begin{aligned} & \mathcal{D}_{d,\delta_d}(\Theta\mathcal{D}_{d,\delta_d}^*u)(\mathbf{x}) \\ &= -2 \int_{\mathbb{R}^d} (u(\mathbf{y}) - u(\mathbf{x})) \alpha_d(\mathbf{x}, \mathbf{y}) \cdot (\Theta(\mathbf{x}, \mathbf{y}) \alpha_d(\mathbf{x}, \mathbf{y})) \mathcal{X}_{B_{\delta_d}(\mathbf{x})}(\mathbf{y}) d\mathbf{y} \end{aligned}$$

and similarly, from (1.13) with  $\nu(\mathbf{x}, \mathbf{y}) = \mu(\mathbf{x}, \mathbf{y})u(\mathbf{x})$ , we have

$$\begin{aligned} \mathcal{D}_{c,\delta_c}(\mu u)(\mathbf{x}) &= \int_{\mathbb{R}^d} (\mu(\mathbf{x}, \mathbf{y})u(\mathbf{x}) + \mu(\mathbf{y}, \mathbf{x})u(\mathbf{y})) \cdot \alpha_c(\mathbf{x}, \mathbf{y}) \mathcal{X}_{B_{\delta_c}(\mathbf{x})}(\mathbf{y}) d\mathbf{y} \\ &= \int_{\mathbb{R}^d} (u(\mathbf{x}) + u(\mathbf{y})) \mu(\mathbf{x}, \mathbf{y}) \cdot \alpha_c(\mathbf{x}, \mathbf{y}) \mathcal{X}_{B_{\delta_c}(\mathbf{x})}(\mathbf{y}) d\mathbf{y}. \end{aligned}$$

Setting

$$\begin{aligned} \gamma_{cd,\delta}(\mathbf{x}, \mathbf{y}) := & \underbrace{2\boldsymbol{\alpha}_d(\mathbf{x}, \mathbf{y}) \cdot (\boldsymbol{\Theta}(\mathbf{x}, \mathbf{y})\boldsymbol{\alpha}_d(\mathbf{x}, \mathbf{y}))\mathcal{X}_{B_{\delta_d}(\mathbf{x})}(\mathbf{y})}_{\text{symmetric part } \gamma_{d,\delta_d}(\mathbf{x}, \mathbf{y})} \\ & - \underbrace{\boldsymbol{\mu}(\mathbf{x}, \mathbf{y}) \cdot \boldsymbol{\alpha}_c(\mathbf{x}, \mathbf{y})\mathcal{X}_{B_{\delta_c}(\mathbf{x})}(\mathbf{y})}_{\text{anti-symmetric part } \gamma_{c,\delta_c}(\mathbf{x}, \mathbf{y})}, \end{aligned} \quad (14.3)$$

we can rewrite (14.2) as

$$\mathcal{L}_{cd,\delta}u(\mathbf{x}) = \int_{\mathbb{R}^d} (u(\mathbf{y})\gamma_{cd,\delta}(\mathbf{y}, \mathbf{x}) - u(\mathbf{x})\gamma_{cd,\delta}(\mathbf{x}, \mathbf{y})) d\mathbf{y} \quad \forall \mathbf{x} \in \mathbb{R}^d. \quad (14.4)$$

In the case of integrable kernel functions and for  $\boldsymbol{\alpha}_c(\mathbf{x}, \mathbf{y}) = \boldsymbol{\alpha}_d(\mathbf{x}, \mathbf{y})$  and  $\delta_d = \delta_c$ , this non-symmetric diffusion operator and the corresponding initial value problem are analyzed in (Du et al. 2014).

Note that with  $\delta = \max\{\delta_d, \delta_c\}$ , we have

$$\gamma_{cd,\delta}(\mathbf{x}, \mathbf{y}) = 0 \quad \forall \mathbf{y} \notin B_\delta(\mathbf{x}). \quad (14.5)$$

Also note that although  $\boldsymbol{\alpha}_d(\mathbf{x}, \mathbf{y})$  and  $\boldsymbol{\alpha}_c(\mathbf{x}, \mathbf{y})$  are often radial functions, in general,  $\boldsymbol{\Theta}(\mathbf{x}, \mathbf{y})$  and  $\boldsymbol{\mu}(\mathbf{x}, \mathbf{y})$  are not, so that, also in general,  $\gamma_{cd,\delta}(\mathbf{x}, \mathbf{y})$  is not radial nor translationally invariant. See Remark 2.3.

In (Tian, Ju and Du 2015, Tian, Ju and Du 2017, Lee and Du 2019a), AC discretizations of nonlocal-convection diffusion problems were considered. In (Du et al. 2014), a convection-diffusion operator in one dimension was considered which turns out to be a special case of the general nonlocal convection diffusion operator (14.2) if one chooses  $\delta_d = \delta_c$ ,  $\boldsymbol{\Theta}(x, y) = \kappa = \text{constant}$ ,  $(\alpha_d(x, y))^2 = \sigma_{d,\delta}(|y - x|)$ ,  $\mu(x, y) = U$  a constant, and  $\alpha_c(x, y) = (y - x)\sigma_{c,\delta}(|y - x|)$ , with  $\sigma_{d,\delta}(\cdot)$  and  $\sigma_{c,\delta}(\cdot)$  being even functions having unit second moments. The resulting operator is given by

$$\begin{aligned} \mathcal{L}_{cd,\delta}u(x) = & 2\kappa \int_{\mathbb{R}} (u(y) - u(x))\sigma_{d,\delta}(|y - x|)dy \\ & - U \int_{\mathbb{R}} (u(y) + u(x))(y - x)\sigma_{c,\delta}(|y - x|)dy \end{aligned}$$

The local counterpart of the operator this operator is  $\mathcal{L}_0u(x) = \kappa u''(x) + Uu'(x)$ . One may also connect this nonlocal convection diffusion models with non-symmetric jump processes; see (Du et al. 2014).

Other nonlocal convection-diffusion models are presented in (Tian et al. 2017), including some that are reminiscent of state-based peridynamic models. For example, a conservative formulation is defined by the nonlocal

convection-diffusion operator

$$\begin{aligned} & \mathcal{L}_{cd,\delta}u(\mathbf{x}) \\ &= \int_{\Omega \cup \Omega_{\mathcal{I}_\delta}} (A(\mathbf{x}) + A(\mathbf{y}))(u(\mathbf{y}) - u(\mathbf{x}))\sigma_{d,\delta}(|\mathbf{y} - \mathbf{x}|)(|\mathbf{y} - \mathbf{x}|)\mathcal{X}_c(\mathbf{x}, \mathbf{y}) d\mathbf{y} \\ &+ \int_{\Omega \cup \Omega_{\mathcal{I}_\delta}} (\mathbf{b}(\mathbf{x})u(\mathbf{x})\mathcal{X}_c(\mathbf{x}, \mathbf{y}) + \mathbf{b}(\mathbf{y})u(\mathbf{y})\mathcal{X}_c(\mathbf{y}, \mathbf{x})) \cdot (\mathbf{y} - \mathbf{x})\sigma_{c,\delta}(|\mathbf{y} - \mathbf{x}|) d\mathbf{y}, \end{aligned}$$

where we have the indicator function

$$\mathcal{X}_c(\mathbf{x}, \mathbf{y}) = \begin{cases} 1 & \text{if } |\mathbf{y} - \mathbf{x}| < \delta \text{ and } \mathbf{b}(\mathbf{x}) \cdot (\mathbf{y} - \mathbf{x}) > 0 \\ 0 & \text{otherwise,} \end{cases}$$

which is generically non-symmetric and is dependent on the velocity field  $\mathbf{b}(\mathbf{x})$ . This operator can be shown to also be a special case of operator given in (14.2). Its local counterpart is  $\mathcal{L}_0u(\mathbf{x}) = \nabla \cdot (A(\mathbf{x})\nabla u(\mathbf{x})) + \nabla \cdot (\mathbf{b}(\mathbf{x})u(\mathbf{x}))$ .

Although AC discretizations of the models using these operators have been discussed in (Tian et al. 2015, Tian et al. 2017, Lee and Du 2019a), the attendant analyses are done using different techniques and for specialized kernels. One may apply the general framework given in (Tian and Du 2020) to possibly offer a unified treatment of systems of non-self-adjoint problems. Indeed, additional studies on asymptotically compatible schemes may also shed new light on improving the robustness of numerical methods based on various nonlocal smoothing approaches that are in use for local PDE models such as the smoothed particle hydrodynamics through the construction of well-posed nonlocal models such as the nonlocal Stokes equation considered in (Du and Tian 2019, Lee and Du 2019a).

#### 14.1.1. Steady-state nonlocal convection-diffusion problems

The nonlocal analog of (14.1) is given by

$$\begin{cases} -\mathcal{L}_{cd,\delta}u = f & \mathbf{x} \in \Omega \\ u = 0 & \mathbf{x} \in \Omega_{\mathcal{I}}. \end{cases} \quad (14.6)$$

Weak formulations of corresponding to (14.6) can be defined in the usual way. Simplifying some notation, for  $\ell = d$  or  $\ell = c$ , one can define the constrained energy space

$$V_\ell^0 := \{v \in L^2(\Omega \cup \Omega_{\mathcal{I}_\delta}) : |v|_{V_\ell^0} < \infty \text{ and } v = 0 \text{ on } \Omega_{\mathcal{I}_\delta}\}$$

for which the semi-norm

$$|v|_{V_\ell^0} := \frac{1}{2} \int_{\Omega \cup \Omega_{\mathcal{I}_\delta}} \int_{\Omega \cup \Omega_{\mathcal{I}_\delta}} |\mathcal{D}_\ell^*(v)(\mathbf{x}, \mathbf{y})|^2 \gamma_{d,\delta_\ell}(\mathbf{x}, \mathbf{y}) d\mathbf{y} d\mathbf{x}$$

is a norm. We assume that the norm  $|v|_{V_\ell^0}$  satisfies the nonlocal Poincaré inequality  $\|v\|_{L^2(\Omega \cup \Omega_{\mathcal{I}_\delta})} \leq C_p |v|_{V_\ell^0}$  for all  $v \in V_d^0$  and that  $V_d \subset V_c$  so that



$|v|_{V_\varepsilon^0} \leq |v|_{V_d^0}$ . The latter assumption implies that solution operators for nonlocal diffusion problems under consideration effect greater smoothing compared to those for nonlocal convection problems, as is the case for local partial differential operators.

Let the bilinear form  $\mathcal{A}_{cd,\delta}(\cdot, \cdot)$  be defined, for all  $u, v \in V_d^0$ , by

$$\begin{aligned} \mathcal{A}_{cd,\delta}(u, v) = & \int_{\Omega \cup \Omega_{\mathcal{I}_\delta}} \int_{\Omega \cup \Omega_{\mathcal{I}_\delta}} \mathcal{D}_{d,\delta}^*(u)(\mathbf{x}, \mathbf{y}) \cdot (\Theta \mathcal{D}_{d,\delta}^* v)(\mathbf{x}, \mathbf{y}) d\mathbf{y} d\mathbf{x} \\ & - \int_{\Omega} \mathcal{D}_{c,\delta}(\boldsymbol{\mu} u)(\mathbf{x}) v(\mathbf{x}) d\mathbf{x} \end{aligned} \quad (14.7)$$

and let the linear functional  $\langle f, v \rangle$  be defined, for all  $v \in V_d^0$ , by

$$\langle f, v \rangle = \int_{\Omega} f(\mathbf{x}) v(\mathbf{x}) d\mathbf{x}. \quad (14.8)$$

Then, a weak formulation of (14.6) is given as follows: given  $f$  belonging to the dual space of  $V_d^0$ , find  $u \in V_d^0$  that satisfies

$$\mathcal{A}_{cd,\delta}(u, v) = \langle f, v \rangle \quad \forall v \in V_d^0. \quad (14.9)$$

In (D'Elia et al. 2017), the well posedness of (14.9) is proved using three different approaches. Here, we state results that mimic what is obtained for local convection-diffusion problems. Specifically,

- if  $f(\mathbf{x})$  belongs to the dual space of  $V_d^0$
- if  $\Theta(\mathbf{x}, \mathbf{y})$  is such that there exist  $\underline{\vartheta}, \bar{\vartheta} > 0$  satisfying

$$0 < \underline{\vartheta} \leq \inf_{\mathbf{x} \in \mathbb{R}^d} (\min_i \theta_i) \quad \text{and} \quad \sup_{\mathbf{x} \in \mathbb{R}^d} (\max_i \theta_i) \leq \bar{\vartheta} < \infty, \quad (14.10)$$

where  $\theta_i$  denote the singular values of  $\Theta$

- if  $\boldsymbol{\mu}$  is such that  $C_p^2 \|\mathcal{D}_c \boldsymbol{\mu}\|_\infty \leq 2\underline{\vartheta}$  and  $\|\boldsymbol{\mu}\|_\infty \leq \bar{\mu}$ ,

then the problem (14.9) has a unique solution  $u \in V_d^0$ . Furthermore, that solution satisfies the a priori estimate

$$|u|_{V_d^0} \leq C \|f\|_{V_d'}, \quad (14.11)$$

where  $C = \frac{1}{C_{\text{coer}}}$  with  $C_{\text{coer}} = \underline{\vartheta} - \frac{1}{2} C_p^2 \|\mathcal{D}_c \boldsymbol{\mu}\|_\infty$  and  $C_{\text{coer}}$  denotes the coercivity constant for the bilinear form  $\mathcal{A}_{cd,\delta}(\cdot, \cdot)$ . Note that the above analysis is effective for diffusion dominated problems. For the convection dominated case, one may use the formulation in (Tian and Du 2020) discussed in Section 13.1 to get results in more general cases.

## 15. Inverse problems

Among the many challenges faced when dealing with nonlocal problems, we have, even more so than for local PDE problems, that mathematical models

are not known with exactitude, e.g., source terms, volume constraint data, coefficients, and even the functional form of the kernel itself may be unknown or subject to uncertainty. If there are experimental data or other a priori information (that may be sparse and/or noisy) available about the state of the system or about an output of interest that depends on the state, one can then resort to control or optimization strategies to identify the unknown entities and thus define a data-driven mathematical model that is more faithful to the physics being considered.

Here we consider inverse problems for the nonlocal diffusion problem (1.5) in which the boundary operator  $\mathcal{V}$  could correspond to Dirichlet, Neumann, or Robin volume constraints. Let  $V(\Omega \cup \Omega_{\mathcal{I}})$  denote a function space for the state  $u(\mathbf{x})$  and let  $W$  denote a set of controls that could consist of function spaces or parameter vectors or a combination of both. Then, a general inverse problem for nonlocal diffusion is given as follows:

$$\begin{aligned} & \text{seek } u(\mathbf{x}) \in V(\Omega \cup \Omega_{\mathcal{I}}) \text{ and } \mu \in W \text{ such that} \\ & \min_{\mu \in W} \mathcal{J}(u; \mu) + \mathcal{R}(\mu) \\ & \text{subject to (1.5) being satisfied.} \end{aligned} \tag{15.1}$$

In (15.1),  $\mathcal{J}(\cdot; \cdot)$  denotes a cost functional that depends on the state and control whereas  $\mathcal{R}(\cdot)$  denotes a regularization functional that serves to guarantee the well posedness of the problem. The control set  $W$  could contain data functions such as  $f$ ,  $g$ , and  $\Theta$  and also parameters appearing in the model definition such as the horizon  $\delta$  or the fractional exponent  $s$  if (1.5) represents a fractional Laplacian problem. The functions may be parameterized in which case  $W$  only contains a parameter vector. Additionally, the control set may contain constraints on the control; constraints on the state may be also be imposed; see Section 16 for an example of the latter. In some such cases, the regularization term in (15.1) may not be needed because such constraints may be sufficient to guarantee well posedness.

The literature about the control and optimization of nonlocal problems is still limited; however, interest in such topics in the setting of nonlocal diffusion is quickly growing. Recent studies in this direction focus on the well posedness and stability of the minimization problem (15.1), the asymptotic behavior of its solution, and its numerical discretization. In particular, with respect to the latter, numerical convergence analyses, error estimates, and solver performance are of interest. In this section, we provide brief reviews of selected contributions devoted to the control and optimization of nonlocal problems, including fractional models, treating both control and identification problems.

### 15.1. Inverse problems for nonlocal diffusion

In this section we focus on operators of the form of (1.6) with  $\gamma_\delta(\mathbf{x}, \mathbf{y})$  given by (2.16), i.e., we have

$$\begin{aligned}\mathcal{L}_\delta u(\mathbf{x}) &= \mathcal{D}_\delta(\Theta_\delta \mathcal{D}^* u)(\mathbf{x}) = -2 \int_{\Omega \cup \Omega_{\mathcal{I}_\delta}} (u(\mathbf{y}) - u(\mathbf{x})) \gamma_\delta(\mathbf{x}, \mathbf{y}) d\mathbf{y} \\ &= -2 \int_{B_\delta(\mathbf{x})} \theta_\delta(\mathbf{x}, \mathbf{y}) (u(\mathbf{y}) - u(\mathbf{x})) \phi_\delta(\mathbf{x}, \mathbf{y}) d\mathbf{y} \quad \forall \mathbf{x} \in \Omega.\end{aligned}\tag{15.2}$$

#### 15.1.1. Distributed optimal control for a matching functional

We consider the minimization problem (15.1) with the state space  $V(\Omega \cup \Omega_{\mathcal{I}}) = V(\Omega \cup \Omega_{\mathcal{I}_\delta})$ , the operator  $\mathcal{L}$  now given by (15.2), and with perhaps the most commonly used cost functional for both PDE and nonlocal optimal control problems, namely

$$\mathcal{J}(u; \mu) = \frac{1}{2} \|u - \hat{u}\|_{U(\Omega)}^2 + \frac{\beta}{2} \|\mathcal{M}(\mu)\|_W^2,\tag{15.3}$$

where the first term is usually referred to as a *matching functional*, the second term as *Tikhonov regularization*, and the given function  $\hat{u}(\mathbf{x})$  for  $\mathbf{x} \in \Omega$  as the *target function*. The operator  $\mathcal{M}$  could be, e.g., a local derivative or a nonlocal operator such as  $\mathcal{D}_\delta^*$ , that is chosen with the purpose of keeping  $\mathcal{M}(\mu)$  under control and to either guarantee well posedness or improve the conditioning of the problem. Furthermore,  $\hat{u}$  need not belong to state space  $V(\Omega \cup \Omega_{\mathcal{I}_\delta})$  and, in (15.3), we have norms  $\|\cdot\|_{U(\Omega)}$  and  $\|\cdot\|_W$  that are well defined for  $\hat{u} \in U(\Omega)$  and  $\mathcal{M}(\mu)$  with  $\mu \in W$ , respectively. Often, target functions are not regular so that a reasonable choice is  $U(\Omega) = L^2(\Omega)$ .

Perhaps (D'Elia and Gunzburger 2014) is the first work that analyzes this problem for integrable and non-integrable kernel functions  $\phi_\delta(\mathbf{x}, \mathbf{y})$ , albeit for  $\theta = 1$  and  $\mathcal{V}u = u$ , i.e., for Dirichlet volume constraints. Specifically, the problem considered is to find the optimal forcing term  $f$  such that the nonlocal solution  $u$  is as close as possible to a given target function  $\hat{u}$ , i.e., we have that  $\mu = f$ ,  $\mathcal{M}$  is the identity operator, and  $\|\cdot\|_W = \|\cdot\|_{L^2(\Omega)}$ . As a result, we have the functional

$$\mathcal{J}(u; f) = \frac{1}{2} \|u - \hat{u}\|_{L^2(\Omega)}^2 + \frac{\beta}{2} \|f\|_{L^2(\Omega)}^2.\tag{15.4}$$

There are no additional constraints on the solution so that the optimization is solely constrained by the nonlocal diffusion equation. The well posedness of that equation is sufficient to guarantee the existence and uniqueness of an optimal pair  $(u^*, f^*)$ . Furthermore, in (D'Elia and Gunzburger 2014), it is shown that in the limit of vanishing nonlocality, i.e., as  $\delta \rightarrow 0$ , the optimal nonlocal state and control converge to the optimal solution  $(u_l^*, f_l^*)$  of the

local counterpart of (15.1) given by

$$\begin{aligned}
 & \text{seek } u_l(\mathbf{x}) \in H^1(\Omega) \text{ and } f_l \in L^2(\Omega) \text{ such that} \\
 & \min_{f_l \in L^2(\Omega)} \mathcal{J}(u_l; f_l) \\
 & \text{subject to } \begin{cases} -\Delta u_l = f_l & \forall \mathbf{x} \in \Omega \\ u_l = g & \forall \mathbf{x} \in \partial\Omega. \end{cases}
 \end{aligned} \tag{15.5}$$

In (D'Elia and Gunzburger 2014), for finite element discretizations of the state and control variables, the convergence of both variables with respect to  $\delta$  and the mesh size  $h$  (the mesh size) is proved as are error estimates. Also, numerical results for discontinuous target functions show that nonlocal models, for which irregular solutions are admissible, allow one to match non-smooth functions in a much better way compared to local models.

An example is provided in Figure 15.1 for the domains  $\Omega = (0, 1)$  and  $\Omega_{\mathcal{I}_\delta} = (-\delta, 0) \cup (1, 1 + \delta)$ , and for a target function having a jump discontinuity at  $x = 0.5$ . Discontinuous piecewise-linear finite element discretizations are used for both the state and control. For comparison purposes, continuous piecewise-linear finite element approximations of the local optimal control problem (15.5) are also computed. In Figure 15.1-left, the target function  $\hat{u}$ , the optimal local state  $u_l^*$  (the solution of (15.5)), and nonlocal optimal state  $u^*$  (for two values of  $\delta$ ) are plotted. Note that for a large horizon  $\delta$  the nonlocal solution perfectly matches the target, whereas for a small horizon the nonlocal optimal solution is visually identical to the local one. In Figure 15.1-right, plots of the corresponding optimal source terms  $f^*$  are given. Here, for a large horizon, the control has a smaller amplitude and a smaller  $L^2$  norm (which can be viewed as indications of a smaller cost of control) even though that control does a better job in matching the target function. As explained in (D'Elia and Gunzburger 2014), this behavior can be justified by the fact that the nonlocal model allows for discontinuous behavior in the optimal state, and, thus, the optimal control has an “easier time” forcing a match between the optimal state and the non-smooth target function.

### 15.1.2. Coefficient identification

The identification of kernel parameters or of the kernel function itself is one of the most important open problems in nonlocal modeling. In fact, in general, the choice of kernel functions and its parameters is based on intuition or designed through heuristic techniques. Here, we report on three approaches that tackle the kernel identification problem using different cost functionals.

In (Fuensanta and Muñoz 2015), the problem of identifying a constitutive function in (15.2) having the form  $\theta(\mathbf{x}, \mathbf{y}) = \vartheta(\mathbf{x}) + \vartheta(\mathbf{y})$  is considered. Thus,

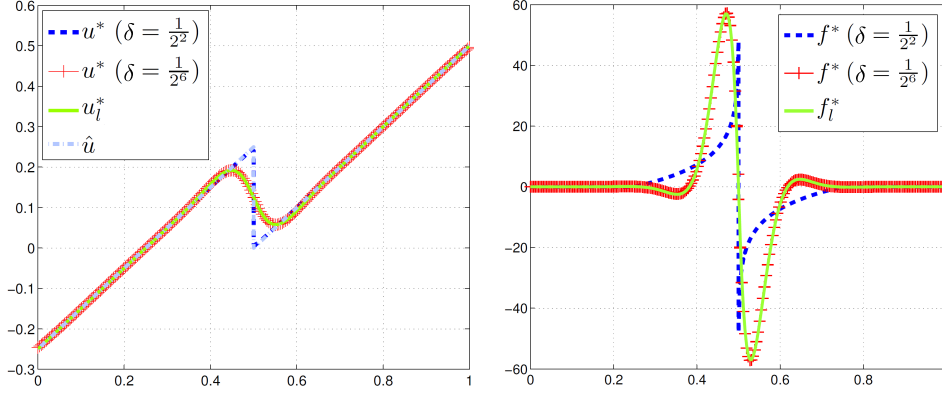


Figure 15.1. Left: the optimal nonlocal state  $u^*$  for  $\delta = 2^{-2}$  and  $2^{-6}$ , the target function  $\hat{u}$ , and the optimal local state  $u_l^*$ . Right: the corresponding optimal source terms.

we have that  $\mu = \vartheta(\mathbf{x})$ . In addition,  $\mathcal{V}u = u$  and  $\phi(\mathbf{x}, \mathbf{y}) = k(\mathbf{x}, \mathbf{y})|\mathbf{y} - \mathbf{x}|^{-2}$  with  $k(\mathbf{x}, \mathbf{y}) \geq C|\mathbf{y} - \mathbf{x}|^{2-d-2s}$  for  $s \in (0, 1)$  and  $\text{support}(k(\mathbf{x})) = B_\delta(\mathbf{x})$ . The set of admissible  $\vartheta(\mathbf{x})$  is defined as

$$W = \left\{ \vartheta(\mathbf{x}) \in [\vartheta_{\min}, \vartheta_{\max}], \vartheta = 0 \text{ on } \Omega_{\mathcal{I}}, \int_{\Omega} \vartheta(\mathbf{x}) d\mathbf{x} = \bar{\vartheta} \right\}$$

for positive constants  $\vartheta_{\min}$ ,  $\vartheta_{\max}$ , and  $\bar{\vartheta}$ . The cost functional in (Fuensanta and Muñoz 2015), referred to as a *compliance* functional, is chosen as

$$\mathcal{J}(u) = \int_{\Omega \cup \Omega_I} \int_{\Omega \cup \Omega_I} F(\mathbf{x}, \mathbf{y}; u) d\mathbf{y} d\mathbf{x} \quad (15.6)$$

and is then minimized over  $\vartheta(\mathbf{x}) \in W$ . First,  $F$  is chosen such that  $\mathcal{J}(u) = |||u|||^2$ , where  $|||\cdot|||$  denotes the “energy” norm corresponding to the kernel function  $\phi(\mathbf{x}, \mathbf{y}) = k(\mathbf{x}, \mathbf{y})|\mathbf{y} - \mathbf{x}|^{-2}$ . For this choice of  $F$  and with no other constraints applied on the state or control, the existence of a solution of the problem of minimizing the functional (15.6) is proved. Note that a regularizing term is not included in this functional because the box constraints on  $\vartheta(\mathbf{x})$  included in the admissibility set  $W$  already guarantee the well posedness of the minimization problem. Extensions to more general functionals are then considered including  $F$  being only required to be measurable with respect to  $u$  and lower semi-continuous with respect to  $\mathbf{x}$ . Furthermore, for the compliance case, the convergence of the optimal nonlocal solution to its local counterpart (15.5) for  $\mu = \vartheta$  is proved. In this work, neither discretizations or numerical tests are provided.

In (D’Elia and Gunzburger 2016), the problem of identifying the constitutive function  $\theta(\mathbf{x}, \mathbf{y})$  in (15.2) is also considered for integrable and non-

integrable kernel functions  $\phi_\delta(\mathbf{x}, \mathbf{y})$ . Specifically, again  $\mathcal{V}u = u$ , and, in the functional (15.3),  $\beta = 0$  and  $\|\cdot\|_{U(\Omega)} = \|\cdot\|_{L^2(\Omega)}$ . The functional is minimized over the set of admissible controls given by

$$W = \{\theta \in W^{1,\infty}(\Omega \cup \Omega_{\mathcal{I}_\delta} \cup \Omega \cup \Omega_{\mathcal{I}_\delta}), \theta \in [\vartheta_{\min}, \vartheta_{\max}], \|\theta\|_{1,\infty} \leq \theta^{\max} < \infty\}.$$

Again, the box constraints on  $\theta$  included in the admissibility set suffice to prove that the problem (15.1) has at least one solution. In (D'Elia and Gunzburger 2016), a mixed finite element discretization of the state and control variable is developed and the convergence of the discretization error as the mesh size is refined is proven. Numerical tests are also provided that show that the approach taken there allows for the identification of both smooth and discontinuous diffusion coefficients for both integrable and (truncated) fractional kernels. A sample result is shown in Figure 15.2. For that figure,  $\Omega = (0, 1)$ ,  $\Omega_{\mathcal{I}_\delta} = (\delta, 0) \cup (1, 1 + \delta)$ ,  $g(x) = 0$ ,  $f(x) = 5$ , and the spatial grid size used to discretize the state is  $2^{-12}$ . A surrogate for the target functional  $\hat{u}$  is a very fine grid finite element approximation of the nonlocal diffusion problem with the data just listed and with

$$\theta(x, y) = \vartheta\left(\frac{x+y}{2}\right) \quad \text{with} \quad \vartheta(z) = \begin{cases} 1 & \forall z \in (0, 0.2) \\ 0.1 & \forall z \in (0.2, 0.6) \\ 1 & \forall z \in (0.6, 1). \end{cases} \quad (15.7)$$

Thus the goal of the minimization problem is to identify this constitutive coefficient function. Figure 15.2 illustrates, for two values of the horizon  $\delta$ , the convergence (with respect to the grid size  $1/N_\vartheta$  used to approximate the coefficient function  $\vartheta(z)$ ) of the approximation.

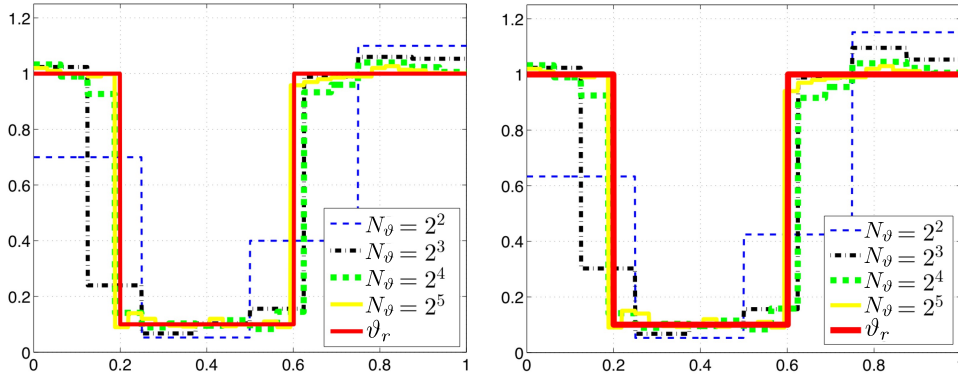


Figure 15.2. Optimal approximate coefficient functions for  $\delta = 2^{-9}$  (left) and  $2^{-4}$  (right) for different numbers of degrees of freedom  $N_\vartheta$  in the discretization of the coefficient function  $\vartheta(z)$  defined in (15.7).

We also mention the approach introduced in (Pang, D'Elia, Parks and

Karniadakis 2019a) in which the task of parameter identification for truncated diffusion operators of fractional type is pursued by including the non-local diffusion equation in the cost functional, i.e., we have

$$\mathcal{J}(u; \mu) = \frac{1}{2} \|u - \hat{u}\|_{L^2(\Omega)}^2 + \frac{\beta}{2} \|\mathcal{L}u - f\|_{L^2(\Omega)}^2. \quad (15.8)$$

Thus, the state equations are only weakly prescribed through the minimization of the residual. In (Pang et al. 2019a), the state and control variables are approximated using fully connected neural networks. Numerical tests on analytic solutions and turbulence models show the ability of this technique to recover kernel parameters such as the interaction radius  $\delta$  and the variable fractional order  $s(\mathbf{x})$ , i.e., we have  $\mu = \{\delta, s(\mathbf{x})\}$ .

### 15.2. Inverse problems for fractional operators

In this section, we focus on control and optimization problems for the fractional Laplace operator. The formulations described in what follows can be easily extended to more general fractional operators (see, e.g., (Meerschaert and Sikorskii 2012)), but at a cost of more complicated analyses.

#### 15.2.1. Distributed optimal control for a matching functional

The formulation presented in the previous section for distributed control can be used for fractional operators with (almost) no modification. We mention several works in the literature that analyze the theoretical and numerical aspects of both the elliptic and parabolic fractional problems.

In (D’Elia, Glusa and Otárola 2019b) the same problem as that introduced in Section 15.1.1 is considered. Specifically, for  $\mathcal{J}$  as in (15.4) and  $\mathcal{V}u = u$ , the problem of minimizing  $\mathcal{J}$  with respect to  $f \in W = \{r \in L^2(\Omega) : r \in [r_{min}, r_{max}]\}$  subject to

$$\begin{cases} (-\Delta)^s u = f & \forall \mathbf{x} \in \Omega \\ u = g & \forall \mathbf{x} \in \mathbb{R}^d \setminus \Omega \end{cases} \quad (15.9)$$

is considered. The well posedness of the control problem is proven, optimality conditions are derived, and regularity estimates for the optimal variables are also proven. Furthermore, based on an a priori error analysis for the state equation, a semidiscrete scheme is constructed for which a priori error estimates for the approximation of the control variable are derived. A fully discrete scheme is also considered for which state and control error estimates are derived. Several two-dimensional numerical illustrations of the theoretical results are also provided.

In the follow-up paper (Glusa and Otárola 2019), the fractional parabolic

equation

$$\begin{cases} u_t + (-\Delta)^s u = f & \forall \mathbf{x} \in \Omega, t \in (0, T) \\ u = g & \forall \mathbf{x} \in \mathbb{R}^d \setminus \Omega, t \in (0, T) \\ u(\cdot, 0) = u_0(\mathbf{x}) & \forall \mathbf{x} \in \Omega. \end{cases} \quad (15.10)$$

is considered. The cost functional, similar to that in (15.4), now involves an integral over time, i.e., we have

$$\mathcal{J}(u; f) = \frac{1}{2} \int_0^T \left( \|u - \hat{u}\|_{L^2(\Omega)}^2 + \beta \|f\|_{L^2(\Omega)}^2 \right) dt. \quad (15.11)$$

Also, the control variable  $f$  is now also time dependent and belongs to the admissibility set  $W(t) = \{r(t) \in L^2(\Omega) : r(t) \in [r_{\min}(t), r_{\max}(t)], \forall t \in (0, T]\}$ . As in (D'Elia et al. 2019b), the existence and uniqueness of optimal solutions are proven and first-order necessary and sufficient optimality conditions are derived. Also derived are regularity estimates for the optimal state and control. Then, discrete stability results and a priori error estimates are derived for the discretized problem resulting from the standard backward Euler scheme for temporal discretization and a piecewise linear finite element spatial discretization. The theoretical findings are illustrated by one- and two-dimensional numerical experiments.

In (Antil, Khatri and Warma 2019a, Antil, Verma and Warma 2019b), the control is chosen as the data  $g$  in the volume constraint for the steady-state and time-dependent cases, respectively. In (15.1), nonlocal Dirichlet, Neumann, and Robin volume constraints are considered for the operator  $\mathcal{V}$ . As an example, in the Robin case, we have

$$\mathcal{V}u = \kappa_N \mathcal{N}u + \kappa_D u = g,$$

where  $\mathcal{N}$  denotes the nonlocal Neumann operator  $\mathcal{N}$  defined as in (1.10) with the appropriate changes made to reflect that here the interaction domain is  $\Omega_{\mathcal{I}_\infty} = \mathbb{R}^d \setminus \Omega$ . Even though the theory is presented for the general functional

$$\mathcal{J}(u; g) = \mathcal{J}_1(u) + \frac{\beta}{2} \int_0^T \|g\|_{L^2(\Omega_T)}^2 dt \quad (15.12)$$

with a convex functional  $\mathcal{J}_1$ , numerical experiments are performed for a matching functional in the usual form; e.g., see (15.11) for the time-dependent version. In the more general formulation, for the time-dependent case, (Antil et al. 2019b) mostly focuses on nonlocal Dirichlet and Robin optimal control problems. Well posedness and regularity are discussed and a discretization scheme is proposed. The theoretical results are illustrated by two-dimensional numerical experiments. The main contribution of (Antil



et al. 2019b) is to show the ability of nonlocal models to take advantage of information outside the domain and not only on the boundary, which is one of the limitations of control problems for PDEs.

Even if not entirely focused on operators such as that in (3.1), we mention that in (Antil and Warma 2019) control problems for both a spectral fractional semilinear operator and for the integral fractional Laplacian are considered. There, existence and regularity results are derived for the spectral case (that is not treated in this section). It is also stated that the results obtained for the spectral case can be extended, after small modifications, to the integral definition of the operator.

**Remark 15.1.** *Kernel identification.* For kernel identification in the setting of fractional operators, we only mention that in (Pang, Lu and Karniadakis 2019b) an algorithm for parameter identification based on physics-informed neural networks is studied. As such, this method is a special instance of the algorithm presented in (Pang et al. 2019a). Specifically, this work is focused on the estimation of the fractional power of the integral fractional Laplacian. Other works on the identification of kernel parameters, more specifically, of the fractional power  $s$ , only deal with the spectral definition of  $(-\Delta)^s u$ .  $\square$

## 16. Variational inequalities and obstacle problems

We consider the nonlocal obstacle problem

$$\left\{ \begin{array}{ll} -\mathcal{L}u \geq f & \forall \mathbf{x} \in \Omega \\ u \geq \psi & \forall \mathbf{x} \in \Omega \\ (-\mathcal{L}u - f)(u - \psi) = 0 & \forall \mathbf{x} \in \Omega \\ u = 0 & \forall \mathbf{x} \in \Omega_{\mathcal{I}_{\infty}}, \end{array} \right. \quad (16.1)$$

where here  $\psi(\mathbf{x})$  denotes the obstacle function. Nonlocal obstacle problems such as this one are used in studying the deformation of elastic membranes, in contact mechanics, and in finance, e.g., the pricing of American put options in Lévy jump-diffusion models. Clearly, (16.1) is a nonlocal analog of the local PDE obstacle problem

$$\left\{ \begin{array}{ll} -\Delta u \geq f & \forall \mathbf{x} \in \Omega \\ u \geq \psi & \forall \mathbf{x} \in \Omega \\ (-\Delta u - f)(u - \psi) = 0 & \forall \mathbf{x} \in \Omega \\ u = 0 & \forall \mathbf{x} \in \partial\Omega. \end{array} \right.$$

The well-posedness analysis of nonlocal obstacle problems require less smooth obstacles than do corresponding local PDE obstacle problems. Moreover, as is illustrated at the end of this section, the behaviors and properties of solutions in the local and nonlocal setting can be quite different.

There is an ever-growing literature on the analysis and approximation of nonlocal obstacle problems, especially in the fractional setting. Here, we give a brief account on an approach used in (Burkovska and Gunzburger 2019b) in which regularity estimates, well-posedness analyses, and finite element methods and their numerical analysis are considered. Using a different approach, the well posedness of nonlocal obstacle problem and the convergence of the finite element approximation are established in (Guan and Gunzburger 2017) for fractional Laplacian and integrable kernels. With respect to other works about obstacle problems for the fractional Laplacian, we mention (Servadei and Valdinoci 2013) in which Lewy-Stampacchia type estimates are obtained that are similar to those obtained in (Burkovska and Gunzburger 2019b), but with restrictions on the fractional exponent and requiring greater smoothness of the obstacle. The regularity of the obstacle problem measured in Hölder and Lipschitz spaces is studied in, e.g., (Silvestre 2017, Caffarelli, Ros-Oton and Serra 2017). In (Borthagaray, Nochetto and Salgado 2018), a finite element approximation of the obstacle problem for the fractional Laplacian is studied and error estimates are proven. Regularity results for the solution are derived in weighted Sobolev spaces under additional regularity assumptions on the right-hand side (Hölder continuity) and the obstacle. In (Bonito, Lei and Salgado 2018), the regularity of the obstacle problem involving integro-differential operators with the fractional Laplacian as the nonlocal term is studied and a finite element based discretization is proposed and analyzed. In the purely nonlocal case, the same regularity for the solution is proven as in (Burkovska and Gunzburger 2019b), but for more restricted cases. Other than (Burkovska and Gunzburger 2019b), none of these works on the obstacle problem for the fractional Laplacian treat truncated kernels.

In (Burkovska and Gunzburger 2019b), the well-posedness and regularity results for the nonlocal obstacle problem (16.1) are obtained and the mixed formulation

$$\begin{aligned} \mathcal{A}(u, v) - \mathcal{B}(\lambda, v) &= \langle f, v \rangle & \forall v \in V \\ \mathcal{B}(\eta - \lambda, u - \psi) &\geq 0 & \forall \eta \in M \subset V_d \end{aligned} \quad (16.2)$$

is used to define, analyze, and apply finite element methods. In (16.2),  $\mathcal{A}(\cdot, \cdot) : V \times V \rightarrow \mathbb{R}$  is the usual bilinear form corresponding to the nonlocal operator  $\mathcal{L}$ ,  $V$  is the energy space associated with that bilinear form and the homogeneous volume constraint,  $V_d$  is the dual space for  $V$ ,  $\mathcal{B}(\cdot, \cdot) : V_d \times V \rightarrow \mathbb{R}$  is defined as  $\mathcal{B}(\eta, v) = \langle \eta, v \rangle$ , and  $M$  denotes the closed convex dual cone  $M := \{\eta \in V_d : \langle \eta, v \rangle \geq 0 \quad \forall v \in V, v \geq 0\}$ . Of course,  $\mathcal{A}(\cdot, \cdot)$  is continuous and coercive in  $V \times V$  and it is shown in (Burkovska and Gunzburger 2019b) that  $\mathcal{B}(\cdot, \cdot)$  is continuous and inf-sup stable on  $V_d \times V$ ,

i.e., we have that

$$\inf_{\eta \in V_d} \sup_{v \in V} \frac{\mathcal{B}(\eta, v)}{\|\eta\|_{V_d} \|v\|_V} \geq \beta_0 > 0.$$

So, the task at hand is to find, for  $f \in V_d$  and  $\psi \in V$ ,  $u \in V$  and  $\lambda \in M$  satisfying (16.2).

Under the assumptions  $f \in L^2(\Omega)$  and  $(-\mathcal{L}_\delta \psi - f)_+|_\Omega \in L^2(\Omega)$ , the improved regularity results

$$\mathcal{L}_\delta u \in L^2(\Omega), \quad \lambda \in L^2(\Omega), \quad \text{and} \quad \lambda \leq (-\mathcal{L}_\delta \psi - f)_+$$

are derived. For the fractional Laplacian obstacle problem, the improved regularity results obtained are given by

$$\begin{aligned} \lambda &\in L^2(\Omega) \quad \text{and} \quad u \in H_\Omega^{s+\beta}(\Omega) \\ \text{with } \beta &= \min\{s, 1/2 - \varepsilon\}, \quad \varepsilon > 0, \quad s \in (0, 1). \end{aligned}$$

Note that these regularity results hold for all  $s \in (0, 1)$ .

Finite element approximations are defined for the space  $V^h \subset V$  of piecewise-linear continuous polynomials and the space  $V_d^h \subset V_d$  of discontinuous linear polynomials for which locally bi-orthogonal basis functions can be constructed, i.e., we have for any basis functions  $\xi_j(\mathbf{x}) \in V_d^h$  and  $\phi_{j'}(\mathbf{x}) \in V^h$  and for any finite element  $K$

$$\int_K \xi_j \phi_{j'} = \delta_{jj'} \int_K \phi_j \geq 0.$$

The inf-sup stability with respect to  $V_d^h \times V^h$  is proven so that the discrete problem is well posed.

An example numerical result is provided in Figure 16.1. Note the differences in the primal solution  $u(\mathbf{x})$  and in the Lagrange multiplier  $\lambda$  obtained using nonlocal and local models. In particular, note that for the nonlocal case,  $\lambda \in L^2(\Omega)$  whereas for the local case,  $\lambda$  consists of Dirac delta functions.

Note that all the results in (Burkovska and Gunzburger 2019b) pertinent to the fractional Laplacian were also proved for the truncated fractional Laplacian kernel introduced in Section 3.1.1. Moreover, the convergence of the solution of the obstacle problem with the truncated kernel is shown to converge to the solution of (the un-truncated) fractional Laplacian obstacle problem.

## 17. Reduced-order modeling

Reduced-order modeling (ROM) is the task of constructing a very low-dimensional discretization for parameterized problems that, in order to achieve a desired fidelity, are usually approximated by a high-dimensional discretization (HDD). The construction of a ROM usually requires an off-line cost

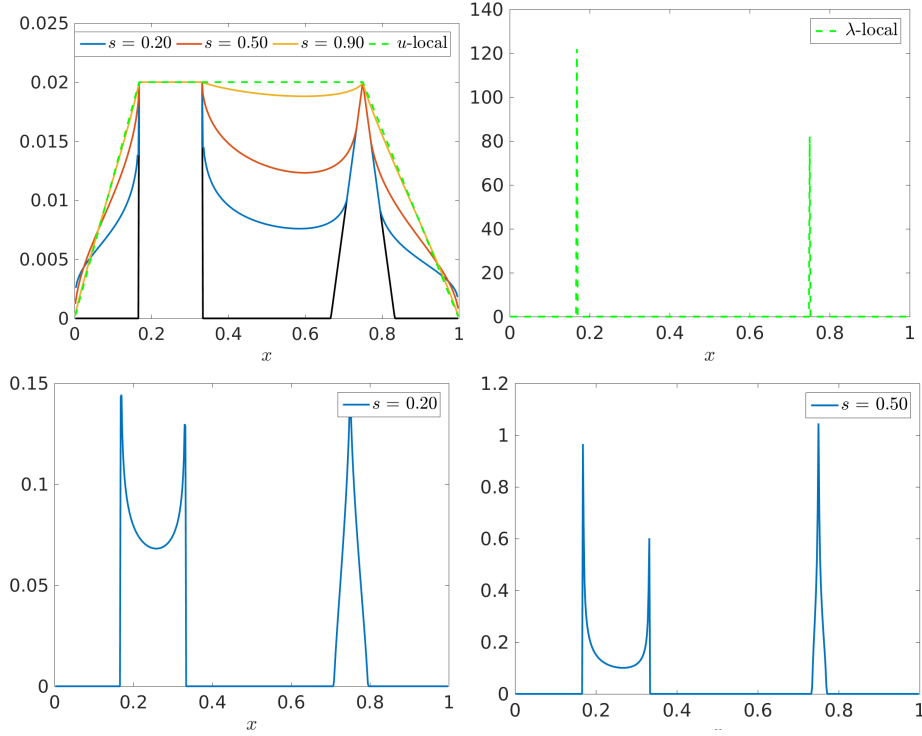


Figure 16.1. Top left: primal nonlocal solutions for three values of the fractional exponent and the primal local solution. Top right: the local Lagrange multiplier. Bottom: the nonlocal Lagrange multiplier for  $s = 0.2$  (left) and  $s = 0.5$  (right). Note the different ordinate scales in the three Lagrange multiplier plots.

incurred by having to do runs of the HDD for a relatively few parameter choices. Once the ROM is constructed, it can be used on line instead of the HDD by, e.g., doing additional simulations for many more parameter choices at much lower cost than if the HDD was used instead. For example, in uncertainty quantification settings, one may need to obtain many simulations in order to obtain good statistical information so that using the ROM instead of the HDD can result in huge computational savings. The huge body of literature available about ROMs for PDEs attest to their usefulness.

PDE discretizations ubiquitously involve large, sparse linear or nonlinear discrete systems. Analogous discretizations of nonlocal models usually involve discrete systems of similar size but, due to nonlocality, having much less sparsity. In some settings such as those involving fractional Laplacians, the discrete systems may even be full. The double curse of high dimension-

ality and lack of sparsity of the discrete systems means that

*reduced-order modeling is needed much more for nonlocal models than for corresponding local PDE models.*

The setting we use to discuss ROMs is parameterized nonlocal diffusion. Thus, we assume that the constitutive function  $\theta_\delta(\mathbf{x}, \mathbf{y}; \mathbf{p}_\theta)$  in (2.16) depends on the components of a parameter vector  $\mathbf{p}_\theta \in \Gamma_\theta \subset \mathbb{R}^{N_\theta}$  and the kernel function  $\phi_\delta(\mathbf{x}, \mathbf{y}; \mathbf{p}_\phi)$  in (2.16) depends on the components of a parameter vector  $\mathbf{p}_\phi \in \Gamma_\phi \subset \mathbb{R}^{N_\phi}$ . We refer to  $\Gamma_\theta$  and  $\Gamma_\phi$  as *parameter domains*. Then, in the weak formulation (2.9) of the nonlocal diffusion problem we have the bilinear form

$$\begin{aligned} \mathcal{A}_{\mathbf{p}}(u, v) &= \int_{\Omega \cup \Omega_{\mathcal{I}_\delta}} \int_{B_\delta(\mathbf{x})} (v(\mathbf{y}) - v(\mathbf{x}))(u(\mathbf{y}) - u(\mathbf{x})) \phi_\delta(\mathbf{x}, \mathbf{y}; \mathbf{p}_\phi) \theta_\delta(\mathbf{x}, \mathbf{y}; \mathbf{p}_\theta) d\mathbf{y} d\mathbf{x}, \end{aligned}$$

where we have used (2.16), i.e.,  $\gamma_\delta(\mathbf{x}, \mathbf{y}) = \phi_\delta(\mathbf{x}, \mathbf{y}; \mathbf{p}_\phi) \theta_\delta(\mathbf{x}, \mathbf{y}; \mathbf{p}_\theta) \chi_{B_\delta(\mathbf{x})}(\mathbf{y})$ . We also assume that we have in hand a finite element or other variational discretization<sup>4</sup> of (2.9) with the bilinear form  $\mathcal{A}_{\mathbf{p}}(\cdot, \cdot)$ , i.e., we have the nonlocal discrete problem for  $u_{\delta, h, \mathbf{p}}(\mathbf{x}) \in V_c^h(\Omega \cup \Omega_{\mathcal{I}_\delta})$  given by

$$\mathcal{A}_{\mathbf{p}}(u_{\delta, h, \mathbf{p}}, v_h) = \langle f, v_h \rangle \quad \forall v_h \in V_c^h(\Omega \cup \Omega_{\mathcal{I}_\delta}), \quad (17.1)$$

where, for economy of exposition, we impose the homogeneous Dirichlet volume constraint  $u_{\delta, h, \mathbf{p}}(\mathbf{x}) = 0$  on  $\Omega_{\mathcal{I}_\delta}$  and where  $V_c^h(\Omega \cup \Omega_{\mathcal{I}_\delta})$  denotes a, e.g., finite element, subspace of  $V_c(\Omega \cup \Omega_{\mathcal{I}_\delta})$ . Thus, given any parameter vectors  $\mathbf{p}_\phi \in \Gamma_\phi$  and  $\mathbf{p}_\theta \in \Gamma_\theta$ , (17.1) can be solved to determine the approximation  $u_{u_{\delta, h, \mathbf{p}}}(\mathbf{x})$  of the exact solution  $u_{\delta, \mathbf{p}}(\mathbf{x})$  of (2.9) with  $\mathcal{A}(\cdot, \cdot)$  replaced by  $\mathcal{A}_{\mathbf{p}}(\cdot, \cdot)$ . We let  $N_h$  denote the dimension of  $V_c^h(\Omega \cup \Omega_{\mathcal{I}_\delta})$ , i.e., of the HDD.

Assume we have a ROM basis  $V_{N_{rom}} := \{v_{n, rom}(\mathbf{x})\}_{n=1}^{N_{rom}}$  consisting of  $N_{rom}$  functions  $v_{n, rom}(\mathbf{x}) \in V_c^h(\Omega \cup \Omega_{\mathcal{I}_\delta})$ . Then, for any  $\mathbf{p}_\phi \in \Gamma_\phi$  and  $\mathbf{p}_\theta \in \Gamma_\theta$ , the *ROM-Galerkin approximation*  $u_{\mathbf{p}, rom}(\mathbf{x}) \in V_{N_{rom}}$  of the solution  $u_{\delta, h, \mathbf{p}}(\mathbf{x})$  of (17.1) is determined by solving the problem

$$\mathcal{A}_{\mathbf{p}}(u_{\mathbf{p}, rom}, v) = \langle f, v \rangle \quad \forall v \in V_{N_{rom}}. \quad (17.2)$$

Thus, the task at hand is to construct a ROM basis such that  $N_{rom} \ll N_h$  that results in ROM solutions  $u_{\mathbf{p}, rom}(\mathbf{x})$  that are acceptably accurate approximations of  $u_{\delta, h, \mathbf{p}}(\mathbf{x})$  for any  $\mathbf{p}_\phi \in \Gamma_\phi$  and  $\mathbf{p}_\theta \in \Gamma_\theta$  or at least for subsets of the parameter domains that are of interest.

Two examples of the use of reduced-order models for nonlocal diffusion are given in (Guan, Gunzburger, Webster and Zhang 2017), where a greedy reduced basis (GRB) approach is used, and (Witman, Gunzburger and

<sup>4</sup> ROMs for discretizations of the strong form of nonlocal models are also of interest.

Peterson 2017), where a proper orthogonal decomposition (POD) approach is used.<sup>5</sup> Both approaches involve only the parameter vector  $\mathbf{p}_\theta$ . The basis construction and application processes for nonlocal and local models are the same, excepting of course that in the local case approximate solutions of PDEs are involved whereas the nonlocal case involves approximate solutions of nonlocal models such as (17.2). Thus, here, we simply refer to (Guan et al. 2017) and (Witman et al. 2017) for detailed descriptions of the GRB and POD approaches, respectively, in the context of nonlocal diffusion models. In (Witman et al. 2017), a time-dependent problem is considered. In (Guan et al. 2017), random parameter vectors are considered and the GRB surrogates are compared to sparse-grid surrogates. In addition to the analyses of the errors incurred by the ROMs, (Guan et al. 2017) and (Witman et al. 2017) provide numerical examples that illustrate the usefulness of the ROMs considered therein.

In (Burkovska and Gunzburger 2019a), the construction and analysis of ROMs for nonlocal models parameterized by the horizon  $\delta$  and, in the case fractional models, by the fractional exponent  $s$  are considered, so that now the parameter vector  $\mathbf{p}_\phi$  is present in the kernel function. The parameter domains for both  $\delta$  and  $s$  are intervals bounded away from the origin and infinity and greedy algorithms are used to construct the reduced bases. Also provided in (Burkovska and Gunzburger 2019b) are illustrative numerical examples.

A very simple one-dimensional, time-dependent illustration of the effectiveness of ROM in the nonlocal setting is given in Figure 17.1. The kernel function is proportional to  $1/|y - x|$  so that it is singular and non-integrable. A manufactured solution that has a jump discontinuity at all times is used to set the data of the problem. A discontinuous finite element Galerkin method is used for both generating the snapshots for the POD basis construction and for comparison purposes. Plots for five time instants are provided. From the figure, it is evident that a one-dimensional POD basis does a poor job of approximating the HDD finite element solution whereas a six-dimensional POD basis does an excellent job.

**Remark 17.1.** As is the case for the local PDE setting, obtaining *solutions* of nonlocal ROM models such as (17.2) incur costs that depend only on the dimension  $N_{rom}$  of the ROM model whereas the naive *assembly* of the ROM models involves steps whose cost depends on the dimension  $N_h$  of the HDD models used to generate the ROM bases. In the PDE setting, several

<sup>5</sup> Although both ROMs we consider, as are most others, involve a “reduced basis,” i.e., a basis of lower dimension than that of the parent HDD model, *reduced-basis methods* usually refer to ROMs in which the basis consists of solutions of (17.2). In contrast, a POD basis consists of linear combinations of such solutions.

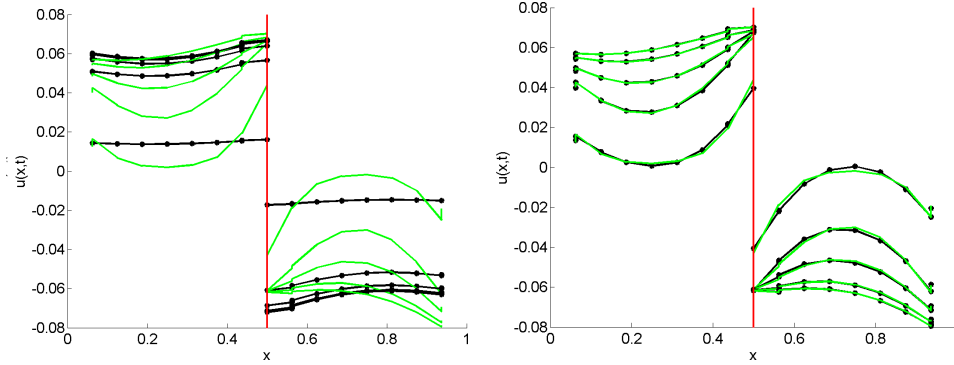


Figure 17.1. Comparison at different times between a fine-grid discontinuous Galerkin finite element approximation (in green) and POD approximations (in black with black dots) with one POD basis function (left) and six POD basis functions (right).

strategies have been developed to overcome this obstacle, all of which can be applied to the nonlocal setting.  $\square$

## 18. Time-dependent nonlocal problems

Although we do not consider nonlocal time-dependent problems other than in this subsection and briefly in some other sections, a brief discussion is warranted. We do not at all delve into nonlocality in time for which there is a vast literature devoted to fractional time derivatives and other settings in which memory effects are present.

Weak formulations of time-dependent problems can be defined in the same manner as that for local PDE time-dependent problems, once one knows how to treat steady-state problems. Likewise, for the discretization of nonlocal time-dependent problems, spatial discretization can be effected using any discretization method for the corresponding steady-state problem, including those discussed in Part 2, and temporal discretization can be effected using any discretization method for the corresponding local PDE problem, e.g., the backward-Euler or Crank-Nicolson method for (18.1) or, for (18.7), a leap-frog or other explicit method. Furthermore, the analysis of weak formulations and discretizations of nonlocal time-dependent problems, including the derivation of well-posedness results and error estimates, also follows the same paths as those for the corresponding local PDE problems.

Here, we just consider a small sample of the differences between time-dependent local and nonlocal problems.

### 18.1. Time-dependent nonlocal diffusion

Using the notation used in (1.5), we have the nonlocal time-dependent diffusion equation

$$\begin{cases} \rho \frac{\partial u}{\partial t} = \mathcal{L}_\delta u + f(\mathbf{x}, t) & \forall \mathbf{x} \in \Omega \times (0, T] \\ \mathcal{V}u = g(\mathbf{x}, t) & \forall \mathbf{x} \in \Omega_{\mathcal{I}_\delta} \times (0, T] \\ u(\mathbf{x}, 0) = u_0(\mathbf{x}) & \forall \mathbf{x} \in \Omega, \end{cases} \quad (18.1)$$

where  $\rho(\mathbf{x}) > 0$  and  $u_0(\mathbf{x})$  are given functions defined on  $\Omega$  and  $f(\mathbf{x}, t)$  and  $g(\mathbf{x}, t)$  are given functions defined on  $\Omega \times (0, T]$  and  $\Omega_{\mathcal{I}_\delta} \times [0, T]$ , respectively.

Using the nonlocal Green's first identity, it is an easy matter to show, for  $f = 0$  and  $g = 0$ , that the nonlocal diffusion equation (18.1) implies that

$$\frac{1}{2} \frac{d}{dt} \int_{\Omega} u^2 d\mathbf{x} + \int_{\Omega \cup \Omega_{\mathcal{I}_\delta}} \int_{\Omega \cup \Omega_{\mathcal{I}_\delta}} \mathcal{D}_\delta^* u \cdot (\Theta_\delta \mathcal{D}_\delta^* u) d\mathbf{y} d\mathbf{x} = 0$$

so that

$$\int_{\Omega} u^2(\mathbf{x}, t) d\mathbf{x} \leq \int_{\Omega} u_0^2(\mathbf{x}) d\mathbf{x} \quad \forall t > 0 \quad (18.2)$$

and for time-independent  $\Theta_\delta$ ,

$$\begin{aligned} & \int_{\Omega \cup \Omega_{\mathcal{I}_\delta}} \int_{\Omega \cup \Omega_{\mathcal{I}_\delta}} \mathcal{D}_\delta^* u(\mathbf{x}, t) \cdot (\Theta_\delta \mathcal{D}_\delta^* u(\mathbf{x}, t)) d\mathbf{y} d\mathbf{x} \\ & \leq \int_{\Omega \cup \Omega_{\mathcal{I}_\delta}} \int_{\Omega \cup \Omega_{\mathcal{I}_\delta}} \mathcal{D}_\delta^* u(\mathbf{x}, 0) \cdot (\Theta_\delta \mathcal{D}_\delta^* u(\mathbf{x}, 0)) d\mathbf{y} d\mathbf{x} \quad \forall t > 0. \end{aligned} \quad (18.3)$$

These are decay characteristics of diffusive processes, e.g., (18.2) and the local version of (18.3) hold for parabolic PDEs. However, for integrable kernels, although solutions of the nonlocal diffusion equation (18.1) satisfy the decay properties (18.2) and (18.3), unlike the case for parabolic PDEs, those solutions may not be much smoother than the data. One can also consider various types of nonlocal-in-time versions of nonlocal diffusion equations; see for example (Chen et al. 2017).

We note that the *fractional heat equation*

$$\begin{cases} \frac{\partial u}{\partial t} + (-\Delta)^s u = f & \text{in } \Omega \times [0, T], \\ u = g & \text{in } \Omega_{\mathcal{I}_\infty} \times [0, T] \\ u(0) = u_0 & \text{in } \Omega \end{cases} \quad (18.4)$$

is perhaps of even greater interest compared to the steady-state case. Similarly, one can consider the fractional heat equation with the regional fractional Laplacian.



### 18.2. Time-dependent convection-diffusion problems

For  $T > 0$ , we introduce the time-dependent function spaces  $L^2(0, T; V_d^0) = \{v(\cdot, t) \in V_d^0 : |v(\cdot, t)|_{V_d} \in L^2(0, T)\}$  and  $L^2(0, T; V_d') = \{f(\cdot, t) \in V_d' : \|f(\cdot, t)\|_{V_d'} \in L^2(0, T)\}$ . The time-dependent nonlocal convection-diffusion problem is then given by

$$\begin{cases} u_t - \mathcal{L}_{cd, \delta} u = f & \forall \mathbf{x} \in \Omega, t \in (0, T] \\ u(\mathbf{x}, t) = 0 & \forall \mathbf{x} \in \Omega_{\mathcal{I}}, t \in (0, T] \\ u(\mathbf{x}, 0) = u_0(\mathbf{x}) & \forall \mathbf{x} \in \Omega. \end{cases} \quad (18.5)$$

The corresponding weak formulation is given as follows: given  $f \in L^2(0, T; V_d')$  and  $u_0 \in V_d^0$ , find  $u \in L^2(0, T; V_d^0)$  that satisfies  $u(\mathbf{x}, 0) = u_0(\mathbf{x})$  and, for all  $v \in V_d^0$  and for almost every  $t \in (0, T]$ ,

$$(u_t, v)_{\Omega} + \mathcal{A}_{cd, \delta}(u, v) = \langle f, v \rangle, \quad (18.6)$$

where  $(\cdot, \cdot)_{\Omega}$  denotes the  $L^2$  inner product over  $\Omega$ . The coercivity and continuity of  $\mathcal{A}_{cd, \delta}(\cdot, \cdot)$  and the continuity of  $\langle \cdot, \cdot \rangle$  guarantee that the weak formulation (18.6) is well posed. However, as pointed out in (D'Elia et al. 2017), standard arguments of variational theory (Evans 1998) imply that actually much weaker assumptions on  $\boldsymbol{\mu}$  are required for well posedness, namely,  $\|\mathcal{D}_{c, \delta} \boldsymbol{\mu}\|_{\infty} < \infty$ .

### 18.3. Nonlocal wave equations

One can also consider the nonlocal wave equation

$$\begin{cases} \rho \frac{\partial^2 u}{\partial t^2} = \mathcal{L}_{\delta} u + f(\mathbf{x}, t) & \forall \mathbf{x} \in \Omega \times (0, T] \\ \mathcal{V} u = g(\mathbf{x}, t) & \forall \mathbf{x} \in \Omega_{\mathcal{I}_{\delta}} \times (0, T] \\ u(\mathbf{x}, 0) = u_0(\mathbf{x}) & \forall \mathbf{x} \in \Omega \\ \frac{\partial u}{\partial t}(\mathbf{x}, 0) = u_1(\mathbf{x}) & \forall \mathbf{x} \in \Omega, \end{cases} \quad (18.7)$$

where  $\rho(\mathbf{x}) > 0$ ,  $u_0(\mathbf{x})$ ,  $f(\mathbf{x}, t)$ , and  $g(\mathbf{x}, t)$  are defined as for (18.1) and  $u_1(\mathbf{x})$  is a given function defined on  $\Omega$ .

For (18.7) with  $f = 0$  and  $g = 0$ , we have conservation of energy, i.e.,

$$\frac{d}{dt} \left( \frac{1}{2} \int_{\Omega} \left( \frac{du}{dt} \right)^2 d\mathbf{x} + \frac{1}{2} \int_{\Omega \cup \Omega_{\mathcal{I}_{\delta}}} \int_{\Omega \cup \Omega_{\mathcal{I}_{\delta}}} \mathcal{D}_{\delta}^* u \cdot (\boldsymbol{\Theta}_{\delta} \mathcal{D}_{\delta}^* u) d\mathbf{y} d\mathbf{x} \right) = 0$$

that is a characteristic of wave processes such as the PDE wave equation. One can find studies related to these nonlocal wave equations in (Guan and Gunzburger 2015, Du et al. 2018d, Du, Lipton and Mengesha 2016a).

One of the stark differences between local and nonlocal models is in their

dispersion relations for wave equations. For the one-dimensional local PDE wave equation

$$\frac{\partial^2 u}{\partial^2 t} = c^2 \frac{\partial^2 u}{\partial^2 x},$$

where  $c$  is a constant, by setting

$$u(x, t) = e^{-i\omega t + ikx},$$

one obtains the dispersion relation

$$\omega^2 = c^2 k^2. \quad (18.8)$$

In fact, this relation shows that there is no dispersion. The velocity of the wave is  $\omega/k = \pm c$  which is independent of  $\omega$  and  $k$ .

In (Guan and Gunzburger 2015), it is shown that the one-dimensional nonlocal wave equation

$$\frac{\partial^2 u}{\partial^2 t} = \frac{2-2s}{\delta^{2-2s}} c^2 \int_{x-\delta}^{x+\delta} \frac{u(y, t) - u(x, t)}{|y-x|^{1+2s}} dy, \quad 0 \leq s < 1/2,$$

has the dispersion relation

$$\omega^2 = \frac{2-2s}{\delta^{2-2s}} c^2 \int_0^\delta \frac{2-2\cos(ky)}{y^{1+2s}} dy. \quad (18.9)$$

Observe that the wave velocity  $\omega/k$  is a nonlinear function of  $k$ . It is also shown in (Guan and Gunzburger 2015) that as  $\delta \rightarrow 0$ ,  $\omega$  given by (18.9) converges (quadratically with respect to  $\delta$ ) to the local  $\omega$  of (18.8). Similar results are obtained there for the two-dimensional case. Similar dispersion relations have been discussed for nonlocal operators; see, e.g., (Zhou and Du 2010, Du and Zhou 2011, Du 2019).

## 19. Connections to stochastic processes

### 19.1. Connection of the fractional heat equation to Lévy processes

The fractional heat equation (18.4) can be associated with a class of stochastic jump processes, namely Lévy jump processes, see, e.g., (Meerschaert and Sikorskii 2012). These are nonlocal counterparts of Brownian motion and, as such, they feature discontinuous sample paths as opposed to continuous ones.

Specifically, let  $W_t$  denote a jump process conditioned on  $W_0 \in \Omega$  and assume that such a process is absorbed whenever  $W_t \in \Omega_{\mathcal{I}_\delta}$ . Also, let  $f = 0$ ,  $g = 0$ , and  $u_0(\mathbf{x})$  denote a nonnegative function such that

$$\int_{\Omega} u_0(\mathbf{x}) d\mathbf{x} = 1. \quad (19.1)$$

Then, for  $T = \infty$ , the fractional system (18.4) describes the evolution of the

probability density for the Lévy process  $W_t$  and we refer to it as the *master equation* for  $W_t$ ; the kernel  $\gamma_\delta$  in (3.1) represents the jump rate. Formally, we have that

$$\mathbb{P}(W_{\tilde{t}} \in \tilde{\Omega}) = \int_{\tilde{\Omega}} u(\mathbf{x}, \tilde{t}) d\mathbf{x} \quad \text{for } \tilde{\Omega} \subset \Omega.$$

The homogeneous volume constraint ensures that the process does not re-enter the domain and condition (19.1) ensures that  $W_0 \in \Omega$ .

The paper (Burch and Lehoucq 2015) describes the connection between nonlocal symmetric diffusion equations and stochastic processes and presents a classification of the latter based on kernel properties. There, the process  $W_t$  introduced in this section is classified as *infinite-activity* process because on any compact time interval the number of jumps in the sample path is infinite. This is a consequence of the fact that  $|\mathbf{x}|^{-d-2s}$  is a non-integrable function on any bounded region containing the origin. These processes can be further characterized by whether or not  $|\mathbf{x}|^{-d+1-2s}$  is an integrable function on any bounded region containing the origin; if it is integrable ( $s < 0.5$ ), the process is of *finite variation*; otherwise, ( $s > 0.5$ ) the process is of *infinite variation* (Burch and Lehoucq 2015).

**Remark 19.1.** Even though the connection to stochastic processes is broadly investigated in the context of fractional operators, more general nonlocal diffusion operators as in (1.6) can also be associated with Markov jump processes (Burch and Lehoucq 2015). When the kernel is of fractional type, such processes are still classified as infinite-activity processes, whereas in case of integrable kernels, they are referred to as *finite-activity* processes, i.e., on any compact time interval the number of jumps in the sample path is finite. The truncation of a kernel simply means that jumps are limited to a finite distance; as a consequence, such processes are classified as being of *finite-range*. In Section 18.2 we discuss the connection of nonlocal convection-diffusion models to non-symmetric stochastic processes.  $\square$

**Remark 19.2.** *The exit-time problem.* An extensively studied problem in the context of Brownian motion is the estimation of the first passage time of a stochastic process through the boundary  $\partial\Omega$ . Instead, due to its discontinuous nature, a Lévy process jumps outside of  $\Omega$  without crossing its boundary. The solution of the evolution equation (18.4) allows one to solve the first *exit-time problem* for jump processes. This problem was first studied in (Burch and Lehoucq 2015) and further analyzed in (Burch, D’Elia and Lehoucq 2014) and (D’Elia et al. 2017).

We introduce the random variable  $\tau := \inf\{t > 0, W_t \in \Omega_{\mathcal{I}_\delta} \mid W_0 \in \Omega\}$  that denotes the first exit time of  $W_t$  from  $\Omega$ . Its probability distribution is

given by

$$F_\tau(t) = 1 - \int_{\Omega} u(\mathbf{x}, t) d\mathbf{x}.$$

The expected exit time from  $\Omega$  is given by the expected value of the random variable  $\tau$ :  $\mathbb{E}(\tau) = \int_0^\infty \int_{\Omega} u(\mathbf{x}, t) d\mathbf{x} dt$ . The paper (Burch and Lehoucq 2015) establishes that, for symmetric infinite and finite activity Lévy jump processes, the expected exit time is finite as long as the initial condition  $u_0$  is square integrable.  $\square$

### 19.2. Connection of nonlocal convection-diffusion to stochastic non-symmetric jump processes

Whereas in general the kernel function  $\gamma_{cd,\delta}(\mathbf{x}, \mathbf{y})$  is allowed to take on negative values, when the nonlocal convection-diffusion equation is associated with a jump process,  $\gamma_{cd,\delta}(\mathbf{x}, \mathbf{y})$  represents a jump rate and, as a consequence, we assume  $\gamma_{cd,\delta}(\mathbf{x}, \mathbf{y}) : \mathbb{R}^d \times \mathbb{R}^d \rightarrow [0, \infty)$ .

As in Section 19.1, we let  $W_t$  denote a jump process conditioned on  $W_0 \in \Omega$  and assume that such a process is absorbed whenever  $W_t \in \Omega_{\mathcal{I}_\delta}$ . For  $f = 0$ ,  $u_0(\mathbf{x})$  satisfying (19.1), and  $T = \infty$ , the nonlocal system (18.5) describes the evolution of the probability density for the process  $W_t$  with jump rate  $\gamma_{cd,\delta}(\mathbf{x}, \mathbf{y}) \geq 0$ ; we refer to (18.5) as the *master equation* for the jump process  $W_t$ . As in the symmetric case, the homogeneous volume constraint ensures that the process does not re-enter the domain and condition (19.1) ensures that  $W_0 \in \Omega$ . The difference in the rates  $\gamma_{cd,\delta}(\mathbf{y}, \mathbf{x}) d\mathbf{x}$  and  $\gamma_{cd,\delta}(\mathbf{x}, \mathbf{y}) d\mathbf{y}$  gives the rate of change of the probability  $u(\mathbf{x}, t) d\mathbf{x}$  and the assumption on  $f$  implies that at the steady state, these rates are equal. Furthermore, standard probability arguments imply that  $W_t$  is Markov; as such, we refer to  $W_t$  as a non-symmetric finite-range Markov jump process. In addition, note that for processes governed by the master equation (18.5), the probability is conserved over  $\Omega$  (D'Elia et al. 2017). On the other hand, the effect of the nonlocal convection term is a *drift of the mean of the position*; the latter becomes more and more pronounced as the extent of the nonlocal interactions vanishes; in fact, the nonlocal convection term converges to pure drift.

**Remark 19.3.** *The exit-time problem for non-symmetric jump processes.* The problem described in Remark 19.2 for Lévy processes can be generalized in a straightforward manner to the non-symmetric finite-range Markov processes described in this section. In fact, following the same arguments of paper (Burch and Lehoucq 2015) for the symmetric case, the paper (D'Elia et al. 2017) shows that the expected exit time is finite as long as the bilinear form in (18.6) is coercive and the initial condition  $u_0$  is square integrable.

Furthermore, the same paper proves that

$$\mathbb{E}(\tau) \leq C_\tau \|u_0\|_{L^2(\Omega)},$$

where  $C_\tau$  only depends on the coercivity constant of the bilinear form  $\mathcal{A}_{cd,\delta}$ .  $\square$

## 20. A turbulent flow application

A fundamental problem of fluid flows is to ascertain information about the paths taken by two initially closely positioned particles, in particular what happens, over a long-time period, to the separation between a pair of particles. Such knowledge is crucial, e.g., to predict how pollutants spread. Intuitively, over a long time period, for *laminar flows* one expects that the separation between initially close particle pairs remains “small” and, in fact, the mean-square separation is proportion to  $t$ . Also intuitively, over a long time period, for *turbulent flows* one expects that at least some initially close particle pairs may become widely separated. What happens to the separation between pairs of particles in turbulent flows is the issue addressed in the classic paper (Richardson 1926). This subject, often referred to *Richardson pair dispersion*, remained of interest to Richardson and to many others, even up to now. Reviews on the subject of Richardson pair dispersion are provided in (Salazar and Collins 2009, Swaford 2001).

Using dimensional analysis arguments, Richardson predicted that the mean-square separation in turbulent flows is proportional to  $t^3$ . Although it is generally accepted that the mean-square separation is *not* proportional to  $t$  and that it grows faster than that, there is some controversy about the exponent 3, referred to as the *Richardson constant*. For example, a  $t^2$  dependence is advocated in (Bourgoin, Ouellette, Xu, Berg and Bodenschatz 2006). Dispersion faster than  $t$  is often referred to as *superdiffusion*. As discussed in Section 3, the fractional Laplace operator, when substituted for the classical Laplacian, is known to result in superdiffusive spread in “parabolic” equations. In (Gunzburger, Jiang and Xu 2018), a modification of the Navier-Stokes equations introduced in (Chen 2006) is studied, where the modification is that a fractional Laplacian viscous term is *added* to the standard Laplacian viscosity term.

The model considered is given by

$$\begin{cases} \mathbf{u}_t + (\mathbf{u} \cdot \nabla) \mathbf{u} - \nu \Delta \mathbf{u} + \sigma (-\Delta)^s \mathbf{u} + \nabla p = \mathbf{f} & \text{in } (0, T] \times \Omega \\ \nabla \cdot \mathbf{u} = 0 & \text{in } (0, T] \times \Omega, \end{cases} \quad (20.1)$$

where  $s \in (0, 1)$ ,  $\Omega \subset \mathbb{R}^d$  denotes a bounded, open domain,  $\sigma$  denotes a constant, and  $[0, T]$  denotes a temporal interval of interest.

In (Gunzburger et al. 2018), the energy spectrum of the modified Navier

Stokes equations (20.1) is investigated. It is shown there that for the special value of the fractional exponent  $s = 1/3$ , the corresponding power law of the energy spectrum in the inertial range has a deviation from the well-known Kolmogorov  $-5/3$  scaling, i.e., instead of a  $k^{-5/3}$  decay in the spectrum, one has  $k^{-5/3+\beta}$  for a constant  $\beta$ , where here  $k$  denotes the frequency. For other values of  $s \in (0, 1)$ , the power law of the energy spectrum is consistent with the Kolmogorov theory.

The connection to Richardson dispersion is made by noting that the fractional Laplacian is the generator of  $2s$ -stable Lévy process. The special value of  $s = \frac{1}{3}$  corresponds to the  $\frac{2}{3}$ -stable Lévy process for which *the mean square displacement is proportional to  $t^3$* . Thus, the fractional Laplacian with  $s = \frac{1}{3}$  introduces the corresponding Lévy flight mechanism into the system and represents Richardson pair dispersion.

An IMEX scheme can be used to discretize the system (20.1); a backward-Euler scheme of that type is considered in (Gunzburger et al. 2018) and is proved to be unconditionally stable and first-order accurate. Both the usual viscous term  $\nu \Delta \mathbf{u}$  and the added fractional viscous term  $\sigma(-\Delta)^s \mathbf{u}$  are treated implicitly. Because of the implicit treatment of the fractional Laplacian term, the scheme requires the solution of a *dense* linear system at each time step. Having to also handle the standard Navier-Stokes terms makes for an even greater computational challenge. Thus, it is tempting to lag the fractional term to the previous time step. Unfortunately, this leads to serious stability issues so that that term has to be treated implicitly. To mitigate these challenges, the following two-stage operator splitting algorithm is introduced in (Gunzburger et al. 2018):

Stage 1: Given  $\mathbf{u}^n$ , find  $\mathbf{w}^{n+1}$  satisfying

$$\begin{cases} \frac{\mathbf{w}^{n+1} - \mathbf{u}^n}{\Delta t} + (\mathbf{u}^n \cdot \nabla) \mathbf{w}^{n+1} - \nu \Delta \mathbf{w}^{n+1} + \nabla p^{n+1} = \mathbf{f}^{n+1} - \sigma(-\Delta)^s \mathbf{u}^n \\ \nabla \cdot \mathbf{w}^{n+1} = 0 \end{cases}$$

Stage 2: Given  $\mathbf{u}^n$  and  $\mathbf{w}^{n+1}$ , find  $\mathbf{u}^{n+1}$  satisfying

$$2\Delta t \sigma(-\Delta)^s (\mathbf{u}^{n+1} - \mathbf{u}^n) + \mathbf{u}^{n+1} - \mathbf{w}^{n+1} = 0.$$

The Stage 1 problem can be solved using a legacy Navier-Stokes code with the only modification necessary being in the construction of the right-hand side. In the second stage, one solves a nonlocal Poisson problem for the fractional Laplace operator which involves a symmetric, positive definite, albeit dense linear system. This two-stage algorithm, although involving two linear system solves per time step, when compared to the algorithm in which the two viscous terms are treated monolithically, requires much less coding effort and introduces efficiencies not possible for the monolithic scheme.

Of course, we have glossed over the fact the the fractional Laplacian involves an integral over all of  $\mathbb{R}^d$ . Moreover, we also have to choose a spatial discretization scheme. For the first of these, we can, e.g., use the truncated approximation discussed in Section 3.1.1, whereas for the latter we can use a finite element method based on, e.g. the Taylor-Hood finite element pair (Girault and Raviart 1986). Such fully discrete schemes involving the two-stage time-stepping algorithm are proven to be unconditionally stable and satisfy the error estimate

$$\|u_\infty(t^n) - u_{h,\lambda}^n\|_{L^2(\Omega)} \leq C\left(\frac{1}{\delta^{2s}} + h^3 + \Delta t\right),$$

where  $u(t^n)$  denotes the exact solution evaluated at time  $t = t_n$  and with no truncation of the fractional Laplace operator involved,  $u_{h,\delta}^n$  denotes the approximate solution, and  $h$  and  $\Delta t$  denote spatial and temporal grid size parameters, respectively. Note that for  $s = \frac{1}{3}$  we have that  $\frac{1}{\delta^{2s}} = \frac{1}{\delta^{2/3}}$ .

## 21. Peridynamics models for solid mechanics

In Sections 1 to 3, we consider nonlocal models for scalar-valued functions that are appropriate for modeling, e.g., anomalous diffusion problems. To provide an example of a nonlocal model for vector-valued functions, in this section we consider a *peridynamics model* for the vector-valued<sup>6</sup> displacement function in solid mechanics. Peridynamics is a nonlocal, continuum model that has been shown to provide an effective means for nucleating and propagating defects such as fractures (Hu, Ha and Bobaru 2012, Lipton 2014, Lipton 2015, Bobaru and Zhang 2015, Du, Tao and Tian 2018c).

The particular model we consider is the linear *state-based peridynamics model* for solid mechanics, introduced and analyzed in (Mengesha and Du 2014), that is a nonlocal analog of the classical Navier equations of linear elasticity. The model of (Mengesha and Du 2014) is a generalization of the peridynamics model introduced in (Silling, Epton, Weckner, Xu and Askari 2007, Silling 2010) when specialized to linear constitutive laws. The model of (Mengesha and Du 2014) is defined through an energy minimization principle for which the corresponding Euler-Lagrange equation provides a weak formulation of the problem. It should be noted that although the model of (Mengesha and Du 2014) generalizes the models in (Silling et al. 2007, Silling 2010), those earlier models are ubiquitous in peridynamic computations. Additionally, it should be noted that the models of (Silling et al. 2007, Silling 2010) cannot be cast in terms of fractional kernels.

<sup>6</sup> The most obvious nonlocal model involving a vector-valued function is the vector Laplacian problem  $-\Delta \mathbf{u} = \mathbf{f}$ , where  $\Delta \mathbf{u}$  is characterized in (1.27). This model can be studied in much same way as is done in this article for the models of Section 1.

To define the model considered, we need to introduce the operators<sup>7</sup>  $\mathcal{D}_\delta^*$  and  $\mathcal{D}_{\delta,\omega}^*$  that are respectively defined through their action on a vector-valued function  $\mathbf{u}(\mathbf{x})$  by

$$(\mathcal{D}^*\mathbf{u})(\mathbf{x}, \mathbf{y}) := -(\mathbf{u}(\mathbf{y}) - \mathbf{u}(\mathbf{x})) \otimes \frac{\mathbf{y} - \mathbf{x}}{|\mathbf{y} - \mathbf{x}|} \quad (21.1)$$

and

$$(\mathcal{D}_{\delta,\omega}^*\mathbf{u})(\mathbf{x}) := \int_{\Omega} (\mathcal{D}^*\mathbf{u})(\mathbf{x}, \mathbf{y}) \omega_\delta(\mathbf{x}, \mathbf{y}) d\mathbf{y},$$

where

$$\omega_\delta(\mathbf{x}, \mathbf{y}) := \frac{d}{m(\mathbf{x})} \gamma_\delta(\mathbf{y} - \mathbf{x}) |\mathbf{y} - \mathbf{x}|.$$

with

$$m_\delta(\mathbf{x}) := \int_{\Omega} \gamma_\delta(\mathbf{y} - \mathbf{x}) |\mathbf{y} - \mathbf{x}|^2 d\mathbf{y}.$$

We define the energy space

$$V_{p,\delta} = \{\mathbf{u} \in [L^2(\Omega \cup \Omega_{\mathcal{I}_\delta})]^d : \|\mathbf{u}\|_{V_{p,\delta}} < \infty, \mathbf{u}|_{\Omega_{\mathcal{I}_\delta}} = 0.\}$$

equipped with the norm

$$\|\mathbf{u}\|_{V_{p,\delta}} = \int_{\Omega \cup \Omega_{\mathcal{I}_\delta}} \int_{\Omega \cup \Omega_{\mathcal{I}_\delta}} \gamma_\delta(|\mathbf{y} - \mathbf{x}|) (\text{Tr}(\mathcal{D}^*\mathbf{u})(\mathbf{x}, \mathbf{y}))^2 d\mathbf{y} d\mathbf{x},$$

where  $\text{Tr}(\cdot)$  denotes the trace operator acting on a tensor. We also define, for functions  $\mathbf{u}(\mathbf{x}) \in V_{p,\delta}$  and  $\mathbf{v}(\mathbf{x}) \in V_{p,\delta}$  the symmetric bilinear form

$$\begin{aligned} \mathcal{P}_\delta(\mathbf{u}, \mathbf{v}) := & \int_{\Omega} \left( \left( k - \frac{\alpha m_\delta(\mathbf{x})}{d^2} \right) \text{Tr}(\mathcal{D}_{\delta,\omega}^*\mathbf{u})(\mathbf{x}) \text{Tr}(\mathcal{D}_{\delta,\omega}^*\mathbf{v})(\mathbf{x}) \right. \\ & \left. + \alpha \int_{\Omega} \gamma_\delta(\mathbf{y} - \mathbf{x}) \text{Tr}(\mathcal{D}^*\mathbf{u})(\mathbf{x}, \mathbf{y}) \text{Tr}(\mathcal{D}^*\mathbf{v})(\mathbf{x}, \mathbf{y}) d\mathbf{y} \right) d\mathbf{x}, \end{aligned} \quad (21.2)$$

where  $k$  and  $\alpha$  denote scalar constants related to the bulk and shear modulus of the material.

With the notation established, the weak formulation of the peridynamics problem considered is given as follows. Use  $V_p(\Omega)$  or  $V_{p,\delta}$  to denote space?

$$\begin{aligned} & \text{seek } \mathbf{u}(\mathbf{x}) \in V_{p,\delta}(\Omega) \text{ such that } \mathbf{u}(\mathbf{x}) = \mathbf{0} \text{ on } \Omega_{\mathcal{I}_\delta} \text{ and} \\ & \mathcal{P}_\delta(\mathbf{u}, \mathbf{v}) = (\mathbf{f}, \mathbf{v}) \quad \forall \mathbf{v} \in V_p(\Omega) \\ & \text{with } \mathbf{v}(\mathbf{x}) = \mathbf{0} \text{ on } \Omega_{\mathcal{I}_\delta}, \end{aligned} \quad (21.3)$$

<sup>7</sup> In (1.15), the operator  $\mathcal{D}_\delta^*$  is defined through its action on a scalar-valued function  $u(\mathbf{x})$ , resulting in  $\mathcal{D}_\delta^*u$  being a vector-valued function of  $\mathbf{x}$  and  $\mathbf{y}$ . In (21.1),  $\mathcal{D}_\delta^*$  is defined through its action on a *vector-valued function*  $\mathbf{u}(\mathbf{x})$ , resulting in  $\mathcal{D}_\delta^*\mathbf{u}$  being a tensor-valued function of  $\mathbf{x}$  and  $\mathbf{y}$ . This is entirely analogous to the local case in which  $\nabla u$  is a vector and  $\nabla \mathbf{u}$  is a tensor.



where  $(\cdot, \cdot)$  denotes the  $[L^2(\Omega)]^d$  inner product. For simplicity, we have imposed a homogeneous volume constraint on the displacement  $\mathbf{u}$ . Nonlocal traction constraints and inhomogeneous volume constraints can also be treated.

In (Mengesha and Du 2014), the coercivity and continuity of the bilinear form  $\mathcal{P}_\delta(\cdot, \cdot)$  with respect to the energy space  $V_p(\Omega)$  is established, so that the well posedness of the problem (21.3) can be rigorously established via the Lax-Milgram theorem. Additional discussions, including studies with other types of nonlocal constraints, can be found in (Mengesha and Du 2015, Mengesha and Du 2016, Du 2019).

**Remark 21.1.** *Some choices for the peridynamics kernel function  $\gamma_\delta(|\mathbf{z}|)$  are those having bounded second moments, including those that are comparable to  $|\mathbf{z}|^{-d-2s}$  in the sense that they have the same singular behavior at the origin as that of the fractional kernel (2.22). Of particular interest in the peridynamics setting are the cases of integrable functions and fractional kernels with  $s < \frac{1}{2}$  because the corresponding function spaces in which the peridynamics model is well posed admit functions with jump discontinuities. As such, discontinuities in the displacement  $\mathbf{u}(\mathbf{x})$  can be viewed as fracture. Functions comparable to  $|\mathbf{z}|^{-1}$  are integrable for  $d \geq 2$  and are the ubiquitous choice made in peridynamics modeling, starting with the papers (Silling 2000, Silling et al. 2007, Silling 2010) in which peridynamics was first introduced.  $\square$*

The strong formulation corresponding to the weak formulation (2.9) is also derived in (Mengesha and Du 2014). In the local limit, i.e., as  $\delta \rightarrow 0$  and for sufficiently smooth  $\mathbf{u}(\mathbf{x})$ , the solutions of the nonlocal state-based peridynamic model converge to that of the classical Navier-Cauchy equation of linear elasticity.

**Remark 21.2.** *Bond breaking.* There is more to peridynamics than just the weak and strong formulations introduced above. Certainly, those models admit, as discussed in Remark 21.1, solutions having jump discontinuities. For example, for integrable functions  $\gamma_\delta$ , solutions are no smoother than the data so that, in general, discontinuities in the boundary data or in the source term will result in discontinuities in the solution. However, in the time dependent setting, fracture and other defects can arise, e.g., due to large tensile loads, even if the initial condition data and other data are smooth. Thus, to model fracture nucleation, the peridynamics model equations, whether in weak or strong form, have been, in some cases, supplemented by a *bond-breaking rule*. Basically, such rules state that two points<sup>8</sup>  $\mathbf{x}$  and  $\mathbf{y}$  that are

<sup>8</sup> Note that peridynamics models, such as those associated with (21.3), are posed in a Lagrangian framework.

initially bonded, i.e., that are within a distance  $\delta$  from each other, become un-bonded if at a later time those points become separated by a distance greater than  $\delta$ . Bond-breaking rules and how they effect the nucleation of cracks are more complicated than the simplistic description just given, but further discussion is beyond the scope of this article. Detailed explanations may be found in, e.g., (Silling 2000, Lipton 2014, Lipton 2017, Lipton, Lehoucq and Sha 2018, Du et al. 2018c).  $\square$

For additional detailed discussions about the material presented in this section, see, e.g., (Du et al. 2012a, Mengesha and Du 2016, Du 2019) as well as (Mengesha and Du 2014).

Numerical methods for both the strong and weak formulations of the peridynamics model have been developed. For example, consider the finite element methods discussed in Section 5. Let  $\{V_{p,\delta,h}\} \subset V_{p,\delta}$  denote a family of finite element subspaces, where  $h$  characterizes the mesh size and for any  $\mathbf{v} \in V_{p,\delta}$ , we have a family of elements  $\{\mathbf{v}_h \in V_{p,\delta,h}\}$  such that  $\|\mathbf{v}_h - \mathbf{v}\|_{V_{p,\delta}} \rightarrow 0$  as  $h \rightarrow 0$  for any fixed  $\delta > 0$ . For the finite element discretization of the state-based linear peridynamic model (21.3), one merely replaces in that equation  $V_{p,\delta}$  by  $V_{p,\delta,h}$  to arrive at the discrete problem

$$\text{find } \mathbf{u}_{\delta,h} \in V_{p,\delta,h} \text{ such that } \mathcal{P}_\delta(\mathbf{u}_{\delta,h}, \mathbf{v}) = (\mathbf{f}, \mathbf{v})_{L^2} \quad \forall \mathbf{v} \in V_{p,\delta,h}. \quad (21.4)$$

The analysis of solutions of this problem can be formulated within the general framework of the AC schemes originally presented in (Tian and Du 2014). It is rigorously shown in (Tian and Du 2014) that, for linear multidimensional state-based peridynamic systems associated with (21.3), all conforming Galerkin approximations of the nonlocal models containing continuous piecewise linear functions are automatically AC. This means that they can recover the correct local limit as long as both  $\delta$  and  $h$  are diminishing, even if the nonlocality measure  $\delta$  is reduced at a much faster pace than the mesh spacing  $h$ .

As was the case for the nonlocal diffusion case, if  $h = o(\delta)$  as  $\delta \rightarrow 0$ , then we are able to obtain the correct local limit even for discontinuous piecewise constant finite element approximations when they are of the conforming type. Practically speaking, this implies that a mild growth of bandwidth in the finite element stiffness matrix is needed as the mesh is refined, in order to recover the correct local limit for Riemann sum like quadratures or piecewise constant finite element schemes. On the other hand, if a constant bandwidth is kept as the mesh is refined, as is often advocated in the peridynamics community, approximations may converge to an incorrect local limit.

## 22. Image denoising

We describe the use of nonlocal diffusion operators in a variational setting for image denoising. In this context, by considering intensity patterns in

neighborhoods of points surrounding a pixel, nonlocal filters allow for simultaneous conservation of structures (patterns) and textures. Classical methods, which use differential operators, do not necessarily guarantee feature preservation because, by definition, they only consider infinitesimal neighborhoods around points.

Even though nonlocal-type filters have been used for decades, we refer to (Buades, Coll and Morel 2010) as the first rigorous work that can be related to a nonlocal diffusion equation as presented in this article. In that paper, the *nonlocal-means* (NL-means) filter for image denoising is proposed. Given a blurred (or noisy) image  $f$  defined by its intensity in the image domain  $\Omega$ , the NL-means filter is defined as

$$NL[f](\mathbf{x}) = \frac{1}{c(\mathbf{x})} \int_{\Omega} e^{-d_a(f(\mathbf{x}), f(\mathbf{y}))/D^2} f(\mathbf{y}) d\mathbf{y} \quad \forall \mathbf{x} \in \Omega \quad (22.1)$$

where

$$d_a(f(\mathbf{x}), f(\mathbf{y})) = \int_{\Omega} G_a(\mathbf{z}) |f(\mathbf{x} + \mathbf{z}) - f(\mathbf{y} + \mathbf{z})| d\mathbf{z},$$

with  $G_a(\mathbf{z})$  a Gaussian with standard deviation  $a$  and with  $c(\mathbf{x})$  a normalizing factor. Note that the nonlocal filter is directly applied to the blurred image, i.e., the nonlocal operator is not associated with a diffusion equation.

The variational interpretation of such a filter is introduced in (Kindermann, Osher and Jones 2005) in which the NL-means and other neighborhood filters are interpreted as regularizing functionals. Specifically, they formulate the denoising problem as an unconstrained optimization problem where the objective is to minimize the nonlocal functional

$$\mathcal{J}_R u = \int_{\Omega} \int_{\Omega} g \left( \frac{|u(\mathbf{x}) - u(\mathbf{y})|}{D^2} \right) \nu(|\mathbf{x} - \mathbf{y}|) d\mathbf{y} + F(u, f), \quad (22.2)$$

where  $\nu$  is a symmetric window that determines the extent of the nonlocal interactions and  $g$  determines the type of filtering. Here,  $F(u, f)$  is a fidelity term, usually a measure of the distance between the reconstructed and noisy images. The outcome of the optimization is the reconstructed image  $u$ . In case of NL-means filtering, (22.2) becomes

$$\mathcal{J}_{NL} u = \int_{\Omega} \int_{\Omega} \left( 1 - e^{-d_a(u(\mathbf{x}), u(\mathbf{y}))/D^2} \right) \nu(|\mathbf{x} - \mathbf{y}|) d\mathbf{y} + F(u, f). \quad (22.3)$$

Such a minimization problem cannot be directly related to the nonlocal diffusion theory reported on this article because of the potential non-convexity of the functionals. For the same reasons, in (Gilboa and Osher 2007), a modified convex functional (still based on nonlocal filters) is introduced that resembles common functionals used in PDE-based imaging approaches such

as total variation ones (Rudin, Osher and Fatemi 1992). In Section 22.1, we describe methods based on this concept and highlight their connection to the solution of nonlocal diffusion problems. In all the examples below, unless otherwise stated, the relation between clean and noisy image is the *additive noise* model, i.e.,  $f = u + \eta$ , where  $u$  denotes the clean image,  $f$  the noisy one, and  $\eta$  the noise.

### 22.1. Image deblurring via minimization of a nonlocal functional

In (Gilboa and Osher 2007), the image deblurring problem is tackled by solving an unconstrained optimization problem with functional

$$\mathcal{J}(u; f) = \frac{1}{2} |u|_{V_c(\Omega)}^2 + \frac{w}{2} \|u - f\|_{L^2(\Omega)}^2, \quad (22.4)$$

where  $|\cdot|_{V_c}$  denotes the energy seminorm defined in (2.5) associated with an appropriate kernel  $\gamma_\delta$ , whose definition depends on the type of filtering (either NL-means or other neighborhood filters) and the fidelity term controls the difference between the reconstructed image and the noisy one. Note that the weight  $w \in \mathbb{R}^+$  could be replaced by a spatially-dependent function that is included within the  $L^2$  norm.

The Euler-Lagrange equation that determines the necessary conditions for optimality is given by the nonlocal reaction-diffusion equation

$$-\mathcal{L}u + w(u - f) = 0, \quad (22.5)$$

whose well posedness can be determined as described in Section 2.1 based on the properties of the kernel  $\gamma_\delta$ .

Figure 22.1 taken from Gilboa2007 provides an example of a nonlocal deblurring reconstruction and also a comparison with a classical method local method, namely the Total Variation (TV) method of (Rudin et al. 1992). The clean and noisy images are given in the top row and the nonlocal and local reconstructions are given in the bottom row. These results show the ability of nonlocal filters to better capture high-contrast features compared to classical methods.

The follow-up paper (Gilboa and Osher 2008) provides additional insights about the theoretical aspects of the method of (Gilboa and Osher 2007) and about other types of filters, and also provides comparisons with other methods.

**Remark 22.1.** A very similar formulation can be used for image deconvolution (Lou et al. 2010) where the relation between clean and noisy image,  $f = \mathcal{K}u + \eta$ , involves a convolution operator  $\mathcal{K}$ . This renders the denoising problem more complicated. In this setting, the cost functional of the

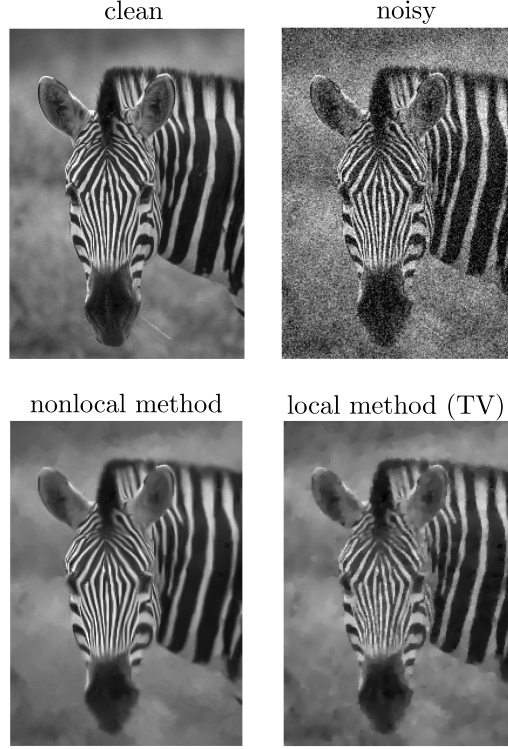


Figure 22.1. Clean, noisy, and nonlocal and local reconstructions of a noisy image featuring high-contrast features.

unconstrained optimization problem is given by

$$\mathcal{J}_c(u) = \frac{1}{2}|u|_{V_c(\Omega)}^2 + \frac{w}{2} \int_{\Omega} (k(\mathbf{x}) * u(\mathbf{x}) - f(\mathbf{x}))^2 d\mathbf{x}$$

and the Euler-Lagrange equation is the nonlocal diffusion equation

$$-\mathcal{L}u = w\tilde{g} * (f - g * u),$$

where  $\tilde{g}$  denotes the adjoint of  $g$ .

**Remark 22.2.** Similar operators to those discussed in this section have also been used for image segmentation (Gilboa and Osher 2007), filtering (Darbon, Cunha, Chan, Osher and Jensen 2008), and image and video recovery (Buades, Coll and Morel 2008).

**Remark 22.3.** In the literature, denoising nonlocal operators are not necessarily associated with nonlocal filters such as NL-means, but can be described by fractional operators, specifically by the spectral fractional Laplacian, see, e.g., (Antil and Bartels 2017).

### 22.1.1. Optimization of the denoising parameters

The quality of the reconstruction strongly depends on model parameters (e.g., parameters in the kernel) and on the weight parameter  $w$ . However, model parameters are often unknown (see Section 15) and the selection of  $w$  is not a trivial task. In (D'Elia, los Reyes and Trujillo 2019c), a bilevel optimization approach is considered for the identification of kernel parameters (in case of integrable kernels, including NL-means) and of the weight function  $w : \Omega \rightarrow \mathbb{R}^+$ . Because the estimation of kernel parameters is discussed in Section 15, here we only consider the formulation for the identification of  $w$ , in its simplest setting.

Given a clean image and the corresponding blurred image,  $(\hat{u}, \hat{f})$ , the bilevel optimization problem is formulated as

$$\begin{aligned} \min_{w \in W} \mathcal{J}_w(u, w) &= \|u - \hat{u}\|_{L^2(\Omega)}^2 + \frac{\beta}{2} \|w\|_{H^1(\Omega)}^2 \\ \text{such that } u &= \arg \min_{u \in V_c} \mathcal{J}_u(u, w) = \frac{1}{2} |u|_{V_c(\Omega)}^2 + \int_{\Omega} w(u - \hat{f})^2 dx, \end{aligned} \quad (22.6)$$

where the feasible set is  $W = \{w \in H^1(\Omega) : 0 \leq \lambda(\mathbf{x}) \leq \Lambda\}$ . Note that the constraint in (22.6) is equivalent to the diffusion-reaction equation in (22.5). The well posedness of the bilevel optimization problem is proven in (D'Elia et al. 2019c). Also introduced there is a second-order optimization algorithm for its solution, and insights are given about implementation aspects and numerical performance. Also, the theory and advantages of using nonlocal models are illustrated through several numerical tests on standard benchmark images.

## Acknowledgements

The research of MD, CG and (partially) MG is supported by Sandia National Laboratories (SNL). SNL is a multimission laboratory managed and operated by National Technology and Engineering Solutions of Sandia, LLC., a wholly owned subsidiary of Honeywell International, Inc., for the U.S. Department of Energy's National Nuclear Security Administration under contract DE-NA-0003525. Specifically, this work was supported by the SNL Laboratory-directed Research and Development (LDRD) program. Note that this paper describes objective technical results and analysis. Any subjective views or opinions that might be expressed in the paper do not necessarily represent the views of the U.S. Department of Energy or the United States Government.

The research of QD is supported in part by the US National Foundation grants NSF DMS-1719699 and NSF CCF-1704833, the US Air Force Office of Scientific Research MURI Center for Material Failure Prediction Through

Peridynamics, and by the US Army Research Office MURI grant W911NF-15-1-0562.

The research of XT is supported in part by the U.S. NSF grant DMS-1819233.

The research of ZZ is supported by a start-up grant from the Hong Kong Polytechnic University and Hong Kong RGC grant 25300818.

Several figures in the article are reproduced by permission. Specifically, Figure 5.1 is reproduced from (Xu et al. 2016a), Figures 12.1 and 12.2 from (Tian and Engquist 2019), Figure 15.1 from (D’Elia and Gunzburger 2014), Figure 15.2 from (D’Elia and Gunzburger 2016), Figure 16.1 from (Burkovska and Gunzburger 2019b), Figure 17.1 from (Witman et al. 2017), and Figure 22.1 from (Gilboa and Osher 2007).

## REFERENCES

- N. Abatangelo and L. Dupaigne (2017), ‘Nonhomogeneous boundary conditions for the spectral fractional Laplacian’, *Ann. Inst. H. Poincaré Anal. Non Linéaire* **34**, 439–467.
- M. Abramowitz and I. Stegun (1972), *Handbook of Mathematical Functions with Formulas, Graphs, and Mathematical Tables*, National Bureau of Standards and Dover.
- G. Acosta and J.-P. Borthagaray (2017), ‘A fractional Laplace equation: regularity of solutions and Finite Element approximations’, *SIAM Journal on Numerical Analysis* **55**, 472–495.
- G. Acosta, F. Bersetche and J. Borthagaray (2017), ‘A short FE implementation for a 2d homogeneous Dirichlet problem of a fractional Laplacian’, *Comput. Math. Appl.* **74**, 784–816.
- G. Acosta, J.-P. Borthagaray and N. Heuer (2019), ‘Finite element approximations of the nonhomogeneous fractional Dirichlet problem’, *IMA J. Numer. Anal.* **39**, 1471–1501.
- G. Acosta, J.-P. Borthagaray, O. Bruno and M. Maas (2018), ‘Regularity theory and high order numerical methods for the (1D)-fractional Laplacian’, *Math. Comp.* **87**, 1821–1857.
- M. Ainsworth and C. Glusa (2017), ‘Aspects of an adaptive finite element method for the fractional Laplacian: a priori and a posteriori error estimates, efficient implementation and multigrid solver’, *Comput. Methods Appl. Mech. Engrg.* pp. 4–35.
- M. Ainsworth and C. Glusa (2018a), ‘Hybrid Finite Element-Spectral Method for the Fractional Laplacian: Approximation Theory and Efficient Solver’, *SIAM Journal on Scientific Computing* **40**, A2383–A2405.
- M. Ainsworth and C. Glusa (2018b), ‘Towards an efficient finite element method for the integral fractional Laplacian on polygonal domains’, in *Contemporary Computational Mathematics - A Celebration of the 80th Birthday of Ian Sloan*, Springer, pp. 17–57.
- M. Ainsworth and Z. Mao (2017), ‘Analysis and approximation of a fractional Cahn-Hilliard equation’, *SIAM Journal on Numerical Analysis* **55**, 1689–1718.

- M. Ainsworth and W. McLean (2003), 'Multilevel diagonal scaling preconditioners for boundary element equations on locally refined meshes', *Numerische Mathematik* **93**, 387–413.
- M. Ainsworth, W. McLean and T. Tran (1999), 'The conditioning of boundary element equations on locally refined meshes and preconditioning by diagonal scaling', *SIAM Journal on Numerical Analysis* **36**, 1901–1932.
- B. Aksoylu and T. Mengesha (2010), 'Results on nonlocal boundary value problems', *Numerical Functional Analysis and Optimization* **31**, 1301–1317.
- B. Aksoylu and M. Parks (2011), 'Variational theory and domain decomposition for nonlocal problems', *Applied Mathematics and Computation* **217**, 6498–6515.
- B. Aksoylu and Z. Unlu (2014), 'Conditioning analysis of nonlocal integral operators in fractional Sobolev spaces', *SIAM Journal on Numerical Analysis* **52**, 653–677.
- B. Alali, M. Gunzburger and K. Liu (2015), 'A generalized nonlocal calculus', *J. Appl. Math. Phys.* **223**, 2807–2828.
- F. Andreu, J. Mazón, J. Rossi and J. Toledo (2010), *Nonlocal Diffusion Problems*, Vol. 165 of *Mathematical Surveys and Monographs*, American Mathematical Society.
- H. Antil and S. Bartels (2017), 'Spectral approximation of fractional PDEs in image processing and phase field modeling', *Computational Methods in Applied Mathematics* **17**(4), 661–678.
- H. Antil and M. Warma (2019), 'Optimal control of fractional semilinear PDEs', *ESAIM Control Optimisation and Calculus of Variations*. To appear.
- H. Antil, R. Khatri and M. Warma (2019a), 'External optimal control of nonlocal PDEs', *Inverse Problems*. To appear.
- H. Antil, J. Pfefferer and S. Rogovs (2018), 'Fractional operators with inhomogeneous boundary conditions: analysis, control, and discretization', *Commun. Math. Sci.* **16**, 1395–1426.
- H. Antil, D. Verma and M. Warma (2019b), 'External optimal control of fractional parabolic PDEs', *arXiv preprint arXiv:1904.07123*.
- K. Atkinson and W. Han (2012), *Spherical harmonics and approximations on the unit sphere: an introduction*, Vol. 2044 of *Lecture Notes in Mathematics*, Springer.
- I. Babuska (1971), 'Error-bounds for finite element method', *Numer. Math.* **16**, 322–333.
- I. Babuska and K. Aziz (1972), Survey lectures on the mathematical foundation of the finite element method, in *The Mathematical Foundations of the Finite Element Method with Application to Partial Differential Equations*, Academic Press, New York, pp. 1–359.
- B. Baeumer and M. Meerschaert (2010), 'Tempered stable Lévy motion and transient super-diffusion', *Journal of Computational and Applied Mathematics* **233**, 2438–2448.
- D. Baleanu, K. Diethelm, E. Scalas and J. Trujillo (2016), *Fractional Calculus: Models and Numerical Methods*, World Scientific, Singapore.
- L. Banjai, J. Melenk, R. Nochetto, E. Otárola, A. Salgado and C. Schwab (2019), 'Tensor FEM for Spectral Fractional Diffusion', *Foundations of Computational Mathematics* **19**, 901–962.



- U. Biccari and V. Hernández-Santamaría (2018), ‘The Poisson equation from non-local to local’, *Electron. J. Differential Equations* pp. Paper No. 145, 13.
- R. Blumenthal, R. Gettoor and D. Ray (1961), ‘On the distribution of first hits for the symmetric stable processes’, *Trans. Amer. Math. Soc.* **99**, 540–554.
- F. Bobaru and M. Duangpanya (2010), ‘The peridynamic formulation for transient heat conduction’, *International Journal of Heat and Mass Transfer* **53**, 4047–4059.
- F. Bobaru and G. Zhang (2015), ‘Why do cracks branch? A peridynamic investigation of dynamic brittle fracture’, *International Journal of Fracture* **196**, 59–98.
- F. Bobaru, M. Yang, L. Alves, S. Silling, E. Askari and J. Xu (2009), ‘Convergence, adaptive refinement, and scaling in 1D peridynamics’, *Inter. J. Numer. Meth. in Eng.* **77**, 852–877.
- K. Bogdan and T. Byczkowski (1999), ‘Potential theory for the  $\alpha$ -stable Schrödinger operator on bounded Lipschitz domains’, *Studia Math.* **133**, 53–92.
- K. Bogdan, K. Burdzy and Z.-Q. Chen (2003), ‘Censored stable processes’, *Probab. Theory Related Fields* **127**, 89–152.
- A. Bonito and J. Pasciak (2015), ‘Numerical approximation of fractional powers of elliptic operators’, *Math. Comp.* **84**, 2083–2110.
- A. Bonito and J. Pasciak (2017), ‘Numerical approximation of fractional powers of regularly accretive operators’, *IMA J. Numer. Anal.* **37**, 1245–1273.
- A. Bonito, W. Lei and J. Pasciak (2019), ‘Numerical approximation of the integral fractional Laplacian’, *Numer. Math.* **142**, 235–278.
- A. Bonito, W. Lei and A. Salgado (2018), ‘Finite element approximation of an obstacle problem for a class of integro-differential operators’, *arXiv:1808.01576*.
- J.-P. Borthagaray, R. Nochetto and A. Salgado (2018), ‘Weighted sobolev regularity and rate of approximation of the obstacle problem for the integral fractional Laplacian’, *arXiv:1806.08048*.
- J. Bourgain, H. Brezis and P. Mironescu (2001), *Another look at Sobolev spaces*, IOS Press, pp. 439–455.
- M. Bourgoïn, N. Ouellette, H. Xu, J. Berg and E. Bodenschatz (2006), ‘The role of pair dispersion in turbulent flow’, *Science* **311**, 835–838.
- J. Boyd (1987), ‘Spectral methods using rational basis functions on an infinite interval’, *J. Comput. Phys.* **69**, 112–142.
- J. Boyd (2001), ‘Rational Chebyshev spectral methods for unbounded solutions on an infinite interval using polynomial-growth special basis functions’, *Comput. Math. Appl.* **41**, 1293–1315.
- S. Brenner and R. Scott (1994), *The Mathematical Theory of Finite Element Methods*, Springer, New York.
- A. Buades, B. Coll and J. Morel (2008), ‘Nonlocal image and movie denoising’, *International Journal of Computer Vision* **76**, 123–139.
- A. Buades, B. Coll and J. Morel (2010), ‘Image denoising methods. a new nonlocal principle’, *SIAM Review* **52**, 113–147.
- C. Bucur (2016), ‘Some observations on the Green function for the ball in the fractional Laplace framework’, *Commun. Pure Appl. Anal.* **15**, 657–699.
- M. Buhmann (2000), ‘Radial basis functions’, **9**, 1–38.
- M. Buhmann (2003), *Radial Basis Functions: Theory and Implementations*, Vol. 12

- of *Cambridge Monographs on Applied and Computational Mathematics*, Cambridge University Press.
- N. Burch and R. Lehoucq (2015), ‘Computing the exit-time for a finite-range symmetric jump process’, *Montecarlo methods and applications* **21**(2), 139–152.
- N. Burch, M. D’Elia and R. Lehoucq (2014), ‘The exit-time problem for a Markov jump process’, *The European Physical Journal Special Topics* **223**, 3257–3271.
- O. Burkovska and M. Gunzburger (2019a), ‘Affine approximation of parametrized kernels and model order reduction for nonlocal and fractional laplace models’, *arXiv:1901.0674*.
- O. Burkovska and M. Gunzburger (2019b), ‘Regularity and approximation analyses of nonlocal variational equality and inequality problems’, *J. Math. Anal. Appl.* **478**, 1027–1048.
- L. Caffarelli and L. Silvestre (2007), ‘An extension problem related to the fractional Laplacian’, *Communications in partial differential equations* **32**, 1245–1260.
- L. Caffarelli and P. R. Stinga (2016), Fractional elliptic equations, caccioppoli estimates and regularity, in *Annales de l’Institut Henri Poincaré (C) Non Linear Analysis*, Vol. 33, pp. 767–807.
- L. Caffarelli, X. Ros-Oton and J. Serra (2017), ‘Obstacle problems for integro-differential operators: regularity of solutions and free boundaries’, *Invent. Math.* **208**, 1155–1211.
- C. Çelik and M. Duman (2012), ‘Crank-Nicolson method for the fractional diffusion equation with the Riesz fractional derivative’, *J. Comput. Phys.* **231**, 1743–1750.
- A. Chen, Q. Du, C. Li and Z. Zhou (2017), ‘Asymptotically compatible schemes for space-time nonlocal diffusion equations’, *Chaos, Solitons and Fractals* **102**, 361–371.
- L. Chen, R. Nochetto, E. Otárola and A. J. Salgado (2016a), ‘Multilevel methods for nonuniformly elliptic operators and fractional diffusion’, *Mathematics of Computation*.
- M. Chen and W. Deng (2014), ‘Fourth order accurate scheme for the space fractional diffusion equations’, *SIAM J. Numer. Anal.* **52**, 1418–1438.
- S. Chen, J. Shen and L.-L. Wang (2016b), ‘Generalized Jacobi functions and their applications to fractional differential equations’, *Math. Comp.* **85**, 1603–1638.
- W. Chen (2006), ‘A speculative study of 2/3-order fractional laplacian modeling of turbulence: some thoughts and conjectures’, *Chaos* **16**, 023126.
- X. Chen and M. Gunzburger (2011), ‘Continuous and discontinuous finite element methods for a peridynamics model of mechanics’, *Computer Methods in Applied Mechanics and Engineering* **200**, 1237–1250.
- Z.-Q. Chen and P. Kim (2002), ‘Green function estimate for censored stable processes’, *Probab. Theory Related Fields* **124**, 595–610.
- A. Chernov, T. von Petersdorff and C. Schwab (2011), ‘Exponential convergence of hp quadrature for integral operators with Gevrey kernels’, *ESAIM: Mathematical Modelling and Numerical Analysis* **45**, 387–422.
- P. Ciarlet (2002), *Finite Element Methods for Elliptic Problems*, SIAM, Philadelphia.
- C. Cortazar, M. Elgueta, J. Rossi and N. Wolanski (2008), ‘How to approximate

- the heat equation with Neumann boundary conditions by nonlocal diffusion problems', *Archive for Rational Mechanics and Analysis* **187**, 137–156.
- T. Coulhon and A. Grigoryan (1998), 'Random walks on graphs with regular volume growth', *Geom. Funct. Anal.* **8**, 656–701.
- J. Curtiss (1950), Sampling methods applied to differential and difference equations, in *Proceedings, Seminar on Scientific Computation, November, 1949*, International Business Machines Corp., pp. 87–109.
- N. Cusimano, F. del Teso, L. Gerardo-Giorda and G. Pagnini (2018), 'Discretizations of the spectral fractional Laplacian on general domains with Dirichlet, Neumann, and Robin boundary conditions', *SIAM J. Numer. Anal.* **56**, 1243–1272.
- J. Darbon, A. Cunha, T. Chan, S. Osher and G. Jensen (2008), 'Fast nonlocal filtering applied to electron cryomicroscopy', *2008 5th IEEE International Symposium on Biomedical Imaging: From Nano to Macro* pp. 1331–1334.
- M. D'Elia and M. Gunzburger (2013), 'The fractional Laplacian operator on bounded domains as a special case of the nonlocal diffusion operator', *Comput. Math. Appl.* **66**, 1245–1260.
- M. D'Elia and M. Gunzburger (2014), 'Optimal distributed control of nonlocal steady diffusion problems', *SIAM Journal on Control and Optimization* **55**, 667–696.
- M. D'Elia and M. Gunzburger (2016), 'Identification of the diffusion parameter in nonlocal steady diffusion problems', *Applied Mathematics and Optimization* **73**, 227–249.
- M. D'Elia, Q. Du, M. Gunzburger and R. B. Lehoucq (2017), 'Nonlocal convection-diffusion problems on bounded domains and finite-range jump processes', *Comput. Meth. in Appl. Math.* **17**, 707–722.
- M. D'Elia, C. Flores, X. Li, P. Radu and Y. Yu (2019a), 'Helmholtz-Hodge decompositions in the nonlocal framework - Well-posedness analysis and applications', *arXiv1906.04259*.
- M. D'Elia, C. Glusa and E. Otárola (2019b), 'A priori error estimates for the optimal control of the integral fractional Laplacian', *SIAM Journal on Control and Optimization* **57**, 2775–2798.
- M. D'Elia, J.-C. D. los Reyes and A. M. Trujillo (2019c), 'Bilevel parameter optimization for nonlocal image denoising models', *arXiv1912.02347*.
- M. D'Elia, X. Tian and Y. Yu (2019d), 'A physically-consistent, flexible and efficient strategy to convert local boundary conditions into nonlocal volume constraints', *arXiv1906.04259*.
- B. Deng, Z. Zhang and X. Zhao (2019), 'Superconvergence points for the spectral interpolation of Riesz fractional derivatives', *Journal of Scientific Computing*.
- E. Di Nezza, G. Palatucci and E. Valdinoci (2012), 'Hitchhiker's guide to the fractional Sobolev spaces', *Bull. Sci. Math.* **136**, 521–573.
- H. Ding, C. Li and Y.-Q. Chen (2015), 'High-order algorithms for Riesz derivative and their applications (II)', *J. Comput. Phys.* **293**, 218–237.
- S. Dipierro, X. Ros-Oton and E. Valdinoci (2017), 'Nonlocal problems with Neumann boundary conditions', *Rev. Mat. Iberoam.* **33**, 377–416.
- Q. Du (2019), *Nonlocal Modeling, Analysis, and Computation*, Vol. 94 of *CBMS-NSF Conference Series in Applied Mathematics*, SIAM.

- Q. Du and X. Feng (2020), The phase field method for geometric moving interfaces and their numerical approximations, in *Geometric Partial Differential Equations - Part I, Handbook of Numerical Analysis*, Vol. 21, Elsevier.
- Q. Du and Z. Huang (2017), 'Numerical solution of a scalar one-dimensional monotonicity-preserving nonlocal conservation law', *J. Math. Res. Appl.* **37**, 1–18.
- Q. Du and X. Tian (2014), 'Asymptotically compatible schemes for peridynamics based on numerical quadratures', *Proc. of ASME 2014 International Mechanical Engineering Congress and Exposition* pp. IMECE2014–39620.
- Q. Du and X. Tian (2015), Robust discretization of nonlocal models related to peridynamics, in *Meshfree Methods for Partial Differential Equations VII*, Vol. 100, Springer, pp. 97–113.
- Q. Du and X. Tian (2018), Heterogeneously localized nonlocal operators, boundary traces and variational problems, in *Proceedings of the International Congress of Chinese Mathematicians*, Vol. 43 of the ALM series, International Press, pp. 217–236.
- Q. Du and X. Tian (2019), 'Mathematics of smoothed particle hydrodynamics via a nonlocal stokes equation', *Foundations of Computational Mathematics* pp. 1–26.
- Q. Du and J. Yang (2016a), 'Asymptotically compatible Fourier spectral approximations of nonlocal Allen-Cahn equations', *SIAM J. Numer. Anal.* **54**, 1899–1919.
- Q. Du and J. Yang (2016b), 'Asymptotically compatible Fourier spectral approximations of nonlocal Allen-Cahn equations', *SIAM J. Numer. Anal.* **54**, 1899–1919.
- Q. Du and J. Yang (2017), 'Fast and accurate implementation of Fourier spectral approximations of nonlocal diffusion operators and its applications', *J. Comput. Phys.* **332**, 118–134.
- Q. Du and X. Yin (2019), 'A conforming dg method for linear nonlocal models with integrable kernels', *J. Scientific Computing* **80**, 1913–1935.
- Q. Du and K. Zhou (2011), 'Mathematical analysis for the peridynamic nonlocal continuum theory', *ESAIM Math. Model. Numer. Anal.* **45**, 217–234.
- Q. Du and Z. Zhou (2017), 'Multigrid finite element method for nonlocal diffusion equations with a fractional kernel', *preprint*.
- Q. Du, M. Gunzburger, R. Lehoucq and K. Zhou (2012a), 'Analysis and approximation of nonlocal diffusion problems with volume constraints', *SIAM Review* **54**, 667–696.
- Q. Du, M. Gunzburger, R. Lehoucq and K. Zhou (2013a), 'A nonlocal vector calculus, nonlocal volume-constrained problems, and nonlocal balance laws', *Math. Mod. Meth. Appl. Sci.* **23**, 493–540.
- Q. Du, H. Han, C. Zheng and J. Zhang (2018a), 'Numerical solution of a two-dimensional nonlocal wave equation on unbounded domains', *SIAM J. Scientific Computing* **40**, A1430–1445.
- Q. Du, Z. Huang and P. LeFloch (2017a), 'Nonlocal conservation laws. I. A new class of monotonicity-preserving models', *SIAM J. Numerical Analysis* **55**, 2465–2489.

- Q. Du, Z. Huang and R. Lehoucq (2014), ‘Nonlocal convection-diffusion volume-constrained problems and jump processes’, *Discrete and Continuous Dynamical Systems Series B* **19**, 961–977.
- Q. Du, L. Ju and J. Lu (2019a), ‘Analysis of fully discrete approximations for dissipative systems and application to time-dependent nonlocal diffusion problems’, *Journal of Scientific Computing* **78**, 1438–1466.
- Q. Du, L. Ju and J. Lu (2019b), ‘A discontinuous Galerkin method for one-dimensional time-dependent nonlocal diffusion problems’, *Mathematics of Computation* **88**, 123–147.
- Q. Du, L. Ju, X. Li and Z. Qiao (2018b), ‘Stabilized linear semi-implicit schemes for the nonlocal Cahn-Hilliard equation’, *Journal of Computational Physics* **363**, 39–54.
- Q. Du, L. Ju, J. Lu and X. Tian (2019c), ‘A discontinuous galerkin method with penalty for one-dimensional nonlocal diffusion problems’, *Communications on Applied Mathematics and Computation* pp. 1–25.
- Q. Du, L. Ju, L. Tian and K. Zhou (2013b), ‘A posteriori error analysis of finite element method for linear nonlocal diffusion and peridynamic models’, *Math. Comp.* **82**, 1889–1922.
- Q. Du, J. Kamm, R. Lehoucq and M. Parks (2012b), ‘A new approach for a nonlocal, nonlinear conservation law’, *SIAM J. Appl. Math.* **72**, 464–487.
- Q. Du, R. Lipton and T. Mengesha (2016a), ‘Multiscale analysis of linear evolution equations with applications to nonlocal models for heterogeneous media’, *ESAIM Math. Model. Numer. Anal.* **50**, 1425–1455.
- Q. Du, Y. Tao and X. Tian (2018c), ‘A peridynamic model of fracture mechanics with bond-breaking’, *Journal of Elasticity* **132**, 197–218.
- Q. Du, Y. Tao, X. Tian and J. Yang (2016b), ‘Robust a posteriori stress analysis for quadrature collocation approximations of nonlocal models via nonlocal gradients’, *Comput. Methods Appl. Mech. Engrg.* **310**, 605–627.
- Q. Du, Y. Tao, X. Tian and J. Yang (2019d), ‘Asymptotically compatible discretization of multidimensional nonlocal diffusion models and approximations of nonlocal green’s functions’, *IMA J. Numerical Analysis* **39**, 607–625.
- Q. Du, L. Tian and X. Zhao (2013c), ‘A convergent adaptive finite element algorithm for nonlocal diffusion and peridynamic models’, *SIAM J. Numer. Anal.* **51**, 1211–1234.
- Q. Du, J. Yang and Z. Zhou (2017b), ‘Analysis of a nonlocal-in-time parabolic equation’, *Discrete Contin. Dyn. Syst. Ser. B* **22**, 339–368.
- Q. Du, J. Zhang and C. Zheng (2018d), ‘Nonlocal wave propagation in unbounded multi-scale media’, *Communications in Computational Physics* **24**, 1049–1072.
- S. Duo and Y. Zhang (2019), ‘Accurate numerical methods for two and three dimensional integral fractional Laplacian with applications’, *Comput. Methods Appl. Mech. Engrg.* **355**, 639–662.
- S. Duo, H.-W. van Wyk and Y. Zhang (2018), ‘A novel and accurate finite difference method for the fractional Laplacian and the fractional Poisson problem’, *J. Comput. Phys.* **355**, 233–252.
- B. Dyda, A. Kuznetsov and M. Kwaśnicki (2016), ‘Fractional Laplace Operator and Meijer G-function’, *Constructive Approximation* pp. 1–22.

- B. Dyda, A. Kuznetsov and M. Kwaśnicki (2017), ‘Eigenvalues of the fractional Laplace operator in the unit ball’, *J. Lond. Math. Soc. (2)* **95**, 500–518.
- A. Ern and J.-L. Guermond (2004a), *Theory and Practice of Finite Elements*, Springer-Verlag.
- A. Ern and J.-L. Guermond (2004b), *Theory and Practice of Finite Elements*, Springer, New York.
- V. Ervin and J. Roop (2007), ‘Variational solution of fractional advection dispersion equations on bounded domains in  $\mathbb{R}^d$ ’, *Numerical Methods for Partial Differential Equations* **23**, 256–281.
- V. Ervin, N. Heuer and J. Roop (2018), ‘Regularity of the solution to 1-d fractional order diffusion equations’, *Mathematics of Computation* **87**, 2273–2294.
- L. Evans (1998), *Partial Differential Equations*, American Mathematical Society.
- M. Faustmann, J. Melenk, M. Parvizi and D. Praetorius (2019), ‘Optimal adaptivity and preconditioning for the fractional Laplacian’, *Proceedings of WONAPDE*.
- M. Felsinger, M. Kassmann and P. Voigt (2015), ‘The Dirichlet problem for nonlocal operators’, *Mathematische Zeitschrift* **279**, 779–809.
- A. Fuensanta and J. Muñoz (2015), ‘Nonlocal optimal design: A new perspective about the approximation of solutions in optimal design’, *Journal of Mathematical Analysis and Applications* **429**, 288–310.
- G. Gilboa and S. Osher (2007), ‘Nonlocal linear image regularization and supervised segmentation’, *Multiscale Model. Simul.* **6**, 595–630.
- G. Gilboa and S. Osher (2008), ‘Nonlocal operators with applications to image processing’, *Multiscale Model. Simul.* **7**, 1005–1028.
- V. Girault and P.-A. Raviart (1986), *Finite Element Methods for Navier-Stokes Equations*, Springer.
- C. Glusa and E. Otárola (2019), ‘Optimal control of a parabolic fractional PDE: analysis and discretization’, *arXiv preprint arXiv:1905.10002*.
- I. Gradshteyn and I. Ryzhik (2007), *Table of Integrals, Series, and Products*, Elsevier/Academic Press.
- G. Grubb (2015a), ‘Fractional Laplacians on domains, a development of Hörmander’s theory of  $\mu$ -transmission pseudodifferential operators’, *Adv. Math.* **268**, 478–528.
- G. Grubb (2015b), ‘Regularity of spectral fractional Dirichlet and Neumann problems’, *Mathematische Nachrichten*.
- G. Grubb (2015c), ‘Spectral results for mixed problems and fractional elliptic operators’, *Journal of Mathematical Analysis and Applications* **421**, 1616–1634.
- Q. Guan and M. Gunzburger (2015), ‘Stability and accuracy of time-stepping schemes and dispersion relations for a nonlocal wave equation’, *Numer. Method. PDE* **31**, 500–516.
- Q. Guan and M. Gunzburger (2017), ‘Analysis and approximation of a nonlocal obstacle problem’, *J. Comput. Appl. Math.* **313**, 102–118.
- Q. Guan, M. Gunzburger, C. Webster and G. Zhang (2017), ‘Reduced basis methods for nonlocal diffusion problems with random input data’, *Comp. Meth. Appl. Mech. Engrg.* **317**, 746–770.
- M. Gunzburger and R. Lehoucq (2010), ‘A nonlocal vector calculus with application to nonlocal boundary value problems’, *Multiscale Modeling & Simulation* **8**, 1581–1598.

- M. Gunzburger, N. Jiang and F. Xu (2018), ‘Analysis and approximation of a fractional laplacian-based closure model for turbulent flows and its connection to richardson pair dispersion’, *Computers and Mathematics with Applications* **75**, 1973–2001.
- B. Guo and L. Wang (2004), ‘Jacobi approximations in non-uniformly Jacobi-weighted Sobolev spaces’, *J. Approx. Theory* **128**, 1–41.
- W. Hackbusch (1985), *Multi-grid methods and applications*, Springer, Berlin.
- W. Hackbusch (1994), *Iterative solution of large sparse systems of equations*, Springer, New York.
- W. Hu, Y. Ha and F. Bobaru (2012), ‘Peridynamic model for dynamic fracture in unidirectional fiber-reinforced composites’, *Computer Methods in Applied Mechanics and Engineering* **217**, 247–261.
- Y. Huang and A. Oberman (2014), ‘Numerical methods for the fractional Laplacian: a finite difference-quadrature approach’, *SIAM J. Numer. Anal.* **52**, 3056–3084.
- P. Jha and R. Lipton (2019a), ‘Finite element convergence for state-based peridynamic fracture models’, *arXiv preprint arXiv:1903.00924*.
- P. Jha and R. Lipton (2019b), ‘Numerical convergence of finite difference approximations for state based peridynamic fracture models’, *Computer Methods in Applied Mechanics and Engineering* **351**, 184–225.
- X. Jiang, L.-H. Lim, Y. Yao and Y. Ye (2011), ‘Statistical ranking and combinatorial Hodge theory’, *Math. Prog.* **127**, 203–244.
- M. Kac (1949), ‘On distributions of certain Wiener functionals’, *Trans. Amer. Math. Soc.* **65**, 1–13.
- G. Karniadakis, ed. (2019), *Handbook of Fractional Calculus with Applications. Vol. 3*, De Gruyter. Numerical methods.
- S. Kindermann, S. Osher and P. Jones (2005), ‘Deblurring and denoising of images by nonlocal functionals’, *SIAM Multiscale Modeling and Simulations* **4**, 1091–1115.
- A. Kyprianou, A. Osojnik and T. Shardlow (2018), ‘Unbiased ‘walk-on-spheres’ Monte Carlo methods for the fractional Laplacian’, *IMA J. Numer. Anal.* **38**, 1550–1578.
- H. Lee and Q. Du (2019a), ‘Asymptotically compatible SPH-like particle discretizations of one dimensional linear advection models’, *SIAM Journal on Numerical Analysis* **57**, 127–147.
- H. Lee and Q. Du (2019b), ‘Nonlocal gradient operators with a nonspherical interaction neighborhood and their applications’, *ESAIM: Mathematical Modelling and Numerical Analysis*.
- R. Lehoucq and S. Rowe (2016), ‘A radial basis function Galerkin method for inhomogeneous nonlocal diffusion’, *Comput. Methods Appl. Mech. Engrg.* **299**, 366–380.
- R. Lehoucq, F. Narcowich, S. Rowe and J. Ward (2018), ‘A meshless Galerkin method for non-local diffusion using localized kernel bases’, *Math. Comp.* **87**, 2233–2258.
- S.-L. Lei and H.-W. Sun (2013), ‘A circulant preconditioner for fractional diffusion equations’, *J. Comput. Phys.* **242**, 715–725.

- Y. Leng, X. Tian, N. Trask and J. Foster (2019), 'Asymptotically compatible reproducing kernel collocation and meshfree integration for nonlocal diffusion', *arXiv preprint arXiv:1907.12031*.
- Y. Leng, X. Tian, N. Trask and J. Foster (2020), 'Asymptotically compatible reproducing kernel collocation and meshfree integration for peridynamic Navier equation', *arXiv preprint arXiv:2001.00649*.
- O. L  zoray, V.-T. Ta and A. Elmoataz (2010), 'Partial differences as tools for filtering data on graphs', *Pattern Recog. Lett.* **31**, 2201–2213.
- C. Li and A. Chen (2018), 'Numerical methods for fractional partial differential equations', *Int. J. Comput. Math.* **95**, 1048–1099.
- S. Li and W. Liu (1996), 'Moving least-square reproducing kernel method part ii: Fourier analysis', *Computer Methods in Applied Mechanics and Engineering* **139**, 159–193.
- X. Li, Z. Qiao and C. Wang (2019), 'Convergence analysis for a stabilized linear semi-implicit numerical scheme for the nonlocal cahn-hilliard equation'.
- R. Lipton (2014), 'Dynamic brittle fracture as a small horizon limit of peridynamics', *J. Elasticity* **117**, 21–50.
- R. Lipton (2015), 'Cohesive dynamics and brittle fracture', *Journal of Elasticity* pp. 1–49.
- R. Lipton (2017), 'Cohesive dynamics and brittle fracture', *J. Elasticity* **124**, 143–191.
- R. Lipton, R. Lehoucq and K. Sha (2018), 'Complex fracture nucleation and evolution with nonlocal elastodynamics', *J. Peridynamics and Nonlocal Modeling* **1**, 122–130.
- W. Liu, S. Jun and Y. Zhang (1995), 'Reproducing kernel particle methods', *International journal for numerical methods in fluids* **20**, 1081–1106.
- Y. Lou, X. Zhang, S. Osher and A. Bertozzi (2010), 'Image recovery via nonlocal operators', *J. Sci. Comput.* **42**, 185–197.
- F. Mainardi (1997), Fractional calculus, in *Fractals and Fractional Calculus in Continuum Mechanics*, Springer, New York and Vienna, pp. 291–348.
- Z. Mao and G. Karniadakis (2018), 'A spectral method (of exponential convergence) for singular solutions of the diffusion equation with general two-sided fractional derivative', *SIAM J. Numer. Anal.* **56**, 24–49.
- Z. Mao and J. Shen (2017), 'Hermite spectral methods for fractional PDEs in unbounded domains', *SIAM J. Sci. Comput.* **39**, A1928–A1950.
- Z. Mao and J. Shen (2018), 'Spectral element method with geometric mesh for two-sided fractional differential equations', *Advances in Computational Mathematics* **44**, 745–771.
- Z. Mao, S. Chen and J. Shen (2016), 'Efficient and accurate spectral method using generalized Jacobi functions for solving Riesz fractional differential equations', *Applied Numerical Mathematics* **106**, 165–181.
- W. McLean (2000), *Strongly elliptic systems and boundary integral equations*, Cambridge University Press, Cambridge.
- M. Meerschaert and A. Sikorskii (2012), *Stochastic models for fractional calculus*, De Gruyter, Berlin-Boston.



- M. Meerschaert and C. Tadjeran (2004), ‘Finite difference approximations for fractional advection-dispersion flow equations’, *J. Comput. Appl. Math.* **172**, 65–77.
- M. Meerschaert and C. Tadjeran (2006), ‘Finite difference approximations for two-sided space-fractional partial differential equations’, *Appl. Numer. Math.* **56**, 80–90.
- M. Meerschaert, D. Benson and B. Bäumer (1999), ‘Multidimensional advection and fractional dispersion’, *Phys. Rev. E* **59**, 5026–5028.
- D. Meidner, J. Pfefferer, K. Schürholz and B. Vexler (2018), ‘hp-finite elements for fractional diffusion’, *SIAM J. Numer. Anal.* **56**, 2345–2374.
- T. Mengesha and Q. Du (2013), ‘Analysis of a scalar nonlocal peridynamic model with a sign changing kernel’, *Discrete Contin. Dyn. Syst. Ser. B* **18**, 1415–1437.
- T. Mengesha and Q. Du (2014), ‘Nonlocal constrained value problems for a linear peridynamic Navier equation’, *J. Elasticity* **116**, 27–51.
- T. Mengesha and Q. Du (2015), ‘On the variational limit of a class of nonlocal functionals related to peridynamics’, *Nonlinearity* **28**, 3999–4035.
- T. Mengesha and Q. Du (2016), ‘Characterization of function spaces of vector fields and an application in nonlinear peridynamics’, *Nonlinear Analysis: Theory, Methods & Applications* **140**, 82–111.
- R. Metzler and J. Klafter (2000), ‘The random walk’s guide to anomalous diffusion: a fractional dynamics approach’, *Phys. Rep.* **339**, 77.
- V. Minden and L. Ying (2018), ‘A simple solver for the fractional laplacian in multiple dimensions’, *arXiv preprint, arXiv:1802.03770*.
- S. Molčanov and E. Ostrovskii (1969), ‘Symmetric stable processes as traces of degenerate diffusion processes’, *Teor. Verojatnost. i Primenen.* **14**, 127–130.
- M. Muller (1956), ‘Some continuous Monte Carlo methods for the Dirichlet problem’, *Ann. Math. Statist.* **27**, 569–589.
- J. Necas (1967), *Les Méthodes Directes en Théorie des Equations Elliptiques*, Masson, Paris.
- J. Necas (2016), ‘Sur un méthode pour résoudre les équations aux dérivées partielles de type elliptique, voisine de la variationnelles’, *Ann. Scuola Norm. Sup. Pisa* **50**, 1425–1455.
- R. Nochetto, E. Otárola and A. Salgado (2015), ‘A PDE approach to fractional diffusion in general domains: a priori error analysis’, *Foundations of Computational Mathematics* **15**, 733–791.
- R. Nochetto, T. von Petersdorff and C.-S. Zhang (2010), ‘A posteriori error analysis for a class of integral equations and variational inequalities’, *Numer. Math.* **116**, 519–552.
- M. Ortigueira (2006), ‘Riesz potential operators and inverses via fractional centred derivatives’, *Int. J. Math. Math. Sci.* pp. Art. ID 48391, 12.
- J. Pan, M. Ng and H. Wang (2016), ‘Fast iterative solvers for linear systems arising from time-dependent space-fractional diffusion equations’, *SIAM J. Sci. Comput.* **38**, A2806–A2826.
- G. Pang, W. Chen and Z. Fu (2015), ‘Space-fractional advection-dispersion equations by the Kansa method’, *J. Comput. Phys.* **293**, 280–296.

- G. Pang, M. D'Elia, M. Parks and G. Karniadakis (2019a), 'nPINNs: nonlocal physics-informed neural networks'.
- G. Pang, L. Lu and G. Karniadakis (2019b), 'fPINNs: Fractional physics-informed neural networks', *SIAM Journal on Scientific Computing* **41**, A2603–A2626.
- I. Podlubny (1999), *Fractional differential equations*, Vol. 198 of *Mathematics in Science and Engineering*, Academic Press, Inc., San Diego, CA. An introduction to fractional derivatives, fractional differential equations, to methods of their solution and some of their applications.
- L. Richardson (1926), 'Atmospheric diffusion shown on a distance-neighbor graph', *Proceedings of the Royal Society of London Series A* **110**, 023126.
- X. Ros-Oton (2016), 'Nonlocal elliptic equations in bounded domains: a survey', *Publ. Mat.* **60**, 3–26.
- X. Ros-Oton and J. Serra (2014), 'The dirichlet problem for the fractional laplacian: regularity up to the boundary', *Journal de Mathématiques Pures et Appliquées* **101**, 275–302.
- J. Rosenfeld, S. Rosenfeld and W. E. Dixon (2019), 'A mesh-free pseudospectral approach to estimating the fractional Laplacian via radial basis functions', *J. Comput. Phys.* **390**, 306–322.
- L. Rudin, S. Osher and E. Fatemi (1992), 'Nonlinear total variation based noise removal algorithms', *Physica D: Nonlinear Phenomena* **60**, 259–268.
- K. Sabelfeld and N. Simonov (1994), *Random walks on boundary for solving PDEs*, VSP, Utrecht.
- J. Salazar and L. Collins (2009), 'Two-particle dispersion in isotropic turbulent flows', *Annual Review of Fluid Mechanics* **41**, 405–432.
- M. Samiee, M. Zayernouri and M. Meerschaert (2019a), 'A unified spectral method for FPDEs with two-sided derivatives; part I: A fast solver', *J. Comput. Phys.* **385**, 225–243.
- M. Samiee, M. Zayernouri and M. Meerschaert (2019b), 'A unified spectral method for FPDEs with two-sided derivatives; Part II: Stability, and error analysis', *J. Comput. Phys.* **385**, 244–261.
- S. Sauter and C. Schwab (2010), Boundary element methods, in *Boundary Element Methods*, Springer, pp. 183–287.
- P. Seleson, Q. Du and M. Parks (2016), 'On the consistency between nearest-neighbor peridynamic discretizations and discretized classical elasticity models', *Comput. Methods Appl. Mech. Engrg.* **311**, 698–722.
- P. Seleson, M. Parks, M. Gunzburger and R. Lehoucq (2009), 'Peridynamics as an upscaling of molecular dynamics', *Multiscale Modeling & Simulation* **8**, 204–227.
- R. Servadei and E. Valdinoci (2013), 'Lewy-Stampacchia type estimates for variational inequalities driven by (non)local operators', *Rev. Mat. Iberoam.* **29**, 1091–1126.
- R. Servadei and E. Valdinoci (2014), 'On the spectrum of two different fractional operators', *Proc. Roy. Soc. Edinburgh Sect. A* **144**, 831–855.
- T. Shardlow (2019), 'A walk outside spheres for the fractional Laplacian: fields and first eigenvalue', *Math. Comp.* **88**, 2767–2792.
- J. Shen and L.-L. Wang (2009), 'Some recent advances on spectral methods for unbounded domains', *Commun. Comput. Phys.* **5**, 195–241.

- J. Shen, T. Tang and L.-L. Wang (2011), *Spectral methods*, Vol. 41 of *Springer Series in Computational Mathematics*, Springer, Heidelberg.
- C. Sheng, J. Shen, T. Tang, L.-L. Wang and H. Yuan (2019), ‘Fast fourier-like mapped chebyshev spectral-galerkin methods for pdes with integral fractional laplacian in unbounded domains’, *arXiv preprint*, *arXiv:1908.10029*.
- S. Silling (2000), ‘Reformulation of elasticity theory for discontinuities and long-range forces’, *Journal of the Mechanics and Physics of Solids* **48**, 175–209.
- S. Silling (2010), ‘Linearized theory of peridynamic states’, *Journal of Elasticity* **99**, 85–111.
- S. Silling, M. Epton, O. Weckner, J. Xu and E. Askari (2007), ‘Peridynamic states and constitutive modeling’, *Journal of Elasticity* **88**, 151–184.
- L. Silvestre (2017), ‘Regularity of the obstacle problem for a fractional power of the Laplace operator’, *Comm. Pure Appl. Math.* **60**, 67–112.
- R. Slevinsky (n.d.), ‘Fast and backward stable transforms between spherical harmonic expansions and bivariate fourier series’, *Appl. Comput. Harmon. Anal.* p. in press.
- R. Slevinsky, H. Montanelli and Q. Du (2018), ‘A spectral method for nonlocal diffusion operators on the sphere’, *J. Computational Phys.* **372**, 893–911.
- I. Sokolov, J. Klafter and A. Blumen (2002), ‘Fractional kinetics’, *Physics Today* **55**, 48–54.
- P. Stinga and J. Torrea (2010), ‘Extension problem and Harnack’s inequality for some fractional operators’, *Comm. Partial Differential Equations* **35**, 2092–2122.
- P. R. Stinga (2019), User’s guide to the fractional Laplacian and the method of semigroups, in *Handbook of fractional calculus with applications. Vol. 2*, De Gruyter, Berlin, pp. 235–r265.
- H.-G. Sun, X. Liu, Y. Zhang, G. Pang and R. Garrard (2017), ‘A fast semi-discrete Kansa method to solve the two-dimensional spatiotemporal fractional diffusion equation’, *J. Comput. Phys.* **345**, 74–90.
- B. Swaford (2001), ‘Turbulent relative dispersion’, *Annual Review of Fluid Mechanics* **33**, 289–317.
- C. Tadjeran, M. Meerschaert and H.-P. Scheffler (2006), ‘A second-order accurate numerical approximation for the fractional diffusion equation’, *J. Comput. Phys.* **213**, 205–213.
- E. Tadmor (2007), ‘Filters, mollifiers and the computation of the Gibbs phenomenon’, *Acta Numer.* **16**, 305–378.
- T. Tang, L.-L. Wang, H. Yuan and T. Zhou (2019), ‘Rational spectral methods for pdes involving fractional laplacian in unbounded domains’, *arXiv preprint arXiv:1905.02476*.
- T. Tang, H. Yuan and T. Zhou (2018), ‘Hermite spectral collocation methods for fractional PDEs in unbounded domains’, *Commun. Comput. Phys.* **24**, 1143–1168.
- Y. Tao, X. Tian and Q. Du (2017), ‘Nonlocal diffusion and peridynamic models with Neumann type constraints and their numerical approximations’, *Appl. Math. Comput.* **305**, 282–298.

- Y. Tao, X. Tian and Q. Du (2019), ‘Nonlocal models with heterogeneous localization and their application to seamless local-nonlocal coupling’, *Multiscale Modeling & Simulation* **17**, 1052–1075.
- H. Tian, L. Ju and Q. Du (2015), ‘Nonlocal convection-diffusion problems and finite element approximations’, *Comput. Methods Appl. Mech. Engrg.* **289**, 60–78.
- H. Tian, L. Ju and Q. Du (2017), ‘A conservative nonlocal convection-diffusion model and asymptotically compatible finite difference discretization’, *Comput. Methods Appl. Mech. Engrg.* **320**, 46–67.
- X. Tian (2017), Nonlocal models with a finite range of nonlocal interactions, PhD thesis, Columbia University.
- X. Tian and Q. Du (2013), ‘Analysis and comparison of different approximations to nonlocal diffusion and linear peridynamic equations’, *SIAM J. Numer. Anal.* **51**, 3458–3482.
- X. Tian and Q. Du (2014), ‘Asymptotically compatible schemes and applications to robust discretization of nonlocal models’, *SIAM J. Numer. Anal.* **52**, 1641–1665.
- X. Tian and Q. Du (2015), ‘Nonconforming discontinuous Galerkin methods for nonlocal variational problems’, *SIAM J. Numer. Anal.* **53**, 762–781.
- X. Tian and Q. Du (2017), ‘Trace theorems for some nonlocal function spaces with heterogeneous localization’, *SIAM J. Math. Anal.* **49**, 1621–1644.
- X. Tian and Q. Du (2020), ‘Asymptotically compatible schemes for robust discretization of parametrized problems with applications to nonlocal models’, *SIAM Review*.
- X. Tian and B. Engquist (2019), ‘Fast algorithm for computing nonlocal operators with finite interaction distance’, *Communications in Mathematical Sciences* **17**, 1653–1670.
- X. Tian, Q. Du and M. Gunzburger (2016), ‘Asymptotically compatible schemes for the approximation of fractional Laplacian and related nonlocal diffusion problems on bounded domains’, *Adv. Comput. Math.* **42**, 1363–1380.
- N. Trask, H. You, Y. Yu and M. Parks (2019), ‘An asymptotically compatible mesh-free quadrature rule for nonlocal problems with applications to peridynamics’, *Computer Methods in Applied Mechanics and Engineering* **343**, 151–165.
- E. Valdinoci (2009), ‘From the long jump random walk to the fractional Laplacian’, *Bol. Soc. Esp. Mat. Apl. SeMA* **49**, 33–44.
- C. Vollmann and V. Schulz (2019), ‘Exploiting multilevel Toeplitz structures in high dimensional nonlocal diffusion’, *Computing and Visualization in Science* **20**, 2946.
- H. Wang and T. S. Basu (2012), ‘A fast finite difference method for two-dimensional space-fractional diffusion equations’, *SIAM J. Sci. Comput.* **34**, A2444–A2458.
- H. Wang and N. Du (2013), ‘A fast finite difference method for three-dimensional time-dependent space-fractional diffusion equations and its efficient implementation’, *J. Comput. Phys.* **253**, 50–63.
- H. Wang and N. Du (2014), ‘Fast alternating-direction finite difference methods for three-dimensional space-fractional diffusion equations’, *J. Comput. Phys.* **258**, 305–318.

- H. Wang and H. Tian (2012), ‘A fast Galerkin method with efficient matrix assembly and storage for a peridynamic model’, *Journal of Computational Physics* **231**, 7730–7738.
- H. Wendland (1995), ‘Piecewise polynomial, positive definite and compactly supported radial functions of minimal degree’, *Adv. Comput. Math.* **4**, 389–396.
- H. Wendland (2005), *Scattered data approximation*, Vol. 17 of *Cambridge Monographs on Applied and Computational Mathematics*, Cambridge University Press, Cambridge.
- D. Witman, M. Gunzburger and J. Peterson (2017), ‘Reduced-order modeling for nonlocal diffusion problems’, *Int. J. Numer. Meth. Fluids* **83**, 307–327.
- F. Xu, M. Gunzburger and J. Burkardt (2016a), ‘A multiscale method for nonlocal mechanics and diffusion and for the approximation of discontinuous functions’, *Computer Methods in Applied Mechanics and Engineering* **307**, 117–143.
- F. Xu, M. Gunzburger, J. Burkardt and Q. Du (2016b), ‘A multiscale implementation based on adaptive mesh refinement for the nonlocal peridynamics model in one dimension’, *Multiscale Model. Simul.* **14**, 398–429.
- K. Xu and E. Darve (2018a), ‘Efficient numerical method for models driven by Lévy process via hierarchical matrices’, *arXiv preprint, arXiv:1812.08324*.
- K. Xu and E. Darve (2018b), ‘Spectral method for the fractional Laplacian in 2D and 3D’, *arXiv preprint, arXiv:1812.08325*.
- C. Yan, W. Cai and X. Zeng (2013), ‘A parallel method for solving Laplace equations with Dirichlet data using local boundary integral equations and random walks’, *SIAM J. Sci. Comput.* **35**, B868–B889.
- H. You, Y. Yu and D. Kamensky (2019), ‘An asymptotically compatible formulation for local-to-nonlocal coupling problems without overlapping regions’, *arXiv preprint arXiv:1912.06270*.
- M. Zayernouri, M. Ainsworth and G. Karniadakis (2015a), ‘Tempered fractional Sturm-Liouville eigenproblems’, *SIAM J. Sci. Comput.* **37**, A1777–A1800.
- M. Zayernouri, M. Ainsworth and G. Karniadakis (2015b), ‘A unified Petrov-Galerkin spectral method for fractional PDEs’, *Comput. Methods Appl. Mech. Engrg.* **283**, 1545–1569.
- M. Zayernouri and G. Karniadakis (2014), ‘Exponentially accurate spectral and spectral element methods for fractional ODEs’, *J. Comput. Phys.* **257**, 460–480.
- L. Zhang, H.-W. Sun and H.-K. Pang (2015), ‘Fast numerical solution for fractional diffusion equations by exponential quadrature rule’, *J. Comput. Phys.* **299**, 130–143.
- W. Zhang, J. Yang, J. Zhang and Q. Du (2017), ‘Artificial boundary conditions for nonlocal heat equations on unbounded domain’, *Commun. Comput. Phys.* **21**, 16–39.
- X. Zhang, M. Gunzburger and L. Ju (2016a), ‘Nodal-type collocation methods for hypersingular integral equations and nonlocal diffusion problems’, *Comp. Meth. Appl. Mech. Eng.* **299**, 401–420.
- X. Zhang, M. Gunzburger and L. Ju (2016b), ‘Quadrature rules for finite element approximations of 1d nonlocal problems’, *Journal of Computational Physics* **310**, 213–236.

- Z. Zhang (2019), 'Error estimates of spectral galerkin methods for a linear fractional reaction-diffusion equation', *Journal of Scientific Computing* **78**, 1087–1110.
- D. Zhou and B. Schölkopf (2005), Regularization on discrete spaces, in *Proceedings of the 27th DAGM Symposium*, Vol. LNCS, 3663,, Springer, pp. 361–36.
- K. Zhou and Q. Du (2010), 'Mathematical and numerical analysis of linear peridynamic models with nonlocal boundary conditions', *SIAM J. Numer. Anal.* **48**, 1759–1780.